HOW THE PLASMID-ENCODED MERCURY RESISTANCE LOCUS ACCELERATES RECOVERY OF *ESCHERICHIA COLI* FROM EXPOSURE TO INORGANIC MERCURY

by

ANDREW GEORGE WIGGINS

(Under the Direction of Anne O. Summers)

ABSTRACT

The element Mercury (Hg) is toxic in all forms. Prokaryotes have evolved an efficient detoxification system widely disseminated by transposons and plasmids. This Hg resistance system (*mer)* encodes transporters that deliver Hg(II) to a specialized mercuric reductase, MerA, that uses NADPH to reduce reactive mercury, Hg(II), to volatile monoatomic Hg(0) vapor which diffuses away. With transcriptomics I examined the whole-cell response to Hg in a model prokaryote, *Escherichia coli* MG1655 (MG), carrying a 94-kb conjugative plasmid, NR1 (NR), bearing a classic *mer* operon. Aim 1 examined the burden of NR1 on chromosomal gene expression of MG and the benefit NR1 provided during Hg exposure. Without Hg exposure, NR1 did not evoke expression of any chromosomal genes and the plasmid itself expressed only its replication genes and several associated with transposons. Upon Hg(II) exposure, NR1's *mer* operon genes expressed strongly but most other plasmid genes decreased or did not change. However, for many chromosomal genes Hg(II) provoked significant differences between MG and its un-exposed condition. These large transcriptional responses by MG diminished or disappeared in MG(NR). Thus, just hosting NR1 adds no expression in chromosomal genes and

with *mer* proteins cells recovered growth sooner. Previous work suggested *E. coli* must increase NADPH production to support observed Hg(II) reduction by MerA. Aim 2 examined expression of chromosomal NADPH-producing enzymes. The only increase (30%) occurred in highly expressed (40,000/cell) TCA cycle enzyme, isocitrate dehydrogenase, ICD, which has a high k_{cat} (72/sec). Those values and RNA-Seq data predicted a mere 30% increase in ICD could produce 18-fold more NADPH than MerA needs to reduce 3 million Hg(II)/min as observed in intact cells. Thus, at typical Hg exposures, MerA's reductant needs are met by a slight tweak in normal metabolism. Aim 3 focused on 310 MG chromosomal genes of proteins we previously observed as highly vulnerable to binding mercurial compounds. Their transcriptional responses revealed distinct patterns consistent with their metabolic functions, notably respiration, sulfur metabolism, and amino acid biosynthesis. Many Hg-vulnerable proteins have homologs in human mitochondria and could be sensitive reporters of Hg exposure and of the efficacy of detoxification measures.

INDEX WORDS: Mercury, Escherichia coli, Transcriptomics, Mercury Resistance, Redox Homeostasis, Mercuric Reductase

HOW THE PLASMID-ENCODED MERCURY RESISTANCE LOCUS ACCELERATES RECOVERY OF *ESCHERICHIA COLI* FROM EXPOSURE TO INORGANIC MERCURY

by

ANDREW GEORGE WIGGINS

B.S., Auburn University, 2009

A Dissertation Submitted to the Graduate Faculty of The University of Georgia in Partial Fulfillment of the Requirements for the Degree

DOCTOR OF PHILOSOPHY

ATHENS, GEORGIA

2022

© 2022

Andrew G. Wiggins

All Rights Reserved

HOW THE PLASMID-ENCODED MERCURY RESISTANCE LOCUS ACCELERATES RECOVERY OF *ESCHERICHIA COLI* FROM EXPOSURE TO INORGANIC MERCURY

by

ANDREW GEORGE WIGGINS

Major Professor:	Anne O. Summers
Committee:	Jorge Escalante-Semerena
	Timothy Hoover
	Anna Karls

Electronic Version Approved:

Ron Walcott
Vice Provost for Graduate Education and Dean of the Graduate School
The University of Georgia
May 2022

DEDICATION

This dissertation is dedicated to my mom, Sammie Wiggins, and in loving memory of my dad, Ron Wiggins. Their endless love, support, and encouragement has guided me throughout this journey of life.

ACKNOWLEDGEMENTS

Most importantly, I would like to acknowledge my mentors. For my advisor, Dr. Anne O. Summers, I am grateful for the opportunities she provided in promoting my understanding of bacterial science and the support of the research presented here. Additionally, I am grateful for my teaching mentor, Dr. Jennifer Walker, for the assistance in my teaching opportunities. My work has afforded me the opportunity to present my research at professional and international venues and participate in various other opportunities offered by the University of Georgia. I am thankful for their assistance, feedback, and support throughout my journey at the University of Georgia. I would also like to thank the members of my committee for their feedback and assistance at various times over the years. Finally, I would like to thank Dr. Stephen LaVoie and Joy Wireman for their assistance during my time in the lab.

TABLE OF CONTENTS

Page

ACKNOWLEDGEMENTS V

CHAPTER

1 INTRODUCTION AND LITERATURE REVIEW 1

2 THE COST TO *ESCHERICHIA COLI* IN CARRYING THE NR1 PLASMID AND THE BENEFIT PROVIDED BY THE MERCURY RESISTANCE OPERON WHEN RECOVERING FROM MERCURY EXPOSURE 23

3 TRANSCRIPTIONAL RESPONSES OF *ESCHERICHIA COLI* GENES ENCONDING PROTEINS HIGHLY VULNERABLE TO DAMAGE BY MERCURY COMPOUNDS 76

4 SUMMARY 109

APPENDIX 123

A SUPPLEMENTAL MATERIAL FOR CHAPTER 2 123

CHAPTER 1

INTRODUCTION AND LITERATURE REVIEW

The Element Mercury

Mercury (Hg), also known as quicksilver, is the 80th element of the periodic table with an atomic mass of 200.592. It is a Group 12 transition metal like zinc (Zn) and cadmium (Cd). Zinc is an essential trace element that plays an important part in many biological processes, but cadmium and mercury have no biological role and are highly toxic. Mercury is unique among metallic elements because at standard temperature and pressure it is a dense silvery liquid with a volatile monoatomic vapor phase. This unusual behavior occurs because of its stable electron configuration and weak Hg-Hg bond, which allows mercury to have the lowest melting point (-39°C) of all pure metals and a low boiling point (357°C). When heated it conducts electricity well, but heat poorly and readily combines to form alloys or amalgams. Because of its unique physical and chemical properties and despite (or because of) its recognized toxicity mercury and its compounds have been used since antiquity.

Biogeochemical Cycle of Mercury

Mercury undergoes a complex biogeochemical cycle that involves biotic and abiotic transformations (Grégoire and Poulain, 2018, Barkay et al., 2003, Morel et al., 1998, Mason et al., 1994). In nature, its common forms are metallic liquid and vapor mercury (Hg^0), ionic mercury (Hg^{2+}, Hg^{1+}, and $(Hg_2)^{2+}$) that combine with nucleophiles such as halides and chalcogens

with varying degrees of solubility in water, and fat soluble organomercurial compounds (RHg^{+}) including methylmercury . The zero valent state (Hg^{0}) is the primary form emitted into the atmosphere where it resides with an approximate 1 year half-life (Huang et al., 2013, Selin et al., 2007). Atmospheric Hg^{0} is oxidized by ozone or lightning and eventually deposited as Hg^{2+} in distant aquatic and terrestrial ecosystems. Hg^{2+} in such deposits can be reduced by sunlight or biotic activities to Hg^{0} which cycles back into the atmosphere, or it can complex at the one or two valence state with different inorganic nucleophiles such as halides. Lastly, and rare among transition metals, it can be methylated by bacteria to monomethylmercury that biomagnifies up food webs into higher organisms. Atmospheric spread coupled with biomagnification, lead to the accumulation of monomethylmercury in biota far removed from natural and anthropogenic sources (Grégoire and Poulain, 2018, Barkay et al., 2003).

Natural occurrences of mercury exist in the Earth's crust in 26 mercury mineral belts. Mercury deposits occur within silica-carbonate formations along convergent plate tectonic boundaries (Rytuba, 2003), in hot springs adjacent to silica-carbonate deposits, near surface environments where meteoric-dominated geothermal systems developed; near felsic volcanic centers (Rytuba, 1996), and in the Almaden mercury mineral belt in central Spain (Saupe, 1990). Cinnabar, mercuric sulfide (HgS), is the primary ore in these deposits and is the major reservoir of mercury in the environment (Rytuba, 2003, Barnes, 1997). Although mineral forms of mercury have a low solubility in water, their products are available for transformation between the Hg^{2+}, Hg^{1+}, and Hg^{0} oxidation states by natural (abiotic or biotic) and anthropogenic processes.

Abiotic Hg transformations include solar photoreduction of ionic mercury (Hg^{2+}) in marine and lacustrine photic zones, solar and ozone oxidation of atmospheric mercury vapor, and solar photodegradation of organomercurials (Barkay et al., 2003). Biotic processes involving microbes play a key environmental role in Hg transformations including sequestration, oxidation, reduction, and methylation reactions. A wide array of chemotrophic and phototrophic microorganisms in oxic and anoxic environments participate directly in the Hg biogeochemical cycle. Chemotrophic mercury transformers include sulfate-reducing bacteria that are the principal methylators of mercury in natural anaerobic sediments (Grégoire and Poulain, 2018, Parks et al., 2013, Barkay et al., 2003, King et al., 2000), although iron-reducing bacteria (Yu et al., 2012) and methanogens (Hamelin et al., 2011) can also be involved. Chemotrophic demethylators include mercury resistant bacteria carrying the *mer* operon (Barkay et al., 2003) that are capable of demethylation by protonlysis of the carbon-mercury bond of organomercurial compounds to Hg^{2+} catalyzed by the organomercury lyase, MerB (Parks et al., 2013, Parks et al., 2009, Pitts and Summers, 2002) with subsequent biotic transformation of Hg^{2+} to Hg^0 by the mercuric reductase, MerA (Ledwidge et al., 2005).

The reduction of mercury to its vapor form is different from most other metal defense mechanisms which typically use active transport or sequestration of metal ions (Ianeva, 2009). Chemotrophic bacteria, instead of effluxion of methylmercury, can demethylate it by an adventitious side reaction of their C1-metabolic pathways yielding Hg^{2+} and CO_2 as products (Hsu-Kim et al., 2013). Other non-dedicated, adventitious Hg transformation pathways unrelated to the *mer* operon can include, for example, Hg^{2+} reduction by microaerophilic magnetotactic bacteria using biogenic membrane-bound magnetite (Fe_3O_4) (Liu and

Wiatrowski, 2018) or by anaerobic Clostridiales fermenting pyruvate (Grégoire et al., 2018). Chemotrophic mercury oxidizers are poorly understood, but apparently oxidize Hg^0 by redox reactions with cell membrane based disulfide management systems of these anaerobes (Colombo et al., 2013) and possibly in other obligate or facultative anaerobes (Lu et al., 2016, Lin et al., 2014, Colombo et al., 2013). Even dead cells that release thiols can produce Hg^0 (Colombo et al., 2013). Catalase in many aerobic bacteria and higher organisms can oxidize Hg^0 to Hg^{2+} in the presence of hydrogen peroxide (Barkay et al., 2003, Clarkson and Magos, 2006, Smith et al., 1998).

Oxygenic phototrophs such as algae, cyanobacteria, diatoms, anoxygenic phototrophic purple non-sulphur bacteria, and the green alga *Chlamydomonas reinhardtii* oxidize elemental Hg^0 to Hg^{2+}(Grégoire and Poulain, 2014). Most studies addressing phototrophic mercury methylation are conducted on periphytic communities where the phototrophs supply nutrients to chemotrophic mercury methylators, but there is very little support for phototrophs directly participating in mercury methylation (Lázaro et al., 2018, Gentès et al., 2017, Olsen et al., 2016, Gionfriddo et al., 2016). Phototrophs can also mitigate mercury exposure by intracellular sequestration or elimination by efflux pumps. Sequestration of mercury occurs by metallochaperones such as phyotchelatins and metallothioneins which serve otherwise in beneficial transition metal homeostasis and by H_2S produced in dissimilatory sulfate respiration by anaerobic sulfate-reducing bacteria forms very stable HgS, cinnabar, with a formation constant of 10^{45}. (Kelly et al., 2007, Kawakami et al., 2006).

Mercury Toxicity

Extensive studies over the past 60 years have greatly advanced our understanding of mercury as a global contaminant. However, the specific molecular basis for mercury's toxic effects inside individual cells is surprisingly poorly understood other than to say that Hg^{2+} disrupts thiol homeostasis. Newer metallomics approaches have described some of the effects of bacterial exposure to sub-lethal concentrations of mercury and the molecular interactions taking place that allow recovery of the biological systems (LaVoie et al., 2015, Polacco et al., 2011, Rao et al., 2010, Trümpler et al., 2009, Krupp et al., 2008). Since no form of mercury is employed in natural biological processes, the metallomics of mercury focuses on how it adversely affects the normal functions of genes and proteins ("i.e., toxic effects"), and how such adverse effects are alleviated by normal cellular processes and/or dedicated mercury resistance systems, the latter limited in only prokaryotes.

The toxic effect of mercury is due to its ability to form nearly covalent bonds with cellular thiol and selenol groups with high affinity (Riccardi et al., 2013). These groups play important roles in many cellular processes which are readily disrupted by their chelating mercury with formation constants ranging from 10^{15} to 10^{40} for thiols (Riccardi et al., 2013, Zhang et al., 2004), which cannot be dissociated by common monothiol buffers such a glutathione. In binding thiol and selenol groups, Hg interrupts key oxidative stress defense molecules such as the abundant tripeptide glutathione and the sources and regulators of their production i.e., thiol homeostasis. Thiol and selenol groups are in amino acids, cysteine and selenocysteine, in the proteins of every biological kingdom where they play important structural and functional roles in protein chemistry and catalysis, but their high affinity for Hg^{2+}

renders them vulnerable to inactivation. Thiol groups are important cofactors for certain enzymes and act as small “redox buffers” against oxidative species.

Elemental mercury vapor, Hg^0, can readily cross cellular membranes, inwardly and outwardly. Upon entering the cell, Hg^0 can be rapidly oxidized to reactive, toxic Hg^{2+} by catalase (Clarkson and Magos, 2006, Clarkson, 2002, Smith et al., 1998). The manner of Hg^{2+}-uptake through the bacterial cell wall is still uncertain, but both passive and facilitated uptake pathways have been suggested. Nonpolar complexes such as $HgCl_2$ and HgS would favor passive uptake. Exposure to mercury compounds induces oxidative stress by inhibiting respiratory enzymes, ATP synthase, and partial reduction of dioxygen to superoxide (LaVoie et al., 2015, Valko et al., 2005). Additionally, mercury directly forms adducts with redox defense proteins, with low molecular weight thiol redox buffers, and exposed thiol groups of proteins and enzymes (LaVoie et al., 2015, Polacco et al., 2011). The thioredoxin and glutaredoxin systems are essential for intracellular redox homeostasis, but both are susceptible to mercury binding directly to these enzymes (Branco and Carvalho, 2019). Mercury compounds decouple oxidative phosphorylation leading to the production of reactive oxygen species (LaVoie et al., 2015) in cytoplasmic membranes of bacteria (Barkay et al., 2003) and in the mitochondria of eukaryotes (Nath et al., 1996).

Roughly half of all enzymes in the six Enzyme Commission functional classes use metal cofactors (Andreini et al., 2008). Transition metal cofactors often bind to cysteine thiols but can easily be displaced by Hg^{2+} with consequent loss of protein function. Electron paramagnetic resonance spectroscopy revealed that iron-sulfur clusters in redox enzymes are susceptible to damage due to mercury exposure and exposure to mercury compounds increased intracellular

concentration of free iron in *E. coli* (LaVoie et al., 2015) at a 250-fold lower concentration than hydrogen peroxide. This further amplifies the damage caused by Hg exposure.

Effects of Mercury Exposure on Transcription

There are limited data on the effects of mercury exposure on transcription and extant studies are on Hg-sensitive cells lacking a *mer* operon. *Saccharomyces cerevisiae* was studied with microarray analysis after exposure to mercuric chloride (19 µM and 47 µM) and found to have increased expression of transporters for polyamine, cation, metal ion, and vitamins, but a decrease in expression of transporters for carbohydrate and secretory pathways. Additionally, increased expression was seen for genes associated with ribosomal proteins, sulfur metabolism, and oxidative stress response (Jin et al., 2008). Transcriptomics of the green alga, *C. reinhardtii,* exposed to sub-nanomolar concentrations (3.7×10^{-10} and 3.6×10^{-11} M) of methylmercury revealed significant dysregulation in expression of genes involved in motility, energy metabolism, lipid metabolism, metal transport, and antioxidant enzymes (Beauvais-Flück et al., 2016). The algal cells could cope with sub-lethal methylmercury exposure, but at a significant cost to energy and metabolic reserves.

In the first phase of this current project we used *Escherichia coli* strain MG1655 to explore significant changes in chromosomal gene expression caused by the effects of exposure to mercuric chloride or phenylmercuric acetate during a 60 minute window to examine how the cell responded and recovered from a dose of 3 µM $HgCl_2$ or phenylmercuric acetate (LaVoie and Summers, 2018). We hypothesized that the cytosolic glutathione pool would be largely sequestered by bis-coordination with Hg^{2+} resulting in up-regulation of cysteine and/or

glutathione biosynthesis pathways as was the case with yeast and green microalga (Jin et al., 2008, Beauvais-Flück et al., 2016). In contrast, cysteine biosynthesis in *E. coli* was down-regulated and glutathione biosynthesis was not statistically distinct from the unexposed culture. However, the oxidoreductases thioredoxin, glutaredoxin, glutathione reductase that maintain thiol homeostasis did increase in *E. coli*. Eukaryotes have the small copper sequestering protein metallothionein to protect thiol homeostasis by sequestering redox active metals and, indeed, metallothionein increased in yeast (Jin et al, 2008).

Genes involved in energy production, which rely on redox-active transition metals and redox-active sulfur compounds, are vulnerable targets to mercury exposure, and were initially sharply down-regulated, as were genes involved in glucose, amino acid, carbohydrate, and nucleotide metabolism, and energy-dependent transporters of these molecules. These results echo the wide functional variety of proteins stably modified by mercury binding to cysteines of *E. coli* proteins. This work now serves as a foundation for studying how a mercury resistance locus assists *E. coli* in recovery from sub-lethal mercury exposure.

Bacterial Mercury Resistance

As noted above, any biotic processes adventitiously reduce low concentrations of mercury simply as a “short circuit” side-reaction of normal physiologic redox processes. However, for Hg concentrations above 10 µM, evolution has quite literally cobbled together paralogs of key flavin disulfide reductases, essential metal chaperones, and essential metal metalloregulators into a mosaic operon to protect the cell from concentration of Hg(II) in excess of ~10 µM. The *mer* operon is broadly distributed among prokaryotes, carried by an

ancient family of transposons, and mounted on a broad host-range of plasmids ubiquitous in proteobacteria, Firmicutes, and Crenarcheotae. Sequences homologous to the core enzyme of Hg resistance, MerA, occurs in 55 prokaryotic lineages at the phylum level (Christakis et al., 2021). The regulatory and structural *mer* genes have been more extensively studied in Gram-negative bacteria, but Gram-positive bacteria have operons of similar genes that are experimentally verified to provide Hg resistance and whose MerA gene yielded the first crystal structure of this remarkable enzyme (Barkay et al., 2003).

The most widely observed mechanism of eubacterial mercury resistance encodes an elaborate detoxification system dedicated to moving inorganic mercury and some organomercury compounds into the cytoplasm of the cell, probably by facilitated diffusion, as there is no evidence of any connection to a source of energy. All proteins encoded by *mer* genes bind to Hg^{2+} with varying affinities appropriate to their tasks via one or more cysteine thiol/thiolate groups. In the periplasm, MerP binds Hg^{2+} with two neighboring cysteines displacing its coordinating nucleophiles (e.g., glutathione) and transfers it to a cysteine pair on the periplasmic side of the inner membrane transporter, MerT, which passes the metal ion to another cysteine pair on its cytoplasmic side. After coordination, MerP transports mercury from the periplasm to a pair of cysteines located in the three transmembrane helices of MerT. MerT is an inner cytosolic membrane protein that transfers mercury to a second pair of cytosolic cysteines located on the interior membrane of the cytoplasm (Liu et al., 2012, Silver and Hobman, 2007, Barkay et al., 2003).

Once mercury is delivered from the periplasm to the inner side of the cytoplasmic membrane, it is accessible to the cytosolic mercuric reductase (MerA) for reduction of Hg^{2+} to a

relatively inert volatile monoatomic gas (Hg^0), which diffuses out of the cell due to its low aqueous solubility and high vapor pressure (Barkay et al., 2003). MerA is a cytosolic flavin disulfide oxidoreductase that uses one NADPH-molecule as its reductant. MerA has a flexible amino-terminal domain (NmerA) homologous to the small periplasmic mercury binding protein (MerP). NmerA is a 70 amino acid extension with homology to other soft metal ion trafficking proteins that allows the delivery of mercury to a vicinal cysteine pair at the carboxyl terminal of the opposite MerA monomer to the cysteine pair of MerA's catalytic core site where the electrons derived from NADPH by the FAD cofactors reduce the thiol bound to Hg^{2+} to Hg^0 (Liu et al., 2012, Ledwidge et al., 2005, Barkay et al., 2003). MerA has been observed to associate with the inner membrane and may directly remove mercury from the cytosolic pair of cysteines located on MerT (Liu et al., 2012, Barkay et al., 2003).

Mercury resistance loci have additional genes involved in mercury uptake, degradation of organomercury compounds, and regulating expression of the *mer* operon. The several small, inner membrane Hg^{2+}-uptake proteins MerT, MerC, MerF, and MerE appear variously in *mer* operons in microbial taxa in diverse environments; all have similar structure to MerT, but with varying numbers of transmembrane spanning domains one with a pair of cysteines on/near the periplasmic side and a 2^{nd} pair in/near the cytoplasm (Liu et al., 2012, Barkay et al., 2003, Hamlett et al., 1992). MerC (Sahlman et al., 1997) and MerH (Schué et al., 2009) transporters contain four predicted transmembrane helices, while MerE (Kiyono et al., 2009) and MerF (Wilson et al., 2000) contain two. MerC is effective in Hg^{2+}-uptake, but less so than MerT (Barkay et al., 2003, Kusano et al., 1990). MerE of Tn*21* takes up methylmercury and Hg(II), whereas MerT of *Pseudomonas spps.* takes up Hg(II) and phenylmercury acetate, but not

methylmercury (Uno et al., 1997). MerG a small periplasmic protein observed in soil pseudomonads appears to prevent organomercurial uptake by limiting transfer of phenylmercury acetate to the cytoplasmic side of the cell (Barkay et al., 2003, Kiyono and Pan-Hou, 1999).

Prokaryotes that are resistant to organomercury compounds encode the organomercury lyase, MerB in which one of two conserved cysteines (Cys96 and Cys159) in the active site donates a proton to a conserved aspartic acid (position Asp99), enabling coordination of two thiolates with the RHg^{2+}. The protonated aspartic acid transfers the proton to the reactive carbanion likely in a trigonal planar intermediate where the bis-thiol-ligated R-Hg^{2+} drives cleavage of the Hg-C bond releasing the hydrocarbon product (Parks et al., 2009). After cleavage, Hg^{2+} remains bound to the MerB cysteines until it is removed by the NmerA domain of MerA and reduced to Hg^0, regenerating bis-thiol MerB for another catalytic cycle. It is also possible that in the absence of MerA, Hg(II) may dissociate spontaneously from MerB to low molecular weight thiols such as glutathione or to other non-*mer* reductases (Christakis et al., 2021, Grégoire and Poulain, 2018).

Transcription of the *mer* operon is controlled by the homodimeric MerR that acts as a repressor in the absence of Hg(II) and as an activator in its presence (Barkay et al., 2003). The MerR homodimer is always bound to the MerOP domain; in the absence of Hg(I), it forms a preinitiation complex preventing access of the bound RNA polymerase to the -10 and -35 hexamers of the structural genes' promoter. Hg^{2+} binds to the metal-binding domains of MerR the protein unwinds the operator DNA allowing access of RNA polymerase to the -10 region of the promoter to begin mRNA polymerization of the structural genes (Song et al., 2007, Barkay

et al., 2003). In *Beta*- and *Gammaproteobacteria* (Barkay et al., 2010), an additional regulatory encoded functional protein in MerD acts as an antagonist to MerR by preventing RNA polymerase from joining the Hg^{2+}/MerR/MerOP complex to begin transcription (Champier et al., 2004) once the intracellular Hg concentration has sufficiently diminished.

The *mer* operon is disseminated by mobile genetic elements as part of group II transposons in both Gram-negative and Gram-positive bacteria (Barkay et al., 2003, Kholodii et al., 2002, Liebert et al., 1997). These *mer*-related transposons often carry integrons with one or more antibiotic resistance genes associated with them (Barkay et al., 2003, Liebert et al., 1999), and are commonly encoded on the chromosome or large, conjugative plasmids of bacteria clinically important for human and animals (Pal et al., 2015). Although both domestic animals and humans are heavily exposed to antibiotics, only humans are heavily exposed to Hg via amalgam dental restorations. We have shown in a primate model that Hg(II) exposure from dental restorations provokes proliferation and spread of Hg and antibiotic-resistance genes genetically linked on plasmids, demonstrating that a non-antibiotic chemical to which well over 50% of the US population is exposed continuously co-selects not only for single antibiotic resistance genes, but for a genetic machine (the integron) that collects and spreads arrays of multiple antibiotic resistance genes (Summers, 1993; Liebert, 1998, Wireman 1996).

MerA requires one NADPH for every Hg(II) ion it detoxifies to volatile Hg(0) vapor

Human intestinal microbiota has been directly exposed to elemental mercury and /or the most common HgS ore, cinnabar, for treating myriad disorders for over two and a half millennia in the East and for at least 500 years in Western medicine. So, our commensal

bacteria have had sufficient time to evolve metabolic pathways and oxidative stress responses to counter the negative effects of mercury. The widely found elimination by reduction mechanism of the *mer* operon has evolved at least once and then spread widely via the mobile element transportation infrastructure. It involves a collaboration between the cell's ability to generate reducing equivalents and the *mer* protein's ability to interact with reactive Hg^{2+} in a nimbler way than the Hg^{2+}-vulnerable proteins from which they evolved. For the cell's part, it must maintain and stabilize its redox state to prevent obstruction of anabolic reactions and repair and replace proteins vulnerable to redox damage provoked by Hg's destabilization of oxidative respiration and the result burst of reactive oxygen species. During normal aerobic growth on glucose by *E. coli*, the primary NADPH-generating reactions are those of the oxidative pentose phosphate pathway that contributes 35% to 45%, isocitrate dehydrogenase in the tricarboxylic acid cycle that contributes 20% to 25%, and the membrane-bound transhydrogenase (PntAB) which catalyzes the energy-dependent transfer of reducing power from NADH to $NADP^+$ forming NADPH and contributes 35% to 45% (Sauer et al., 2004). Bacteria can respond to extra NADPH demand from ordinary reactive oxygen species alone by rerouting the glycolytic flux towards the pentose phosphate pathway which can lead to a NADPH surplus to supply the glutathione-based redox repair proteins, thioredoxin and glutaredoxins (Nikel et al., 2021, Christodoulou et al., 2018, Rui et al., 2010).

In Hg-resistant bacteria, the ability of the cell to supply MerA with NADPH places a larger demand on the NADPH-generating pathways and their response to this Hg-challenge is unknown. *In vivo* measurements of MerA enzymatic activity in aerobically growing *E. coli* cells at mid- and late-log growth indicated an average reduction rate of metallic mercury of 3.22 ±

2.62 x 10^6 Hg^0-atoms/min/cell and places a NADPH-demand of 3.22 ± 2.62 x 10^6 molecules/min/cell (Engst and Miller, 1998, Hamlett et al., 1992, Fox and Walsh, 1982, Summers et al., 1982, Summers and Lewis, 1973, Summers and Silver, 1972). NADPH steady state levels in unchallenged *E. coli* MG1655 aerobically growing in minimal medium with glucose were reported as 0.05 x 10^6 (Bennett et al., 2009) and 0.08 ± 0.2 10^6 (Fuhrer and Sauer, 2009) NADPH molecules per cell. Consequently, the available NADPH concentration does not suffice for successful detoxification. Thus, the work presented in this dissertation is to use global transcriptomics to identify changes in enzymes producing or consuming NADPH after Hg-exposure induces synthesis of MerA. To this end, we are comparing mercury exposure with and without mercury resistance to quantify transcriptional changes compared to unexposed cultures. This is also the only examination of how all genes of plasmid NR1 are expressed under unchallenged and Hg-challenged growth.

Objectives

There has been little research on the global transcriptional responses in any organism during recovery from mercury exposure. Our group has previously employed *Escherichia coli* strain MG1655 as the model organism for such studies because it has become the universal standard in *E. coli* 'omics work. We have long worked with the Hg resistance locus on plasmid NR1, a naturally and globally distributed large, conjugative IncFII plasmid carrying Tn*21* encoding the most thoroughly characterized *mer* operon. Moreover, the NR1 plasmid has extensive physiological, biochemical, and genetic information making it the definitive tool for identifying the global chromosomal- and plasmid-encoded effects of mercury exposure and

how the tools evolution has packaged into a mobile element assist the chromosomal genes to survive this toxicant.

My objectives in this dissertation have been to use a whole cell (aka global) approach to identify the transcriptional response to inorganic mercury exposure in a model prokaryote. The information from this study will illuminate how bacteria recover from exposure to toxic, but sub-lethal concentrations of inorganic mercury and what metabolic pathways adjust to supply NADPH to the mercuric reductase, MerA, to reduce and thereby detoxify it. My study will provide insight for future studies narrowing down the ideal systems to measure when Hg^{2+} intoxication is suspected and perhaps inform design of diets or pharmaceuticals optimized for removal of Hg^{2+} in organisms that lack a *mer* operon, such as in our own chromosomes. In chapter 2, I compared the transcriptional responses of *E. coli* with or without a *mer* resistance locus. To observe cells responding in real time to this toxicant, I first identified mercuric chloride concentrations that sharply diminished growth rate when applied during mid-log phase but allowed recovery of growth only in the Hg-resistant strain. Then for each experiment using carefully established growing cultures I took replicate samples just before adding Hg (time zero) and at 10, 30, 60, and 90 min after adding Hg. Such an experiment was repeated from 4 - 6 times (biological replicated) for each strain (plasmid-free and plasmid-carrying) and the three most statistically similar biological replicate were used for RNA isolation and RNA-seq analysis. The data for differential plasmid and chromosomal gene expression were analyzed by the conventional method of comparing the exposed cells to the non-exposed cells and then focused on the behavior of chromosomal genes known to produce or to consume NADPH or NADH. For linear expression of the plasmid genes, the read count of a given gene was plotted as a line

graph to describe changes in read abundance as expression changes over time in reference to growth rate recovery (OD_{595}) indicated by the growth curves.

In chapter 3, the transcriptional response of *E. coli* with and without *mer* resistance is considered for the 310 genes whose proteins were previously observed in proteomics experiments to be especially vulnerable to binding Hg or RHg. The primary conclusion is that one cannot infer in any simple way from a protein susceptibility for binding to Hg(II) in which direction its transcriptional profile will respond. However, several distinct patterns reveal that the mode of regulation of expression of some genes can affect its recovery trajectory.

The results presented in this dissertation are the most comprehensive view of how mercury exposure influences expression of chromosomal and plasmid genes responsible for recovery from mercury exposure in any organism to date. The strong conservation of several of these genes and pathways can inform development of diagnostic tools and therapeutic interventions for Hg exposure which remains surprisingly widespread in the developed world (Wiggins et al., 2018, Yin et al., 2016) and nearly universal in the developing world.

References

ADEDIRAN, G. A., LIEM-NGUYEN, V., SONG, Y., SCHAEFER, J. K., SKYLLBERG, U. & BJÖRN, E. 2019. Microbial biosynthesis of thiol compounds: implications for speciation, cellular uptake, and methylation of Hg (II). *Environmental science & technology,* 53**,** 8187-8196.

ANDREINI, C., BERTINI, I., CAVALLARO, G., HOLLIDAY, G. L. & THORNTON, J. M. 2008. Metal ions in biological catalysis: from enzyme databases to general principles. *JBIC Journal of Biological Inorganic Chemistry,* 13**,** 1205-1218.

BARKAY, T., KRITEE, K., BOYD, E. & GEESEY, G. 2010. A thermophilic bacterial origin and subsequent constraints by redox, light and salinity on the evolution of the microbial mercuric reductase. *Environmental Microbiology,* 12**,** 2904-2917.

BARKAY, T., MILLER, S. M. & SUMMERS, A. O. 2003. Bacterial mercury resistance from atoms to ecosystems. *FEMS microbiology reviews,* 27**,** 355-384.

BARNES, H. L. 1997. *Geochemistry of hydrothermal ore deposits*, John Wiley & Sons.

BEAUVAIS-FLÜCK, R., SLAVEYKOVA, V. I. & COSIO, C. 2016. Transcriptomic and physiological responses of the green microalga Chlamydomonas reinhardtii during short-term exposure to subnanomolar methylmercury concentrations. *Environmental science & technology,* 50**,** 7126-7134.

BENNETT, B. D., KIMBALL, E. H., GAO, M., OSTERHOUT, R., VAN DIEN, S. J. & RABINOWITZ, J. D. 2009. Absolute metabolite concentrations and implied enzyme active site occupancy in Escherichia coli. *Nature chemical biology,* 5**,** 593-599.

BRANCO, V. & CARVALHO, C. 2019. The thioredoxin system as a target for mercury compounds. *Biochimica et Biophysica Acta (BBA)-General Subjects,* 1863**,** 129255.

CHAMPIER, L., DUARTE, V., MICHAUD-SORET, I. & COVÈS, J. 2004. Characterization of the MerD protein from Ralstonia metallidurans CH34: a possible role in bacterial mercury resistance by switching off the induction of the mer operon. *Molecular microbiology,* 52**,** 1475-1485.

CHRISTAKIS, C. A., BARKAY, T. & BOYD, E. S. 2021. Expanded diversity and phylogeny of mer genes broadens mercury resistance paradigms and reveals an origin for MerA among thermophilic Archaea. *Frontiers in microbiology,* 12.

CHRISTODOULOU, D., LINK, H., FUHRER, T., KOCHANOWSKI, K., GEROSA, L. & SAUER, U. 2018. Reserve flux capacity in the pentose phosphate pathway enables Escherichia coli's rapid response to oxidative stress. *Cell systems,* 6**,** 569-578. e7.

CLARKSON, T. W. 2002. The three modern faces of mercury. *Environ Health Perspect,* 110 Suppl 1**,** 11-23.

CLARKSON, T. W. & MAGOS, L. 2006. The toxicology of mercury and its chemical compounds. *Critical reviews in toxicology,* 36**,** 609-662.

COLOMBO, M. J., HA, J., REINFELDER, J. R., BARKAY, T. & YEE, N. 2013. Anaerobic oxidation of Hg (0) and methylmercury formation by Desulfovibrio desulfuricans ND132. *Geochimica et Cosmochimica Acta,* 112**,** 166-177.

CÁRDENAS, C. S., GEREA, M., QUEIMALIÑOS, C., GUEVARA, S. R. & DIÉGUEZ, M. C. 2018. Inorganic mercury (Hg2+) accumulation in autotrophic and mixotrophic planktonic protists: Implications for Hg trophodynamics in ultraoligotrophic Andean Patagonian lakes. *Chemosphere,* 199**,** 223-231.

ENGST, S. & MILLER, S. M. 1998. Rapid reduction of Hg (II) by mercuric ion reductase does not require the conserved C-terminal cysteine pair using HgBr2 as the substrate. *Biochemistry,* 37**,** 11496-11507.

FOX, B. & WALSH, C. T. 1982. Mercuric reductase. Purification and characterization of a transposon-encoded flavoprotein containing an oxidation-reduction-active disulfide. *Journal of Biological Chemistry,* 257**,** 2498-2503.

FUHRER, T. & SAUER, U. 2009. Different biochemical mechanisms ensure network-wide balancing of reducing equivalents in microbial metabolism. *Journal of bacteriology,* 191**,** 2112-2121.

GENTÈS, S., TAUPIAC, J., COLIN, Y., ANDRÉ, J.-M. & GUYONEAUD, R. 2017. Bacterial periphytic communities related to mercury methylation within aquatic plant roots from a temperate freshwater lake (South-Western France). *Environmental Science and Pollution Research,* 24**,** 19223-19233.

GIONFRIDDO, C. M., TATE, M. T., WICK, R. R., SCHULTZ, M. B., ZEMLA, A., THELEN, M. P., SCHOFIELD, R., KRABBENHOFT, D. P., HOLT, K. E. & MOREAU, J. W. 2016. Microbial mercury methylation in Antarctic sea ice. *Nature microbiology,* 1**,** 1-12.

GRÉGOIRE, D., LAVOIE, N. & POULAIN, A. 2018. Heliobacteria reveal fermentation as a key pathway for mercury reduction in anoxic environments. *Environmental science & technology,* 52**,** 4145-4153.

GRÉGOIRE, D. S. & POULAIN, A. 2014. A little bit of light goes a long way: the role of phototrophs on mercury cycling. *Metallomics,* 6**,** 396-407.

GRÉGOIRE, D. S. & POULAIN, A. J. 2018. Shining light on recent advances in microbial mercury cycling. *Facets,* 3**,** 858-879.

HAMELIN, S., AMYOT, M., BARKAY, T., WANG, Y. & PLANAS, D. 2011. Methanogens: principal methylators of mercury in lake periphyton. *Environmental science & technology,* 45**,** 7693-7700.

HAMLETT, N., LANDALE, E., DAVIS, B. & SUMMERS, A. 1992. Roles of the Tn21 merT, merP, and merC gene products in mercury resistance and mercury binding. *Journal of bacteriology,* 174**,** 6377-6385.

HSU-KIM, H., KUCHARZYK, K. H., ZHANG, T. & DESHUSSES, M. A. 2013. Mechanisms regulating mercury bioavailability for methylating microorganisms in the aquatic environment: a critical review. *Environmental science & technology,* 47**,** 2441-2456.

HUANG, J., CHANG, F.-C., WANG, S., HAN, Y.-J., CASTRO, M., MILLER, E. & HOLSEN, T. M. 2013. Mercury wet deposition in the eastern United States: characteristics and scavenging ratios. *Environmental Science: Processes & Impacts,* 15**,** 2321-2328.

IANEVA, O. 2009. Mechanisms of bacteria resistance to heavy metals. *Mikrobiolohichnyi zhurnal (Kiev, Ukraine: 1993),* 71**,** 54-65.

JIN, Y. H., DUNLAP, P. E., MCBRIDE, S. J., AL-REFAI, H., BUSHEL, P. R. & FREEDMAN, J. H. 2008. Global transcriptome and deletome profiles of yeast exposed to transition metals. *PLoS genetics,* 4**,** e1000053.

KAWAKAMI, S. K., GLEDHILL, M. & ACHTERBERG, E. P. 2006. Production of phytochelatins and glutathione by marine phytoplankton in response to metal stress 1. *Journal of phycology,* 42**,** 975-989.

KELLY, D. J., BUDD, K. & LEFEBVRE, D. D. 2007. Biotransformation of mercury in pH-stat cultures of eukaryotic freshwater algae. *Archives of microbiology,* 187**,** 45-53.

KHOLODII, G., GORLENKO, Z., MINDLIN, S., HOBMAN, J. & NIKIFOROV, V. 2002. Tn5041-like transposons: molecular diversity, evolutionary relationships and distribution of distinct variants in environmental bacteriabbThe accession numbers for the nucleotide sequences reported in this work are given in the legends for Figs 1F1 and 2. ccA comparison of the sequence of INT5041C with other proteins is available as supplementary data on Microbiology Online (http://mic. sgmjournals. org). *Microbiology,* 148**,** 3569-3582.

KING, J. K., KOSTKA, J. E., FRISCHER, M. E. & SAUNDERS, F. M. 2000. Sulfate-reducing bacteria methylate mercury at variable rates in pure culture and in marine sediments. *Applied and environmental microbiology,* 66**,** 2430-2437.

KIYONO, M. & PAN-HOU, H. 1999. The merG gene product is involved in phenylmercury resistance in Pseudomonas strain K-62. *Journal of bacteriology,* 181**,** 726-730.

KIYONO, M., SONE, Y., NAKAMURA, R., PAN-HOU, H. & SAKABE, K. 2009. The MerE protein encoded by transposon Tn21 is a broad mercury transporter in Escherichia coli. *FEBS letters,* 583**,** 1127-1131.

KRUPP, E. M., MILNE, B. F., MESTROT, A., MEHARG, A. A. & FELDMANN, J. 2008. Investigation into mercury bound to biothiols: structural identification using ESI–ion-trap MS and introduction of a method for their HPLC separation with simultaneous detection by ICP-MS and ESI-MS. *Analytical and Bioanalytical Chemistry,* 390**,** 1753-1764.

KUSANO, T., JI, G., INOUE, C. & SILVER, S. 1990. Constitutive synthesis of a transport function encoded by the Thiobacillus ferrooxidans merC gene cloned in Escherichia coli. *Journal of bacteriology,* 172**,** 2688-2692.

LAVOIE, S. P., MAPOLELO, D. T., COWART, D. M., POLACCO, B. J., JOHNSON, M. K., SCOTT, R. A., MILLER, S. M. & SUMMERS, A. O. 2015. Organic and inorganic mercurials have distinct effects on cellular thiols, metal homeostasis, and Fe-binding proteins in Escherichia coli. *JBIC Journal of Biological Inorganic Chemistry,* 20**,** 1239-1251.

LAVOIE, S. P. & SUMMERS, A. O. 2018. Transcriptional responses of Escherichia coli during recovery from inorganic or organic mercury exposure. *BMC genomics,* 19**,** 1-24.

LEDWIDGE, R., PATEL, B., DONG, A., FIEDLER, D., FALKOWSKI, M., ZELIKOVA, J., SUMMERS, A. O., PAI, E. F. & MILLER, S. M. 2005. NmerA, the metal binding domain of mercuric ion reductase, removes Hg2+ from proteins, delivers it to the catalytic core, and protects cells under glutathione-depleted conditions. *Biochemistry,* 44**,** 11402-11416.

LIEBERT, C. A., HALL, R. M. & SUMMERS, A. O. 1999. Transposon Tn 21, flagship of the floating genome. *Microbiology and molecular biology reviews,* 63**,** 507-522.

LIEBERT, C. A., WIREMAN, J., SMITH, T. & SUMMERS, A. O. 1997. Phylogeny of mercury resistance (mer) operons of gram-negative bacteria isolated from the fecal flora of primates. *Applied and Environmental Microbiology,* 63**,** 1066-1076.

LIN, H., MORRELL-FALVEY, J. L., RAO, B., LIANG, L. & GU, B. 2014. Coupled mercury–cell sorption, reduction, and oxidation on methylmercury production by Geobacter sulfurreducens PCA. *Environmental science & technology,* 48**,** 11969-11976.

LIU, G., CAI, Y., O'DRISCOLL, N., FENG, X. & JIANG, G. 2012. Overview of mercury in the environment. *Environmental chemistry and toxicology of mercury***,** 1-12.

LIU, S. & WIATROWSKI, H. A. 2018. Reduction of Hg (II) to Hg (0) by biogenic magnetite from two magnetotactic bacteria. *Geomicrobiology Journal,* 35**,** 198-208.

LU, X., LIU, Y., JOHS, A., ZHAO, L., WANG, T., YANG, Z., LIN, H., ELIAS, D. A., PIERCE, E. M. & LIANG, L. 2016. Anaerobic mercury methylation and demethylation by Geobacter bemidjiensis Bem. *Environmental science & technology,* 50**,** 4366-4373.

LÁZARO, W. L., DÍEZ, S., DA SILVA, C. J., IGNÁCIO, Á. R. & GUIMARÃES, J. R. 2018. Seasonal changes in peryphytic microbial metabolism determining mercury methylation in a tropical wetland. *Science of the Total Environment,* 627**,** 1345-1352.

MASON, R. P., FITZGERALD, W. F. & MOREL, F. M. 1994. The biogeochemical cycling of elemental mercury: anthropogenic influences. *Geochimica et cosmochimica acta,* 58**,** 3191-3198.

MOREL, F. M., KRAEPIEL, A. M. & AMYOT, M. 1998. The chemical cycle and bioaccumulation of mercury. *Annual review of ecology and systematics,* 29**,** 543-566.

NATH, K. A., CROATT, A. J., LIKELY, S., BEHRENS, T. W. & WARDEN, D. 1996. Renal oxidant injury and oxidant response induced by mercury. *Kidney international,* 50**,** 1032-1043.

NIKEL, P. I., FUHRER, T., CHAVARRÍA, M., SÁNCHEZ-PASCUALA, A., SAUER, U. & DE LORENZO, V. 2021. Reconfiguration of metabolic fluxes in Pseudomonas putida as a response to sub-lethal oxidative stress. *The ISME journal,* 15**,** 1751-1766.

OLSEN, T. A., BRANDT, C. C. & BROOKS, S. C. 2016. Periphyton biofilms influence net methylmercury production in an industrially contaminated system. *Environmental Science & Technology,* 50**,** 10843-10850.

PAL, C., BENGTSSON-PALME, J., KRISTIANSSON, E. & LARSSON, D. J. 2015. Co-occurrence of resistance genes to antibiotics, biocides and metals reveals novel insights into their co-selection potential. *BMC genomics,* 16**,** 1-14.

PARKS, J. M., GUO, H., MOMANY, C., LIANG, L., MILLER, S. M., SUMMERS, A. O. & SMITH, J. C. 2009. Mechanism of Hg− C protonolysis in the organomercurial lyase MerB. *Journal of the American Chemical Society,* 131**,** 13278-13285.

PARKS, J. M., JOHS, A., PODAR, M., BRIDOU, R., HURT JR, R. A., SMITH, S. D., TOMANICEK, S. J., QIAN, Y., BROWN, S. D. & BRANDT, C. C. 2013. The genetic basis for bacterial mercury methylation. *Science,* 339**,** 1332-1335.

PITTS, K. E. & SUMMERS, A. O. 2002. The roles of thiols in the bacterial organomercurial lyase (MerB). *Biochemistry,* 41**,** 10287-10296.

POLACCO, B. J., PURVINE, S. O., ZINK, E. M., LAVOIE, S. P., LIPTON, M. S., SUMMERS, A. O. & MILLER, S. M. 2011. Discovering mercury protein modifications in whole proteomes using natural isotope distributions observed in liquid chromatography-tandem mass spectrometry. *Molecular & cellular proteomics,* 10.

RAO, Y., MCCOOEYE, M., WINDUST, A., BRAMANTI, E., D'ULIVO, A. & MESTER, Z. N. 2010. Mapping of selenium metabolic pathway in yeast by Liquid Chromatography− Orbitrap Mass Spectrometry. *Analytical chemistry,* 82**,** 8121-8130.

RICCARDI, D., GUO, H.-B., PARKS, J. M., GU, B., SUMMERS, A. O., MILLER, S. M., LIANG, L. & SMITH, J. C. 2013. Why mercury prefers soft ligands. *The Journal of Physical Chemistry Letters,* 4**,** 2317-2322.

RUI, B., SHEN, T., ZHOU, H., LIU, J., CHEN, J., PAN, X., LIU, H., WU, J., ZHENG, H. & SHI, Y. 2010. A systematic investigation of Escherichia coli central carbon metabolism in response to superoxide stress. *BMC systems biology,* 4**,** 1-12.

RYTUBA, J. Genozoic mittallgeny of California: Geology and Ore Deposits of the American Cordillera. Symposium Proceedings., 1996. 803-822.

RYTUBA, J. J. 2003. Mercury from mineral deposits and potential environmental impact. *Environmental Geology,* 43**,** 326-338.

SAHLMAN, L., WONG, W. & POWLOWSKI, J. 1997. A mercuric ion uptake role for the integral inner membrane protein, MerC, involved in bacterial mercuric ion resistance. *Journal of Biological Chemistry,* 272**,** 29518-29526.

SAUER, U., CANONACO, F., HERI, S., PERRENOUD, A. & FISCHER, E. 2004. The soluble and membrane-bound transhydrogenases UdhA and PntAB have divergent functions in NADPH metabolism of Escherichia coli. *Journal of Biological Chemistry,* 279**,** 6613-6619.

SAUPE, F. 1990. Geology of the Almadén mercury deposit, province of Ciudad Real, Spain. *Economic Geology,* 85**,** 482-510.

SCHAEFER, J. K., SZCZUKA, A. & MOREL, F. M. 2014. Effect of divalent metals on Hg (II) uptake and methylation by bacteria. *Environmental science & technology,* 48**,** 3007-3013.

SCHUÉ, M., DOVER, L. G., BESRA, G. S., PARKHILL, J. & BROWN, N. L. 2009. Sequence and analysis of a plasmid-encoded mercury resistance operon from Mycobacterium marinum identifies MerH, a new mercuric ion transporter. *Journal of bacteriology,* 191**,** 439-444.

SELIN, N. E., JACOB, D. J., PARK, R. J., YANTOSCA, R. M., STRODE, S., JAEGLÉ, L. & JAFFE, D. 2007. Chemical cycling and deposition of atmospheric mercury: Global constraints from observations. *Journal of Geophysical Research: Atmospheres,* 112.

SILVER, S. & HOBMAN, J. L. 2007. Mercury microbiology: resistance systems, environmental aspects, methylation, and human health. *Molecular microbiology of heavy metals.* Springer.

SMITH, T., PITTS, K., MCGARVEY, J. A. & SUMMERS, A. O. 1998. Bacterial oxidation of mercury metal vapor, Hg (0). *Applied and environmental microbiology,* 64**,** 1328-1332.

SONG, L., TENG, Q., PHILLIPS, R. S., BREWER, J. M. & SUMMERS, A. O. 2007. 19F-NMR reveals metal and operator-induced allostery in MerR. *Journal of molecular biology,* 371**,** 79-92.

STENZLER, B., HINZ, A., RUUSKANEN, M. & POULAIN, A. J. 2017. Ionic strength differentially affects the bioavailability of neutral and negatively charged inorganic Hg complexes. *Environmental Science & Technology,* 51**,** 9653-9662.

SUMMERS, A., KNIGHT-OLLIFF, L. & SLATER, C. 1982. Effect of catabolite repression on the mer operon. *Journal of bacteriology,* 149**,** 191-197.

SUMMERS, A. O. & LEWIS, E. 1973. Volatilization of mercuric chloride by mercury-resistant plasmid-bearing strains of Escherichia coli, Staphylococcus aureus, and Pseudomonas aeruginosa. *Journal of bacteriology,* 113**,** 1070-1072.

SUMMERS, A. O. & SILVER, S. 1972. Mercury resistance in a plasmid-bearing strain of Escherichia coli. *Journal of bacteriology,* 112**,** 1228-1236.

TRÜMPLER, S., LOHMANN, W., MEERMANN, B., BUSCHER, W., SPERLING, M. & KARST, U. 2009. Interaction of thimerosal with proteins—ethylmercuryadduct formation of human serum albumin and β-lactoglobulin A. *Metallomics,* 1**,** 87-91.

UNO, Y., KIYONO, M., TEZUKA, T. & PAN-HOU, H. 1997. Phenylmercury transport mediated by merT-merP genes of Pseudomonas K-62 plasmid pMR26. *Biological and Pharmaceutical Bulletin,* 20**,** 107-109.

VALKO, M., MORRIS, H. & CRONIN, M. 2005. Metals, toxicity and oxidative stress. *Current medicinal chemistry,* 12**,** 1161-1208.

WIGGINS, A. G., LAVOIE, S. P., WIREMAN, J. & SUMMERS, A. O. 2018. Thinking outside the (pill) box: Does toxic metal exposure thwart antibiotic stewardship best practices? *Plasmid,* 99**,** 68-71.

WILSON, J. R., LEANG, C., MORBY, A. P., HOBMAN, J. L. & BROWN, N. L. 2000. MerF is a mercury transport protein: different structures but a common mechanism for mercuric ion transporters? *FEBS letters,* 472**,** 78-82.

YIN, L., YU, K., LIN, S., SONG, X. & YU, X. 2016. Associations of blood mercury, inorganic mercury, methyl mercury and bisphenol A with dental surface restorations in the US population, NHANES 2003–2004 and 2010–2012. *Ecotoxicology and Environmental Safety,* 134**,** 213-225.

YU, R.-Q., FLANDERS, J., MACK, E. E., TURNER, R., MIRZA, M. B. & BARKAY, T. 2012. Contribution of coexisting sulfate and iron reducing bacteria to methylmercury production in freshwater river sediments. *Environmental science & technology,* 46**,** 2684-2691.

ZHANG, J., WANG, F., HOUSE, J. D. & PAGE, B. 2004. Thiols in wetland interstitial waters and their role in mercury and methylmercury speciation. *Limnology and Oceanography,* 49**,** 2276-2286.

CHAPTER 2

THE COST TO *ESCHERICHIA COLI* IN CARRYING THE NR1 PLASMID AND THE BENEFIT PROVIDED BY THE MERCURY RESISTANCE OPERON WHEN RECOVERING FROM MERCURY EXPOSURE

[1]WIGGINS, A.G., SUMMERS, A.O.; To be submitted to *Metallomics*.

Abstract

Mercury (Hg) is a persistent global pollutant and exposure to its compounds results in a variety of toxic effects. The World Health Organization has adopted the Minamata Treaty advocating discontinuing Hg use. Concern for identifying Hg's various syndromes and assisting in their remediation motivates our research into the effects Hg has at the molecular level to cellular processes and their recovery. Prokaryotes have evolved a mercury (*mer*) resistance operon carried on plasmids and transposons. Detoxification involves reducing reactive, ionic Hg(II) to relatively inert Hg(0) vapor. Mercuric reductase uses NADPH as a reductant, which is at insufficient levels prior to Hg exposure. Here we use RNA-seq in a model organism, *Escherichia coli*, to discover how the cell rapidly supplies large amounts of NADPH after Hg exposure. Since these resistance genes are commonly carried on plasmids, there is also a cost to the cell in maintaining its replicon. This study is the first transcriptional study of a natural plasmid-encoded resistance system analyzing the "upkeep" costs and "payback" when its cellular host is exposed to the toxicant. Upon Hg exposure, the *mer* operon genes were strongly expressed, but expression of only a few other plasmid genes increased and many decreased. When directly comparing the expression of chromosomal genes of Hg-resistant (HgR) to Hg-sensitive (HgS) strains in the absence of Hg exposure, I found essentially no genes were being expressed differentially. Hg(II) provoked rapid significant differential (up and down) expression of many chromosomal genes in the HgS most of which barely returned to levels of the unexposed control during the 90-minute post-exposure. In contrast, the strain with mercury resistance made similar rapid changes in the same genes, but recovered almost normal, unexposed levels of expression sooner. A key NADPH-producing TCA cycle enzyme, isocitrate dehydrogenase

(*icd*), increased its mRNA expression by 30% under Hg exposure. Due to ICD's high copy number and k_{cat} rate, the mere 30% increase would be sufficient to allow the mercuric reductase to rapidly dispatch 4 µM Hg(II). Thus, the plasmid and *mer* resistance places only trivial, transient burden on the cell in the absence or presence of mercury.

Introduction

The chemical versatility of mercury (Hg) and its compounds have been exploited by humans since antiquity. Natural sources of Hg in the form of cinnabar (HgS) ore, have been mined since the Neolithic era making Hg one of the great seven metals of antiquity (Goren et al., 2001, Farrar and Williams, 1977). As a Group 12 element, life has evolved to utilize zinc as an essential trace mineral for numerous cellular process (Frassinetti et al., 2006), yet cadmium and mercury have no known biological role and are toxic at minute concentrations (Xu and Imlay, 2012).

In modern times, industrial and medical uses of Hg is being phased down. In 2015, the World Health Organization adopted a treaty to eliminate the use of Hg. Dental restorations are currently the primary source of non-occupational Hg exposure (Yin et al., 2021, Joy and Qureshi, 2020, Bjørklund et al., 2018). Unfortunately, apart from the European Union and Japan, actual implementation has been desultory (Zhongming et al., 2013), especially in the US where Hg still accounts for ~ 50% of all dental restorations (Yin et al., 2021). Given that amalgams have been used for decades by most US dentists, there are millions of US residents with amalgam fillings, and their replacement for a more benign material is not covered by dental health insurance. Additionally, amalgams remain the default restoration for all active

and retired military and their families, and intervention for indigenous people on reservations. A positive sign is that the major US amalgam manufacturers are discontinuing production and sale of this product (Sirona, 2020).

As the developed world begins to step away from the use of dental amalgams, the developing world in the global south expand very dangerous artisanal gold mining. The extraction of gold uses liquid Hg as a lixiviant to dissolve pure placer gold particles from low value ores in deposits. These practices are carried out in countries ranging from Amazonia to the African mid-continent and far south (Veiga et al., 2006, Malm, 1998). There is essentially no control of this practice in any country. The process emits toxic mercury vapor, and its unregulated waste is contaminating soil and freshwater resources over thousands of square miles. Unregulated emissions are compromising the health of the impoverished miners and their families as well as the surrounding ecosystems, which have already been exploited by deforestation for production of grain and animal protein.

Human toxicity varies depending on the dose and rate of exposure to a given Hg compound (Bernhoft, 2012). There is no demonstrated non-toxic level of Hg(II) exposure at the cellular level (LaVoie et al., 2015, Bernhoft, 2012). With this in mind, *in vivo* bacterial cultures without mercury resistance can slowly recover some semblance of normal growth after exposure to low levels of Hg (LaVoie and Summers, 2018). However in both environmental and commensal anaerobic niches, bacteria methylate Hg resulting in it being “bioaccumulated up the food chain” into higher organisms (Barkay et al., 2003, Council, 2000). The molecular details of this phenomenon and the physiological sequelae of residual Hg in, for example, fish muscle are undefined (Zheng et al., 2019). For bacteria, Hg(0) volatilization is a fast, cheap, and easy

way to rid themselves of reactive Hg(II). Although mercury resistance enzymes, MerA and MerB, have been expressed in plants (Meagher et al., 1999), to remediate transfer of Hg(II) and RHg compounds from soil and water, this is not possible in animals. In animals, Hg and other toxic metals are slowly eliminated by sequestering them on small cysteine-rich proteins called metallothionines that are also part of homeostasis systems for essential metals including zinc and copper. In the interests of finding ways to support and perhaps enhance Hg(II) and RHg(I) detoxification by multicellular organisms such as humans, we began by examining what chromosomal genes a simple bacterium uses to recover normal growth after a bolus exposure to inorganic or organic Hg (LaVoie, 2015).

Prokaryotes exposed to higher levels of environmentally common Hg concentrations use their normal repertoire of housekeeping genes, or an evolved mobile set of resistance genes in the mercury (*mer*) operon (Barkay et al., 2003). The *mer* proteins exploit Hg(II)'s high affinity for thiol to readily sequester and transport it into the cytoplasm for enzymatic reduction, by the mercuric reductase. (Barkay et al., 2003). Enzymatic reduction by MerA volatilizes Hg at a rate of $3.22 \pm 2.62 \times 10^6$ atoms/min/cell, and requires the same number of NADPH-molecules/min/cell (Engst and Miller, 1998, Hamlett et al., 1992, Fox and Walsh, 1983, Summers et al., 1982, Summers and Lewis, 1973, Summers and Silver, 1972). Steady state levels of NADPH are insufficient (Bennett et al., 2009, Fuhrer and Sauer, 2009), and normal production is ~60% of the required amount for growth (Sauer et al., 2004). The deficiency is balanced by two transhydrogenase (Chou et al., 2015). The oxidative stress response, which is caused by Hg exposure, could indirectly up-regulate production of NADPH by enzymes associated with central carbon metabolism by rerouting glycolytic flux towards the pentose

phosphate pathway and balancing the overproduction via the activity of the transhydrogenases (Nikel et al., 2021, Christodoulou et al., 2018, Ahn et al., 2016, Rui et al., 2010).

In the work presented here, I applied RNA-Seq to $HgCl_2$-challenged cells to monitor the global transcriptional response as *E. coli* MG1655 cells (HgS) and *E. coli* MG1655 carrying plasmid-born *mer* resistance (HgR) recovered from Hg(II) exposure (Fig. 2.1). This is also the first report of how all the NR1 plasmid genes are expressed under normal and $HgCl_2$-challenged conditions. My aim here is first to assess the metabolic burden of simply carrying the NR1 plasmid, so I have compared the transcriptomes of HgR cultures and HgS cultures in the absence of Hg challenge. Secondly, I have described the response of all plasmid genes under Hg exposure. Thirdly, I have assessed the metabolic benefit of having the *mer* operon during Hg(II) exposure by (a) comparing transcriptional changes during Hg(II) exposure of HgR or HgS cultures compared to their respective unchallenged cultures and (b) directly comparing the global transcriptional changes of HgR cultures vs. HgS cultures at the same level of Hg(II) exposure (Fig. 2.2). My hypotheses regarding carriage of the plasmid were that: (1) since HgR and HgS cultures have nearly identical growth curves in the absence of $HgCl_2$-challenge, there will be very little change in chromosomal genes due to maintaining the plasmid and, (2) minimal plasmid genes will be differentially expressed in Hg(II) exposure, except genes of the *mer* operon. My hypotheses regarding chromosomal gene expression were that: (3) during $HgCl_2$-challenge, expression of genes for NAD(P)H production will be higher in HgR cultures to supply MerA with NADPH, and (4) initially both HgR and HgS cultures increase expression of stress repair genes, decrease expression of genes for normal cell growth, and HgR cultures will

recover expression of genes for normal cell growth while declining in stress response gene sooner than the HgS cultures.

As noted in previous proteomic (LaVoie 2015) and transcriptomic (LaVoie, 2018) studies, the mercury-damaged proteins and their genes that are responding to Hg are of direct relevance to Hg exposure in humans and other higher animals. Many of the proteins and metabolic pathways affected by Hg compounds in *E. coli* are highly conserved, especially in the human mitochondrion, an organelle whose malfunctioning is implicated in disorders ranging from autism to cancer. Enhancing basic knowledge of Hg's effects in the most vulnerable proteins and pathways we share can facilitate design of nutritional or pharmaceutical interventions for those chronically exposed iatrogenically (e.g., dental amalgam fillings) or occupationally (electronics recycling, artisanal gold mining). Moreover, because the bacteria themselves affect our health as members of our commensal microbiota, their response to Hg exposure by any of the above routes is also of relevance. For example, reduction of ionic Hg(II) by intestinal bacteria to Hg(0) makes it more membrane permeant, potentially fostering enterohepatic recycling (Sangvanich et al., 2014).

Methods

Bacterial strain and plasmid

Escherichia coli strain MG1655 (Blattner et al., 1997) without (MG) or with the NR1 plasmid MG(NR) that encodes mercury resistance (Williams et al., 2006) were removed from cryostorage onto Luria-Bertani (LB) agar containing 25 µg/ml chloramphenicol and incubated at 37°C overnight. Then a half-dozen well isolated colonies of each strain were inoculated into 20

ml starter cultures of Neidhardt MOPS Minimal Medium (NM3) (Neidhardt et al., 1974) containing 2 g/L glucose, 20 mg/L uracil, and 500 µg/L thiamine, which was incubated at 37°C with agitation at 250 rpm overnight (~18 hrs).

Optimizing culture conditions to distinguish the contribution of the mer locus

Mercuric ion exposure conditions were chosen to observe recovery of a culture from Hg-exposure for one 90-minute growth period in a strain without the *mer* locus, MG, or the same strain with the *mer locus* MG(NR). We found in NM3 medium that 3 µM mercuric chloride ($HgCl_2$) restricted growth in both MG and NR compared to their respective unexposed control conditions. In addition, the *mer* operon, allowed growth to resume equivalent to the unexposed cells (i.e., recovery) by 30 min, whereas MG recovered growth equivalent to the unexposed cells by 90 min. Here, we refer to 3 µM $HgCl_2$ as sub-acute exposure (Figure 2.3). We also found that 4 µM Hg restrained growth for both strains but allowed the growth rate of MG(NR) to match that of its unexposed culture by 90 min; however, MG did not resume a normal growth rate during the 90-minute window. We refer to 4 µM Hg as acute Hg exposure (Fig. 2.3).

mRNA extraction

For each biological replicate (Fig. 2.2), an overnight starter culture was diluted 1:30 into Neidhardt MOPs minimal medium (N3M) making a total volume of 350 mL, thoroughly mixed, and 100 ml of each diluted culture was dispensed into each of three 500 ml flasks. Each flask was incubated at 37°C with 250 rpm aeration. As the cultures reached an OD_{595} of 0.40 (~200

min), each was exposed to the indicated $HgCl_2$ concentration of 0 $HgCl_2$ µM, 3 $HgCl_2$ µM or 4 $HgCl_2$ µM Hg with a fresh 1 mM stock of $HgCl_2$ (Alfa Aesar) in ultra-pure Milli-Q water (MilliporeSigma). Thereafter, 1 ml aliquots of each culture were collected at 0 min (0 µM $HgCl_2$ only) and 10, 30, 60, and 90 min after Hg exposure. Aliquots were immediately centrifuged at 20,800 *x g* for 3 min at 4°C. Spent medium was aspirated and the cell pellets were immediately frozen (<3 min) at -70°C. Six biological replicates for each condition were prepared following this protocol. The three biological replicates with the lowest variance between optical density measurements during the Hg exposure period (range 0.00008 – 0.00049 for all time points) were used to isolate total RNA for mRNA extraction.

Purification of mRNA

A single cell pellet for each condition and sampling time point was thawed on ice for each of three biological replicates. Total RNA was isolated by RNA*snap™* (Stead et al., 2012). The supernatant was immediately extracted with acidic phenol:chloroform (Ambion pH 4.5) and the aqueous phase transferred to a fresh microcentrifuge tube for ethanol precipitation with 3M sodium acetate (Ambion pH 5.5). The precipitate of each aliquot was then reconstituted in 50 µl of RNase-free water for 30 min on ice at 4°C. Trace DNA was digested with one treatment with Turbo-DNase (Ambion; Life Technologies). Total RNA concentrations and A_{260}/A_{280} ratios were determined using a Nanodrop™ 1000 spectrophotometer (Thermo Scientific) and stored at -70°C.

Library preparation and Illumina sequencing

Total RNA preparations were depleted of ribosomal RNA with the Ribo-Zero rRNA kit for Gram-negative bacteria (Epicentre) by the Georgia Genomics and Bioinformatics Core facility (GGBC, https://dna.uga.edu) who also assessed the quality and quantity of rRNA-depleted RNA using a 2100 Bioanalyzer RNA pico chip (Agilent Technologies) per manufacture's recommendations. Next-generation sequencings (NGS) libraries were prepared with the Kapa Biosystems NGS stranded library preparation kit for RNA-Seq with dual indexed iTru adapters developed by GGBC (Glenn et al., 2016). The average library insert size was 276 bp as determined by the high-sensitivity NGS fragment analysis kit for Fragment Analyzer™ (Advanced Analytical Technologies) using manufacture's recommendations (GGBC, personal communication). Quantification of each library was done with Qubit® 2.0 fluorometer (Life Technologies) and all 78 libraries were pooled in equal concentrations by GGBC. Paired-end (2 x 75 bp) sequencing of the pooled libraries with the Illumina Next Seq 2500 platform was performed by GGBC. Raw sequence data for each library was uploaded to NCBI Gene Expression Omnibus database (http://www.ncbi.nlm.nih.gov/geo/) with dataset ID: To Be Determined.

Data processing and differential expression analysis

Quality control processing of sequence data was performed with a local Galaxy instance using a customized Galaxy workflow created from various tools in the Galaxy Toolshed (https://toolshed.g2.bx.psu.edu/) (Appendix A, Table A1). The raw read quality and presence of adapter sequences were assessed by FastQC (Galaxy v0.52). Low quality reads (≤ Q20) and poly-

G sequences (n > 10) were removed, then read quality was improved with a sliding window step size of 4 with a mean quality score ≥ 20 by *fastp* (Galaxy v0.19.5)(Chen et al., 2018). Forward- and reverse-read mate pairs were assembled and aligned to *E. coli* K-12 MG1655 (U00096.3) and plasmid NR1 (NC_009133.1) using Bowtie2 (Galaxy 0.6)(Langmead and Salzberg, 2012). The resulting BAM alignments were tabulated by the HTSeq-count program with intersection non-empty mode (Galaxy v0.9.1)(Anders et al., 2015). Mapped read-counts were analyzed for significant differential expression (**standard criteria**: false discovery rate ≥ 0.01 and $\log_2$-fold ≥ ±1 and **relaxed criteria**: false discovery rate ≥ 0.01 and $\log_2$-fold ≥ ±0.50) using DESeq2 (v1.30.1)(Love et al., 2014) package in R. Within DESeq2, pairwise comparisons were made for determination of significant differentially expressed genes (DEGs) for all three biological replicates for a given (1) $HgCl_2$-challenged time point (**traditional DEG:** HgS or HgR) versus the unexposed control time point and (2) the HgR time point versus HgS time point (**direct DEG:** HgR vs. HgS) (Fig. 2.2).

COG analysis

The Clusters of Orthologous Genes (COGs) database is a useful tool for functional annotation and provides a consistent classification of proteins based on orthologous groups (Galperin et al., 2021). All chromosomal DEGs were classified based on the 2020 COG annotation for *Escherichia coli* MG1655 (http://www.ncbi.nlm.nih.gov/COG/). The significance of difference for HgS and HgR values between each COG categories at a given condition and time point was performed by Mann-Whitney U test and given a *p*-value less than 0.05 for statistical significance.

Results

Transcriptomic benchmarks

Paired-end libraries averaged over 22 million reads in both HgS and HgR cultures (Appendix, Table A.S1). Quality of the sequence data was high requiring minimal processing (<1%) of raw reads (Appendix, Table A.S1, A). Of the high-quality reads, on average 95% of reads mapped to the chromosome and a range of 1.5% to 6% for the plasmid, of the mapped reads 95% of chromosomal and 2.5% of plasmid reads properly paired, and of properly paired reads, 88% and 71% matched an annotated feature on the chromosome and plasmid.

Annotated features for rRNA averaged 0.77% for HgS libraries and 1.00% of HgR libraries indicating the effectiveness of the Ribo-Zero™ rRNA removal (Appendix Table A.S1). In unexposed cultures, non-coding RNAs (ncRNAs) were 6.29% of total reads in HgS libraries and 5.65% of total reads in HgR libraries; these percentages increased during Hg exposure and more so in the HgS libraries. In the unexposed conditions, tmRNA (*ssrA*) responsible for rescuing stalled ribosomes was 6.30% of total reads in HgS libraries and 6.16% in HgR libraries. The *ssrA* percentage increased with Hg exposure, slightly more so for the HgS strain, but was never differentially expressed for any time point comparison at our standard criteria (criteria defined in Materials and Methods section). Pseudogenes were ~0.5% or less of total reads for all conditions. In all conditions, tRNA's were less than 1.0% of total reads because the library preparation method excludes small RNAs (> 100 bp). Thus, we removed read counts for all annotated tRNA and rRNA from the subsequent differential expression analysis performed by DESeq2.

Effects of $HgCl_2$ on Growth

Our lab had previously used longitudinal RNA-Seq to compare significantly changed chromosomal genes in *E. coli* MG1655 lacking a *mer* operon as it recovers from sub-acute (3 µM) exposure to inorganic mercury ($HgCl_2$) versus organic mercury (phenylmercury acetate, PMA) compounds (LaVoie and Summers, 2018). Here my focus is just on exposure to inorganic mercury because plasmid NR1 carries a "narrow spectrum" Hg resistance locus based on only MerA. It lacks MerB, the organomercurial lyase necessary for having "broad spectrum" Hg resistance. Thus, I ask how *E. coli* MG1655 chromosomal gene expression differs as it recovers from exposure to 3 µM Hg or 4 µM Hg concentrations with or without a plasmid conferring narrow spectrum HgR. As noted above, I also consider the response of all genes encoded by NR1. Since this plasmid is well-studied biochemically and genetically, I will first consider the transcriptional response of genes located on the plasmid as they change after exposure to sub-3 µM Hg or 4 µM Hg. My two key questions regarding the plasmid were: under standard criteria for a DEG (1) to what degree are plasmid genes differentially expressed compared to the unexposed culture, and (2) in what order do plasmid genes return to their normal levels of expression after a bolus challenge of Hg(II). Similar questions of the quality and quantity and the temporal course of the chromosomal "recovery proteome" will be taken up when we consider chromosomal genes of the HgS plasmid-free and HgR plasmid-bearing strains.

As detailed in the Methods and depicted in Figure 2.3, this study is a continuation of our transcriptomics study of sub-acute $HgCl_2$ in the same HgS strain, *E. coli* MG1655. At 3 µM Hg, growth is arrested in both HgS and HgR cultures, but is recovered within 90 min. Here, I also challenged *E. coli* more severely with a 4 µM Hg, that prevented recovery in the HgS strain for

90 min. Surprisingly, as little as a ~30% increase in the Hg(II) concentration was enough to require the *mer* operon for recovery. The absolute concentration of Hg involved here likely reflects the concentration of nucleophilic ligands in the medium and the cells under these experimental conditions. Results would be different in a rich medium or if adding this amount of mercuric chloride at a lower cell concentration. Indeed, when I challenged cultures in NM3 medium at mid-exponential growth with 5 - 10µM Hg restoration of growth was prevented for both HgS and HgR strains. When using less than 3 µM Hg growth arrest did not occur.

Attenuation of the mer operon

Expression of the Tn*21 mer* operon exhibits sharp natural polarity within the transcript. In the initial transcriptional analysis of the *mer* operon using Northern blotting (Gambill and Summers, 1992), a 5-fold mid-operon decrease in the mRNA signal occurred approximately at the junction of *merC* and *merA*. The abundance of paired-end reads for *mer* genes, also shows this difference in the *mer* operon (Fig. 2.4). For both Hg concentrations, the 10-minute time point had a 2.2-fold difference in read abundance at/near the junction of *merC* and *merA* in 3 µM Hg and a 2.9-fold difference in 4 µM Hg. This drop in the read coverage profile persisted at 30 min as a 1.6-fold difference at 3 µM or 2.0 at 4 µM Hg (Table 2.3, Fig. 2.4). By 60 and 90 min, the drop-off in expression was ~1.5-fold (Table A.S2, Fig. 2.4). In the original work, no obvious sequence structures were identified as agents of natural polarity within the operon, but with the advantage of this refined resolution and 30 years of research on mid-transcript regulation we will be revisiting this question.

With the *mer* operon as an example of the temporal response to a dose of Hg, I could examine whether any other plasmid-borne genes exhibited a similar temporal response to this challenge. Simple line graphs for each *mer* gene depict the reads/gene length at each time point for the repressor-activator, *merR,* and each of the *merTPCADE* structural gene transcripts from their divergent overlapping promoters (Fig. 2.5) (Barkay et al., 2003, Caguiat et al., 1999, Park et al., 1992, Ross et al., 1989). Although the copy number of reads differs from the 5'- to the 3'-ends of the structural gene transcript (Fig. 2.4), each transcript abundance follows a similar trajectory over all time points. In 3 µM and 4 µM Hg, each segment of the *mer* structural gene transcript peaks at 10 min and all sharply decrease by 30 min and continue to decline at 60 and 90 min (Fig. 2.4A). The divergent *merR* mRNA has a low abundance that is little changed throughout all time points as expected for a regulatory gene (Fig. 2.4). A strong correlation of coverage appears within the promoter-proximal- and promoter-distal-ends of the *mer* transcript (Table A.S3A, Table A.S4A) on either side of the *merC-merA* junction*,* consistent with the previously reported mid-operon drop-off observed by Northern analysis (Gambill and Summers, 1992). We have suggested (Barkay, 2003) that as a flavin disulfide oxidoreductase, MerA generates reactive oxygen species in the absence of its normal substrate and the strong natural polarity within the operon may have evolved to limit over-expression of MerA.

Differential expression of NR1 plasmid genes

To quantify differentially expressed genes (DEGs) of the NR1 plasmid, I compared the Hg-challenged HgR strain to the non-challenged HgR strain at the same time point (criteria defined in Materials and Methods section). Fifty of NR1's 114 plasmid genes were not

differentially expressed when challenged with Hg (Fig. 2.6). However, the other 64 non-*mer* plasmid genes did change - up or down - in synchrony with the *mer* genes. The *mer* locus is one of three important components in the 19-kb Class II replicative transposon, Tn*21*. The second is Tn21's own set of mobility genes including a transposase (*tnpA*), a resolvase (*tnpR*), and a regulatory gene (*tnpM*) that increases *tnpA* and its own expression (Liebert et al., 1999). In response to 3 µM Hg, only *tnpA* and *tnpM* were up-regulated until 10 min; in 4 µM Hg all three genes were down-regulated at 10 and 30 min but were not differentially expressed by 60 and 90 min (Fig. 2.7). So, Hg exposure may promote Tn*21* spread by transposition to other replicons in the same cell; this could have important medical implications, given the third important element of Tn*21*.

The third important element in Tn*21* is a class 1 integron (In2) that accounts for over half of its total length (11 Kbp), but cannot transpose itself due to having only vestigial transposition (*tni*) genes (Liebert et al., 1999). In2 itself contains three distinct regions: (1) the 5'-conserved region consisting of the integrase (*intI1*) and an aminoglycoside adenylytransferase (*aadA1*) conferring streptomycin resistance, (2) the 3'-conserved region containing three ORFs for a truncated quaternary ammonium efflux pump (*qacEΔ1*) conferring disinfectant resistance, and the sulfonamide-resistance "cassette" dihydropteroate synthase (*sul1*), and (3) the vestigial integron transposition module (*tniA* and *tniBΔ1*)(Liebert et al., 1999, Brown et al., 1996). In2's *tni* genes are modestly up-regulated at 10 and 30 min after 3 µM Hg but only *tniA* is up-regulated at 30 min in 4 µM Hg (Fig. 2.7). Expression of the gene-capturing integrase enzyme *intI1* declines through 30 min in 4 µM Hg and the hallmark resistance cassette

aadA1 is not differentially expressed (Fig. 2.7). In the 3'-conserved region, expression of the sulfadiazine resistance cassette *sul1* declines through 30 min in 4 μM Hg (Fig. 2.7).

The NR1 plasmid also includes the original example of the Tn*9* transposon encoding a chloramphenicol acetyltransferase (*cat*) resistance gene and the separate Tn*10* transposon encoding the *tetAB* operon for tetracycline resistance (Partridge and Hall, 2004, Liebert et al., 1997). Upon Hg-challenge, *cat* is down-regulated at 10 min (Fig. 2.7). Likewise, all tetracycline resistance genes (*tetRBCD*) are down-regulated at 10 min and further down-regulated, except *tetD*, to 30 min in 4 μM Hg. Overall, in the domain of antibiotic resistance and mobilization loci Hg exposure tends to turn down their normal constitutive expression.

Other well-defined components of the NR1 plasmid are genes for self-transmissibility (*tra* and *trb*), plasmid stability (*stb*), plasmid SOS inhibitor (*psi*), autonomous replication (*rep*), and toxin-antitoxin systems. Early during $HgCl_2$-challenge, only 1 of 31 self-transmission genes (*traX*) up-regulated at 10 min (Fig. 2.7). At later timepoints, self-transmission genes down-regulated. In 3 μM Hg, down-regulation was sporadic for *traY* at 30 min, *traB* at 60 min, and *traC* at 90 min (Fig. 2.7). In 4 μM Hg, down-regulation occurred in *traY* and *traB* at 60 min and in 8 genes (*traYALKBDVC)* at 90 min (Fig. 2.7). The plasmid stability gene responsible for plasmid partitioning (*stbB*) down-regulated at 10 min in 3 μM Hg but delayed down-regulation until 30 min in 4 μM Hg 30 (Fig. 2.7). The plasmid segregation protein (*stbA*) was not differentially expressed in 3 μM Hg but up-regulated at 10 min in 4 μM Hg (Fig. 2.7). Both plasmid SOS inhibitor proteins (*psiAB*) up-regulated at 10 min and further up-regulated at 30 min for 4 μM Hg (Fig. 2.7).

The frequency of NR1 replication is controlled by the replication initiation protein (RepA1), whose synthesis is repressed by RepA2 which itself is controlled positively by a leader peptide (*tap*) (Wu et al., 1992). RepA1 down-regulated at 10 min after $HgCl_2$-challenge and further down-regulated to 30 min for 4 μM Hg (Fig. 2.7). Transcription of its repressor, RepA2, was not differentially expressed in 3 μM Hg but up-regulated at 10 m in 4 μM Hg (Fig. 2.7), consistent with down-regulation of the replication initiator. Again, overall NR1 on exposure to Hg lowers expression of its transfer and replication genes.

NR1 has two post-segregational killing systems: (1) *pemIK* and (2) *hok*/*sok* (Gerdes et al., 1997, Jensen and Gerdes, 1995). Only the *pemIK* system was differentially expressed. Upon $HgCl_2$-challenge, *pemI* up-regulated at 10 min in 3 μM Hg, but both *pemIK* up-regulated at 10 and 30 min in 4 μM Hg (Fig. 2.7). Although, generalizations about toxin-antitoxin systems must be made cautiously, the one non-*mer* system exhibiting Hg-provoked changes is acting to stabilize inheritance of NR1.

Lastly, the NR1 plasmid has 43 putative coding sequences annotated as hypothetical proteins. At 3 μM Hg, five of the hypothetical genes were up-regulated at 10 min and three down-regulated. At later time points, none of the hypothetical genes were differentially expressed (Fig. 2.6). In response to 4 μM Hg, two of the previously observed hypothetical genes were up-regulated with the addition of three new ones, and four of the previously observed genes were down-regulated with the addition of one new gene (Fig. 2.6). By 30 min, three of the observed genes being up-regulated at 10 min and an additional four new ones were up-regulated at 30 min (Fig. 2.6). Likewise, three of the observed genes being down-regulated at 10 min and an additional new gene were down-regulated at 30 min (Fig. 2.6). At later time

points, none of the hypothetical genes were differentially expressed (Fig. 2.6). For this group of unknown proteins, expression changes are modest, and short-lived.

Observed chromosomal DEGs in non-Hg-challenged cultures using the standard criteria

When comparing chromosomal gene expression in the unexposed condition between HgR cultures and HgS cultures (HgR $HgCl_2$ 0 µM vs. HgS $HgCl_2$ 0 µM) only one DEG using our standard criteria at 10 min occurred for the signal recognition 4.5s RNA (*ffs*) and was down-regulated (log_2 = -1.02) (criteria defined in Materials and Methods section). No other DEGs occurred at any other time point suggesting there is little, or no burden placed on cellular metabolism due to the presence of the plasmid and expression of its genes (Table 2.6A).

Observed chromosomal DEGs in $HgCl_2$-challenged cultures using the standard criteria

Given that the HgR cell culture recovered a normal growth rate sooner than HgS cell culture, I first describe the bulk changes of chromosomal genes using here a traditional and direct DEG comparison with standard criteria to look at the overarching recovery process between arrested growth and recovery (criteria defined in Materials and Methods section). At 10 min in 3 µM Hg, a direct comparison of HgR to HgS had a single DEG at 10 min (Table 2.6, F), indicating system-wide transcriptional responses of HgR and HgS cultures at 10 min were the same. Both HgR and HgS cultures resumed growth by 30 min (Fig. 2.3, green), but HgR cultures had recovered all but 270 genes compared to those expressed in the unexposed condition. HgS cultures present a very different picture, expressing 1172 genes in the exposed versus unexposed condition (Table 2.6, B – C). In other words, having the *mer* locus allows the cells to

express 77% fewer chromosomal genes during $HgCl_2$-challenge. By 60 min after Hg exposure, HgS and HgR strains had similar growth rates (Fig. 2.6, green), differing in only 123 DEGs (Table 2.6, F); the increase in DEGs at 90 min owes to the HgR culture's decreased rate as, having exhausted its nutrients, it begins stationary phase. (Fig. 2.6, green, dashed). Acute 4 μM Hg arrested growth of the HgR cells for 30 min (Fig. 2.3, orange, dashed) resulting in zero DEGs for the direct comparison at 10 min and only 67 DEGs at 30 min (Table 2.6 G), i.e., large-scale responses of the HgR and HgS strain were highly similar until 30 min. The HgR strain took 60 min to restart growth in 4 μM Hg, and the HgS cultures remained arrested managing just a 3.7% increase in optical density by 90 min (Fig. 2.3, orange, solid).

COG categories of DEGs observed

I organized a traditional DEG comparison based on our standard criteria by their Clusters of Orthologous Genes (COGs)(Table A.S5 – A.S8) to ask, "How and when does *Escherichia coli* recover specific functional groups with and without the help of the *mer* operon (criteria defined in Materials and Methods section) (Fig. 2.8 – 2.10)?" Of the 12 COG categories showing many DEGs at 10 min, COG category E, amino acids biosynthesis (panel A) has the most DEGs and COG category F, nucleotides biosynthesis, has the fewest DEGs under all four conditions (Fig. 2.8). It is noteworthy at this time point there is no significant difference in the number of DEGs for each strain. This complements the findings in the previous section where at 10 min the system-wide response to $HgCl_2$-challenge by direct DEG comparison was the same for HgR vs. HgS. In addition, the absolute sizes of each COG category are also indistinguishable and indicating each strain is simply responding to Hg, which is consistent with all strains for a given

condition had arrested growth (Fig. 2.3 green, orange, 10 min). Panel B reveals a common shape (densities) for the 12 COG categories in the HgS or HgR strains for their upward or downward responses in both the 3 µM Hg and 4 µM Hg. This is consistent with some uniformity in these "early responder" COG categories that are dealing with Hg, but cells have not yet recovered from the degree of damage. By 30 min (Fig. 2.9), there are 13 COGs visible with the addition of COG category V (defense mechanisms). In every COG category, the green bars for 3 µM Hg are strikingly different in size than the HgR (pale green) bar, which is consistently much smaller than the HgS (dark green) bar. HgR strain is behaving like the unexposed control – it has mostly accomplished recovery from Hg exposure. Panel B also shows this dramatic difference between dark and light fiddles for the HgR and HgS cultures. In sharp contrast at just 33% higher [$HgCl_2$], the orange bars and fiddles at 30 min look very much like they did at 10 min; both strains are still deploying the "early responders" and have turned up a small set of defense systems and turned down even fewer (Fig. 2.9, Table A.S6).

By 60 min (Fig. 2.10, Table A.S7), only 10 COG categories are shown with the greatest decrease in those confronting 4 µM Hg, which have dwindled to numbers quite like those appearing to respond to 3 µM Hg. These latter green bars are again very similar in length for both strains. However, about half of the orange bars show a much shorter pale bars (HgR) than dark orange bars. At 60 min, all 4 Hg conditions are biased towards increasing gene expression with the sole exception being COG category C (energy production), which is uniformly declining in expression and consistent with Hg being reduced (Fig. 2.10, Table A.S7). In Panel B, the 3 µM Hg fiddles are more compact and nearly identical in shape for up-regulated and down-regulated genes (Fig. 2.10, Table A.S7). In contrast, HgS at 4 µM Hg shows a much greater dispersion.

Lastly, at 90 min (Fig. 2.11, Table A.S8), only 6 COG categories are present. This is consistent with the resumption of normal growth in all conditions expect HgS at 4 μM Hg. Also, it is consistent for HgR at 3 μM Hg as it begins to transition into stationary phase like its non-exposed condition (Fig. 2.3).

Metabolic source increasing NADPH production

For reduction of Hg(II) to Hg^0, MerA uses NADPH (Barkay et al., 2003), but NADPH concentrations in *E. coli* prior to $HgCl_2$-challenge are insufficient to meet the demand of MerA. *In vivo* measurements of Hg(II) reduction by intact cells with plasmid encoded MerA (Table 2.11) determined a volatilization rate of 3.22 ± 2.62 x 10^6 Hg^0-atoms/min/cell, which places a demand of 3.22 ± 2.62 x 10^6 NADPH-molecules/min/cell (Engst and Miller, 1998, Hamlett et al., 1992, Fox and Walsh, 1983, Summers et al., 1982, Summers and Lewis, 1973, Summers and Silver, 1972). In non-stressed *E. coli,* available NADPH steady state measurements when aerobically growing in minimal media indicate a NADPH concentration of 0.05 x 10^6 (Bennett et al., 2009) and 0.08 ± 0.2 10^6 (Fuhrer and Sauer, 2009) molecules per cell (Table 2.12), which are not initially sufficient for detoxification of $HgCl_2$. Additionally, *E. coli* naturally functions in a NADPH deficit requiring 10.6 ± 0.2 mmol/g/h, but only produces 6.2 ± 1.5 mmol/g/h (Sauer et al., 2004). The deficit is balanced and maintained by two transhydrogenase: energy-dependent reduction of $NADP^+$ with NADH by PntAB and reoxidation of NADPH by SthA (Chou et al., 2015). However, changes in metabolic fluxes induced by oxidative stress could resolve this paradox. *E. coli* increases NADPH production while decreasing NADH production by rerouting glycolytic flux towards the pentose phosphate pathway and balancing the overproduction by increasing

expression of both transhydrogenases (Nikel et al., 2021, Christodoulou et al., 2018, Ahn et al., 2016, Rui et al., 2010). Thus, I hypothesize that under $HgCl_2$-challenge expression of one or more of these genes increases to supply MerA.

To find genes producing NAD(P)H that might be consistently, but more moderately increased or decreased, I used a traditional DEG comparisons with both standard criteria (FDR ≥ 0.01 and $\log_2$-fold ≥ ±1) and then relaxed criteria (FDR ≥ 0.01 and $\log_2$-fold ≥ ±0.50) for a less stringent threshold of up- and down-regulated genes (criteria defined in Materials and Methods section). Using the standard criteria for DEG revealed a consistent increase at 10 min of exposure to 4 µM Hg in the very abundant TCA cycle enzyme, isocitrate dehydrogenase (*icd*), a major source of NADPH. However, there was down-regulation at 4 µM Hg for *sthA* in HgS cultures only and *pntAB* at 3 µM Hg (Fig 2.11A). At 30 min, only *gnd* was down-regulated in HgS cultures at 4 µM Hg (Fig. 2.12A). This indicates that the $HgCl_2$-challenge was not eliciting a typical oxidative stress response for increases production of NADPH to supply MerA for detoxification.

To further explore NAD(P)H sources, I used the relaxed DEG criteria, and it tells a more complete picture of how NAD(P)H sources are responding to $HgCl_2$ exposure (Fig. 2.12B). For all 10-minute time points, *icd* is up-regulated and further up-regulate at 30 min in HgS cultures at 3 µM Hg (Fig. 2.12B), which further complements an early and positive response from *icd* to supply NADPH under $HgCl_2$-challenge. Key NADPH-producing genes (*zwf* and *gnd*) in the Pentose Phosphate pathway are not significantly changed at 10 min, but *gnd* is down-regulated at 30 min under 4 µM Hg exposure and further down-regulate at 60 min in HgS cultures. There was no indication that the oxidative branch of the Pentose Phosphate pathway was being

recruited for increased NADPH production early under $HgCl_2$-challenge. Both transhydrogenases was down regulated for HgS and HgR cultures at 10 min in 3 µM Hg and *pntAB* was further down-regulated at 30 min (Fig. 2.12B). At 4 µM Hg exposure, down-regulation in *pntAB* was delayed until 30 min for both HgS and HgR cultures where it returned to normal expression levels in HgR cultures but is further down-regulated at 60 and 90 min for HgS (Fig. 2.12B). Up-regulation occurred in *sthA*, but not until 60 min in all conditions, and it returned to normal expression levels in HgR cultures at 90 min in 3 µM Hg (Fig. 2.12B). This indicated both transhydrogenases elicited a negative response to $HgCl_2$-challenge until growth was restored. Another NADPH-producer in the TCA cycle *maeB* was up-regulated at 10 min in 4 µM Hg for HgS and HgR cultures but returned to normal expression levels by 30 min This indicates *maeB* was transcriptionally responding early during $HgCl_2$-challenge for increase production of NADPH.

The transcriptional profile in both HgR and HgS strains showed that *icd* and *maeB* elicit a positive response to increase NADPH during $HgCl_2$-challenge (Fig. 2.13 – 2.14). I revisited my quantitative approach using Pearson correlations of their line graphs as done with the *mer* operon to ask whether the temporal expression patterns of HgR and HgS strains correlate between and with one another at the same [$HgCl_2$]. In both $HgCl_2$-challenge conditions, *icd* sharply increased at 10 min (Fig. 2.13). In 3 µM Hg, the HgS strain continued to increase *icd*'s expression to 30 min until steadily decreasing through 90 min, but for HgR it steadily decreased to 90 min (Fig. 2.13 A - B). In 4 µM Hg, *icd* sharply decreased at 30 min before remaining relatively the same at 60 min, and then increasing again at 90 min for both HgR and HgS strains (Fig. 2.13 C - D). A strong correlation was observed between HgR and HgS in 3 µM Hg but was

not significant (Table A.S9 and A.S10). However, a very strong and significant correlation was seen in 4 µM Hg(Table A.S9 and A.S10). There were no similarities within exposure conditions for either HgR or HgS comparisons (Table A.S9 and A.S10). For *maeB*, a moderate increase occurred at 10 min in 3 µM Hg and a sharp increase at 4 µM Hg(Fig. 2.14 A – D). In 3 µM Hg, the HgS strain continued to increase expression to 30 min until steadily decreasing through 90 min, but for HgR it steadily decreased to 90 min (Fig. 2.13A – B). In 4 µM Hg, *maeb* sharply decreased at 30 min before remaining relatively the same at 60 min, and then increasing again at 90 min for both HgR and HgS strains (Fig. 2.13A – B). A strong correlation was observed between HgR and HgS in 3 µM Hg but was not significant (Table A.S10 and A.S11). However, a very strong and significant correlation occurred in 4 µM Hg (Table A.S10 and A.S11). There were no similarities within exposure conditions for either HgR or HgS comparisons (Table A.S10 and A.S11). Even though *icd* and *maeB* both initially increased in expression under $HgCl_2$-challenge, there was no correlation for the response between HgS and HgR in 3 µM Hg, but there is correlation between the two in 4 µM Hg. Additionally, there is no correlation between 3 µM Hg and 4 µM Hg conditions for either gene in either HgS or HgR strain.

Genes that respond to oxidative stress during $HgCl_2$-challenge

I used the standard criteria for a traditional DEG comparison to investigate genes involved in oxidative stress to determine if HgR was allowing for faster recovery from reactive oxygen species caused by $HgCl_2$ (criteria defined in Materials and Methods section). The thioredoxin (Trx) and glutaredoxin (Grx) systems are important as antioxidants for maintain cellular redox balance and providing electrons for thiol-dependent reactions, but both systems

are primary targets for mercury binding (Branco and Carvalho, 2019). However, the ability of MerA to remove the bis-coordinate Hg(II) ions will allow for recovery of both these systems (Ledwidge et al., 2005). The initial response to oxidative stress caused by $HgCl_2$ was identical in HgS and HgR cultures, except *katG* was not differentially expressed in HgR cultures at 3 µM Hg (Fig. 2.15). At 30 min for both $HgCl_2$-challenge conditions, HgR returned *trxB* to normal expression levels and *grxD* in 4 µM Hg(Fig. 2.15). Both *trxC* and *grxA* were up-regulated through 60 min, but response at later time points in the HgR strain was not elicited as strongly (Fig. 2.15).

E. coli encodes three H_2O_2-scavenging enzymes (*katG*, *katE*, and *ahpCF*), which are under the regulation of (Mishra and Imlay, 2012). Both *katG* and *ahpCF* are regulated by *oxyR*, which was not differentially expressed. KatE production increases in stationary phase and was not differentially expressed by HgS until later time points where it was down-regulated (Fig. 2.15); however, it was up-regulated at 30 min in 3 µM Hg for HgR before being down regulated at 60 min (Fig. 2.15). Both *katG* and *ahpCF* were activated by *oxyR* and both were initially up-regulated during $HgCl_2$-challenge, except in 3 µM Hg for HgR. Expression of *ahpCF* returned to normal in the HgR culture before it did in the HgS culture(Fig. 2.15), and expression of *katG* returned to normal by 90 min for HgR culture under 3 µM Hg exposure (Fig. 2.15). Additionally, the expression of the gene for the reactive oxygen scavenger, SodA, was activated by *soxRS*, which was up-regulated early, but *sodA* was delayed to 60 min, except in HgS in 4 µM Hg(Fig. 2.15). Overall, the HgR strain returned several oxidative stress scavengers to normal or down-regulated their expression earlier than HgS.

Discussion

The NR1 plasmid was originally isolated in *Proteus mirabilis* (and differs from widely used R100 (Barkay et al., 2003) by only 15 substitutions in 94 kb (Williams et al., 2006). Despite the potential benefits the NR1 plasmid provides *Escherichia coli* during mercury exposure, large plasmids have been assumed to exact a fitness cost that might slow its growth (Carroll and Wong, 2018, San Millan and MacLean, 2017). A putative fitness cost just of hosting a plasmid might manifest in differentially expressed chromosomal genes in the absence of $HgCl_2$-challenge. Initially, I observed that HgR and HgS cultures grew in a very similar manner in minimal medium (Fig. 2.3, blue). This result was corroborated when using the standard criteria for a DEG, which only identified a single gene being differentially expressed at 10 min and none at any other time point (Table 2.6). These results indicate that in *Escherichia coli* there were no chromosomal genes differentially expressed due to carriage of the NR1 plasmid.

This is the first study to describe the expression of all NR1 plasmid genes during $HgCl_2$-challenge. As I expected, the genes of the *mer* operon were highly expressed because MerR traps RNA polymerase permanently at the structural gene promoter so it is always ready to go (Barkay et al., 2003). During $HgCl_2$-challenge, all of the transposon-borne antibiotic resistant genes in the transposon Tn*9* (chloramphenicol) and Tn*10* (tetracycline) were down-regulated and their corresponding transposases ere down-regulated or not changed.

Bulk transcriptional response of chromosomal genes

The bulk response of chromosomal genes at 3 µM Hg of the HgR strain recovered faster than the similarly exposed HgS strain did not recover from 4 µM Hg during 90 min. These

expression differences were quite obvious using the standard criteria for DEGs and showed the largest benefits accruing to energy production, amino acid biosynthesis, carbohydrate metabolism, translation, and transcription. Among these very dynamically changing genes we were most interested in the ones for energy production (category C), which is always active and defense mechanisms (category V), which only appears at 30 min.

Oxidative stress response

The cytosolic pool of glutathione (GSH) can sequester $HgCl_2$ to protect protein thiols from damage (Helbig et al., 2008). However, Hg(II) binds thioredoxin and glutathione strongly limiting their effectiveness at mitigating the subsequent burst of oxidative stress (Branco and Carvalho, 2019, Oram et al., 1996, Kapoor et al., 1965, Stricks and Kolthoff, 1953). Since proteins of the stress response and repair pathways all contain two or more thiols in their active sites, the Hg(II) chelates they form can only be rescued by the proteins of the *mer* locus (Ledwidge et al., 2005). Specifically, the NmerA "Hg(II) extraction" domain of MerA very efficiently chelates Hg(II) and can remove Hg(II) chelated by thioredoxin or glutathione (Hong et al., 2010, Ledwidge et al., 2005). During the initial response to $HgCl_2$, the regulator OxyR was not differentially expressed; however, at 10 min stress repair genes it is known to regulate increased notably. And, again, in the HgR strain expression of several of these "first responders" declined sooner than in HgS strain.

Supplying NADPH for the mercuric reductase

Both the standard and the relaxed criteria for a DEG revealed isocitrate dehydrogenase (ICD) immediately increased expression by 31.5% or 26% when exposed to 3 µM Hg or 4 µM Hg, respectively a departure from its well established decrease during oxidative stress in *Escherichia coli* (Christodoulou et al., 201*8)* and was also seen at just over a 2-fold increase meeting the standard criteria for a DEG in our previous study of the HgS strain (LaVoie and Summers, 2018). Moreover, in *E. coli*, oxidative stress response decreases *icd* expression (Nikel et al., 2021) bypassing it altogether by switching to the glyoxylate shunt to supply NADPH through the pentose phosphate pathway (*zwf* and *gnd*). Oxidative stress has also been found to increase expression of the membrane-bound transhydrogenase PntAB and its soluble partner, SthA; instead, we found both transhydrogenases were down-regulated. At mid-logarithmic growth in identical medium, *Escherichia coli* MG1655 is measured to have ~40,000 molecules of Icd (Table 2.10) (Li et al., 2014). Based on the *in vitro*-determined k*cat* for Icd (Muslin et al., 1995) *in vivo* NADPH could be 1.8 x10^8 molecules/min/cell (Table 2.10). Our observation of a ~30% increase in Icd expression in the HgR strain suggest that NADPH production would exceed by ~17-fold the amount of NADPH necessary for MerA to detoxify Hg exposure. So, the open question is in the face of oxidative stress provoked by Hg(II), how does the cell avoid switching to the glyoxylate shunt, preferring instead to just tweak expression of *icd* up a bit to dispatch enough of this toxic metal ion as a relatively harmless vapor!

References

AHN, S., JUNG, J., JANG, I.-A., MADSEN, E. L. & PARK, W. 2016. Role of glyoxylate shunt in oxidative stress response. *Journal of Biological Chemistry,* 291**,** 11928-11938.

ANDERS, S., PYL, P. T. & HUBER, W. 2015. HTSeq—a Python framework to work with high-throughput sequencing data. *bioinformatics,* 31**,** 166-169.

BARKAY, T., MILLER, S. M. & SUMMERS, A. O. 2003. Bacterial mercury resistance from atoms to ecosystems. *FEMS microbiology reviews,* 27**,** 355-384.

BENNETT, B. D., KIMBALL, E. H., GAO, M., OSTERHOUT, R., VAN DIEN, S. J. & RABINOWITZ, J. D. 2009. Absolute metabolite concentrations and implied enzyme active site occupancy in Escherichia coli. *Nature chemical biology,* 5**,** 593-599.

BERNHOFT, R. A. 2012. Mercury toxicity and treatment: a review of the literature. *Journal of environmental and public health,* 2012.

BJØRKLUND, G., LINDH, U., AASETH, J., MUTTER, J. & CHIRUMBOLO, S. 2018. Mercury in dental amalgams: a great concern for clinical toxicology in developing countries? *Journal of Trace Elements in Medicine and Biology: Organ of the Society for Minerals and Trace Elements (GMS),* 51**,** 9-11.

BLATTNER, F. R., PLUNKETT III, G., BLOCH, C. A., PERNA, N. T., BURLAND, V., RILEY, M., COLLADO-VIDES, J., GLASNER, J. D., RODE, C. K. & MAYHEW, G. F. 1997. The complete genome sequence of Escherichia coli K-12. *science,* 277**,** 1453-1462.

BRANCO, V. & CARVALHO, C. 2019. The thioredoxin system as a target for mercury compounds. *Biochimica et Biophysica Acta (BBA)-General Subjects,* 1863**,** 129255.

BROWN, H. J., STOKES, H. & HALL, R. M. 1996. The integrons In0, In2, and In5 are defective transposon derivatives. *Journal of Bacteriology,* 178**,** 4429-4437.

CAGUIAT, J. J., WATSON, A. L. & SUMMERS, A. O. 1999. Cd (II)-responsive and constitutive mutants implicate a novel domain in MerR. *Journal of bacteriology,* 181**,** 3462-3471.

CARROLL, A. C. & WONG, A. 2018. Plasmid persistence: costs, benefits, and the plasmid paradox. *Canadian journal of microbiology,* 64**,** 293-304.

CHEN, S., ZHOU, Y., CHEN, Y. & GU, J. 2018. fastp: an ultra-fast all-in-one FASTQ preprocessor. *Bioinformatics,* 34**,** i884-i890.

CHOU, H.-H., MARX, C. J. & SAUER, U. 2015. Transhydrogenase promotes the robustness and evolvability of E. coli deficient in NADPH production. *PLoS genetics,* 11**,** e1005007.

CHRISTODOULOU, D., LINK, H., FUHRER, T., KOCHANOWSKI, K., GEROSA, L. & SAUER, U. 2018. Reserve flux capacity in the pentose phosphate pathway enables Escherichia coli's rapid response to oxidative stress. *Cell systems,* 6**,** 569-578. e7.

COUNCIL, N. R. 2000. Toxicological effects of methylmercury.

ENGST, S. & MILLER, S. M. 1998. Rapid reduction of Hg (II) by mercuric ion reductase does not require the conserved C-terminal cysteine pair using HgBr2 as the substrate. *Biochemistry,* 37**,** 11496-11507.

FARRAR, W. & WILLIAMS, A. 1977. A history of mercury. *The chemistry of mercury.* Springer.

FDA, U. 2020. Advice about eating fish for women who are or might become pregnant, breastfeeding mothers, and young children.

FERNANDES, A. P., FLADVAD, M., BERNDT, C., ANDRÉSEN, C., LILLIG, C. H., NEUBAUER, P., SUNNERHAGEN, M., HOLMGREN, A. & VLAMIS-GARDIKAS, A. 2005. A novel monothiol glutaredoxin (Grx4) from Escherichia coli can serve as a substrate for thioredoxin reductase. *Journal of Biological Chemistry,* 280**,** 24544-24552.

FOX, B. & WALSH, C. T. 1982. Mercuric reductase. Purification and characterization of a transposon-encoded flavoprotein containing an oxidation-reduction-active disulfide. *Journal of Biological Chemistry,* 257**,** 2498-2503.

FOX, B. S. & WALSH, C. T. 1983. Mercuric reductase: homology to glutathione reductase and lipoamide dehydrogenase. Iodoacetamide alkylation and sequence of the active site peptide. *Biochemistry,* 22**,** 4082-4088.

FRASSINETTI, S., BRONZETTI, G. L., CALTAVUTURO, L., CINI, M. & DELLA CROCE, C. 2006. The role of zinc in life: a review. *Journal of environmental pathology, toxicology and oncology,* 25.

FUHRER, T. & SAUER, U. 2009. Different biochemical mechanisms ensure network-wide balancing of reducing equivalents in microbial metabolism. *Journal of bacteriology,* 191**,** 2112-2121.

GALPERIN, M. Y., WOLF, Y. I., MAKAROVA, K. S., VERA ALVAREZ, R., LANDSMAN, D. & KOONIN, E. V. 2021. COG database update: focus on microbial diversity, model organisms, and widespread pathogens. *Nucleic acids research,* 49**,** D274-D281.

GAMBILL, B. D. & SUMMERS, A. O. 1992. Synthesis and degradation of the mRNA of the Tn21 mer operon. *Journal of molecular biology,* 225**,** 251-259.

GERDES, K., GULTYAEV, A. P., FRANCH, T., PEDERSEN, K. & MIKKELSEN, N. D. 1997. Antisense RNA-regulated programmed cell death. *Annual review of genetics,* 31**,** 1-31.

GLENN, T. C., NILSEN, R. A., KIERAN, T. J., FINGER, J. W., PIERSON, T. W., BENTLEY, K. E., HOFFBERG, S. L., LOUHA, S., GARCÍA-DE LEÓN, F. J. & DEL RIO PORTILLA, M. A. 2016. Adapterama I: universal stubs and primers for thousands of dual-indexed Illumina libraries (iTru & iNext). *BioRxiv***,** 049114.

GOREN, Y., GORING-MORRIS, A. N. & SEGAL, I. 2001. The technology of skull modelling in the Pre-Pottery Neolithic B (PPNB): regional variability, the relation of technology and iconography and their archaeological implications. *Journal of Archaeological Science,* 28**,** 671-690.

HAMLETT, N., LANDALE, E., DAVIS, B. & SUMMERS, A. 1992. Roles of the Tn21 merT, merP, and merC gene products in mercury resistance and mercury binding. *Journal of bacteriology,* 174**,** 6377-6385.

HELBIG, K., BLEUEL, C., KRAUSS, G. J. & NIES, D. H. 2008. Glutathione and transition-metal homeostasis in Escherichia coli. *Journal of bacteriology,* 190**,** 5431-5438.

HONG, B., NAUSS, R., HARWOOD, I. M. & MILLER, S. M. 2010. Direct measurement of mercury (II) removal from organomercurial lyase (MerB) by tryptophan fluorescence: NmerA domain of coevolved γ-proteobacterial mercuric ion reductase (MerA) is more efficient than MerA catalytic core or glutathione. *Biochemistry,* 49**,** 8187-8196.

JENSEN, R. B. & GERDES, K. 1995. Programmed cell death in bacteria: proteic plasmid stabilization systems. *Molecular microbiology,* 17**,** 205-210.

JOY, A. & QURESHI, A. 2020. Mercury in dental amalgam, online retail, and the Minamata convention on mercury. *Environmental Science & Technology,* 54**,** 14139-14142.

KAPOOR, R., DOUGHTY, G. & GORIN, G. 1965. The reaction and assay of glutathione with Hg2+ and alkali. *Biochimica et Biophysica Acta (BBA)-General Subjects,* 100**,** 376-383.

LANGMEAD, B. & SALZBERG, S. L. 2012. Fast gapped-read alignment with Bowtie 2. *Nature methods,* 9**,** 357-359.

LAVOIE, S. P., MAPOLELO, D. T., COWART, D. M., POLACCO, B. J., JOHNSON, M. K., SCOTT, R. A., MILLER, S. M. & SUMMERS, A. O. 2015. Organic and inorganic mercurials have distinct effects on cellular thiols, metal homeostasis, and Fe-binding proteins in Escherichia coli. *JBIC Journal of Biological Inorganic Chemistry,* 20**,** 1239-1251.

LAVOIE, S. P. & SUMMERS, A. O. 2018. Transcriptional responses of Escherichia coli during recovery from inorganic or organic mercury exposure. *BMC genomics,* 19**,** 1-24.

LEDWIDGE, R., PATEL, B., DONG, A., FIEDLER, D., FALKOWSKI, M., ZELIKOVA, J., SUMMERS, A. O., PAI, E. F. & MILLER, S. M. 2005. NmerA, the metal binding domain of mercuric ion reductase, removes Hg2+ from proteins, delivers it to the catalytic core, and protects cells under glutathione-depleted conditions. *Biochemistry,* 44**,** 11402-11416.

LI, G.-W., BURKHARDT, D., GROSS, C. & WEISSMAN, J. S. 2014. Quantifying absolute protein synthesis rates reveals principles underlying allocation of cellular resources. *Cell,* 157**,** 624-635.

LIEBERT, C. A., HALL, R. M. & SUMMERS, A. O. 1999. Transposon Tn 21, flagship of the floating genome. *Microbiology and molecular biology reviews,* 63**,** 507-522.

LIEBERT, C. A., WIREMAN, J., SMITH, T. & SUMMERS, A. O. 1997. Phylogeny of mercury resistance (mer) operons of gram-negative bacteria isolated from the fecal flora of primates. *Applied and Environmental Microbiology,* 63**,** 1066-1076.

LOVE, M. I., HUBER, W. & ANDERS, S. 2014. Moderated estimation of fold change and dispersion for RNA-seq data with DESeq2. *Genome biology,* 15**,** 1-21.

MALM, O. 1998. Gold mining as a source of mercury exposure in the Brazilian Amazon. *Environmental research,* 77**,** 73-78.

MEAGHER, R. B., SUMMERS, A. O. & RUGH, C. L. 1999. Metal resistance sequences and transgenic plants.

MISHRA, S. & IMLAY, J. 2012. Why do bacteria use so many enzymes to scavenge hydrogen peroxide? *Archives of biochemistry and biophysics,* 525**,** 145-160.

MUSLIN, E. H., LI, D., STEVENS, F. J., DONNELLY, M., SCHIFFER, M. & ANDERSON, L. E. 1995. Engineering a domain-locking disulfide into a bacterial malate dehydrogenase produces a redox-sensitive enzyme. *Biophysical journal,* 68**,** 2218-2223.

NEIDHARDT, F. C., BLOCH, P. L. & SMITH, D. F. 1974. Culture medium for enterobacteria. *Journal of bacteriology,* 119**,** 736-747.

NIKEL, P. I., FUHRER, T., CHAVARRÍA, M., SÁNCHEZ-PASCUALA, A., SAUER, U. & DE LORENZO, V. 2021. Reconfiguration of metabolic fluxes in Pseudomonas putida as a response to sub-lethal oxidative stress. *The ISME journal,* 15**,** 1751-1766.

ORAM, P. D., FANG, X., FERNANDO, Q., LETKEMAN, P. & LETKEMAN, D. 1996. The formation constants of mercury (II)− glutathione complexes. *Chemical research in toxicology,* 9**,** 709-712.

PARK, S.-J., WIREMAN, J. & SUMMERS, A. 1992. Genetic analysis of the Tn21 mer operator-promoter. *Journal of bacteriology,* 174**,** 2160-2171.

PARTRIDGE, S. R. & HALL, R. M. 2004. Complex multiple antibiotic and mercury resistance region derived from the r-det of NR1 (R100). *Antimicrobial agents and chemotherapy,* 48**,** 4250-4255.

ROSS, W., PARK, S. & SUMMERS, A. 1989. Genetic analysis of transcriptional activation and repression in the Tn21 mer operon. *Journal of bacteriology,* 171**,** 4009-4018.

RUI, B., SHEN, T., ZHOU, H., LIU, J., CHEN, J., PAN, X., LIU, H., WU, J., ZHENG, H. & SHI, Y. 2010. A systematic investigation of Escherichia coli central carbon metabolism in response to superoxide stress. *BMC systems biology,* 4**,** 1-12.

SAN MILLAN, A. & MACLEAN, R. C. 2017. Fitness costs of plasmids: a limit to plasmid transmission. *Microbiology spectrum,* 5**,** 5.5. 02.

SAUER, U., CANONACO, F., HERI, S., PERRENOUD, A. & FISCHER, E. 2004. The soluble and membrane-bound transhydrogenases UdhA and PntAB have divergent functions in NADPH metabolism of Escherichia coli. *Journal of Biological Chemistry,* 279**,** 6613-6619.

SCHOBER, P., BOER, C. & SCHWARTE, L. A. 2018. Correlation coefficients: appropriate use and interpretation. *Anesthesia & Analgesia,* 126**,** 1763-1768.

SIRONA, D. 2020. Dentsply Sirona: 2020 Annual Report. 140.

SONG, L., TENG, Q., PHILLIPS, R. S., BREWER, J. M. & SUMMERS, A. O. 2007. 19F-NMR reveals metal and operator-induced allostery in MerR. *Journal of molecular biology,* 371**,** 79-92.

STEAD, M. B., AGRAWAL, A., BOWDEN, K. E., NASIR, R., MOHANTY, B. K., MEAGHER, R. B. & KUSHNER, S. R. 2012. RNA snap™: a rapid, quantitative and inexpensive, method for isolating total RNA from bacteria. *Nucleic acids research,* 40**,** e156-e156.

STRICKS, W. & KOLTHOFF, I. 1953. Reactions between mercuric mercury and cysteine and glutathione. Apparent dissociation constants, heats and entropies of formation of various forms of mercuric mercapto-cysteine and-glutathione. *Journal of the American Chemical Society,* 75**,** 5673-5681.

SUMMERS, A., KNIGHT-OLLIFF, L. & SLATER, C. 1982. Effect of catabolite repression on the mer operon. *Journal of bacteriology,* 149**,** 191-197.

SUMMERS, A. O. & LEWIS, E. 1973. Volatilization of mercuric chloride by mercury-resistant plasmid-bearing strains of Escherichia coli, Staphylococcus aureus, and Pseudomonas aeruginosa. *Journal of bacteriology,* 113**,** 1070-1072.

SUMMERS, A. O. & SILVER, S. 1972. Mercury resistance in a plasmid-bearing strain of Escherichia coli. *Journal of bacteriology,* 112**,** 1228-1236.

VEIGA, M. M., MAXSON, P. A. & HYLANDER, L. D. 2006. Origin and consumption of mercury in small-scale gold mining. *Journal of cleaner production,* 14**,** 436-447.

WILLIAMS, L. E., DETTER, C., BARRY, K., LAPIDUS, A. & SUMMERS, A. O. 2006. Facile recovery of individual high-molecular-weight, low-copy-number natural plasmids for genomic sequencing. *Applied and environmental microbiology,* 72**,** 4899-4906.

WU, R., WANG, X., WOMBLE, D. & ROWND, R. 1992. Expression of the repA1 gene of IncFII plasmid NR1 is translationally coupled to expression of an overlapping leader peptide. *Journal of bacteriology,* 174**,** 7620-7628.

XU, F. F. & IMLAY, J. A. 2012. Silver (I), mercury (II), cadmium (II), and zinc (II) target exposed enzymic iron-sulfur clusters when they toxify Escherichia coli. *Applied and environmental microbiology,* 78**,** 3614-3621.

YEUNG, N., GOLD, B., LIU, N., PRATHAPAM, R., STERLING, H., WILLAMS, E. & BUTLAND, G. 2011. The E. coli monothiol glutaredoxin GrxD forms homodimeric and heterodimeric FeS cluster containing complexes. *Biochemistry,* 50**,** 8957-8969.

YIN, L., LIN, S., SUMMERS, A. O., ROPER, V., CAMPEN, M. J. & YU, X. 2021. Children with amalgam dental restorations have significantly elevated blood and urine mercury levels. *Toxicological Sciences,* 184**,** 104-126.

ZHENG, N., WANG, S., DONG, W., HUA, X., LI, Y., SONG, X., CHU, Q., HOU, S. & LI, Y. 2019. The toxicological effects of mercury exposure in marine fish. *Bulletin of environmental contamination and toxicology,* 102**,** 714-720.

ZHONGMING, Z., LINONG, L., XIAONA, Y., WANGQIANG, Z. & WEI, L. 2013. Global Mercury Assessment 2013: Sources, emissions, releases, and environmental transport.

Table 2.1 The average of total paired reads by chromosomal feature type from three biological replicates for each condition. Values are percentages of sum of total paired reads for each feature type in a condition divided by the total amount of paired reads in that condition.

A.

Feature	Total Count	unexposed	3 µM $HgCl_2$	4 µM $HgCl_2$	Avg	STDV
CDS	4241	86.81	84.16	82.30	84.42	2.27
tRNA	86	0.63	0.35	0.20	0.39	0.22
tmRNA	1	6.30	7.71	8.64	7.55	1.18
rRNA	22	0.36	1.01	0.93	0.77	0.35
Pseudogene	145	0.48	0.32	0.35	0.38	0.09
ncRNA	77	5.11	6.29	7.46	6.29	1.18

B.

Feature	Total Count	unexposed	3 µM $HgCl_2$	4 µM $HgCl_2$	Avg	STDV
CDS	4241	87.36	85.51	84.52	85.80	1.44
tRNA	86	0.62	0.44	0.44	0.50	0.10
tmRNA	1	6.16	6.68	6.97	6.60	0.41
rRNA	22	0.10	1.18	1.73	1.00	0.83
Pseudogene	145	0.51	0.40	0.42	0.44	0.06
ncRNA	77	5.24	5.78	5.92	5.65	0.36

Table 2.2: Total DEGs for each comparison and at indicated time point. Abbreviation: MG = MG1655; NR= MG1655(pNR1); 0, 3, 4 = [$HgCl_2$] µM.

A.

NR0 vs MG0	0 minute	10 minute	30 minute	60 minute	90 minute
Up-regulated	0	0	0	0	0
Down-regulated	0	1	0	0	0
Total DEGs	0	1	0	0	0

B.

MG3 vs MG0	10 minute	30 minute	60 minute	90 minute
Up-regulated	610	540	391	412
Down-regulated	743	632	261	293
Total DEGs	1353	1172	652	705

C.

NR3 vs NR0	10 minute	30 minute	60 minute	90 minute
Up-regulated	706	163	393	60
Down-regulated	815	107	323	54
Total DEGs	1521	270	716	114

D.

MG4 vs MG0	10 minute	30 minute	60 minute	90 minute
Up-regulated	884	941	682	331
Down-regulated	908	890	507	295
Total	1792	1831	1189	626

E.

NR4 vs NR0	10 minute	30 minute	60 minute	90 minute
Up-regulated	852	778	342	519
Down-regulated	883	683	241	394
Total	1735	1461	583	913

F.

NR3 vs MG3	10 minute	30 minute	60 minute	90 minute
Up-regulated	1	358	44	189
Down-regulated	0	196	79	240
Total DEGs	1	554	123	429

G.

NR4 vs MG4	10 minute	30 minute	60 minute	90 minute
Up-regulated	0	19	544	352
Down-regulated	0	48	522	406
Total DEGs	0	67	1066	758

Table 2.3: *In vivo* measurements of Hg(II) reduction by intact *Escherichia coli* cells.

Strain(Plasmid)	Growth Conditions	Detection Method	Avg. Rate (Hg^0 Atoms/min/cell)
E. coli AB1932-1 (JJ1) E. coli DU1040 (pDU202) *E. coli* JM103 (pDU202)	Tryptone broth Aerobic growth Hg-induced Mid- Late-log phase	$^{203}HgCl_2$	$3.22 \pm 2.62 \times 10^6$

Summers and Silver, 1972
Summers and Lewis, 1973
Summers, et al., 1982
Fox and Walsh, 1983
Hammlett, et al., 1992
Engst and Miller, 1998

Table 2.4: Intracellular concentrations of pyridine nucleotides for *Escherichia coli* MG1655 growing in minimal medium.

[Intracellular]	Fuhrer, *et al*. 2009 Molecules/cell	Bennet, *et al*. 2009 Molecules/cell
NAD^+	$0.35\pm0.24 \times 10^6$	1.05×10^6
$NADP^+$	0.08×10^6	0.001×10^6
NADH	$0.12\pm0.03 \times 10^6$	0.03×10^6
NADPH	$0.08\pm0.02 \times 10^6$	0.05×10^6
Total Pyridine Nucleotide Pool	0.63×10^6	1.13×10^6

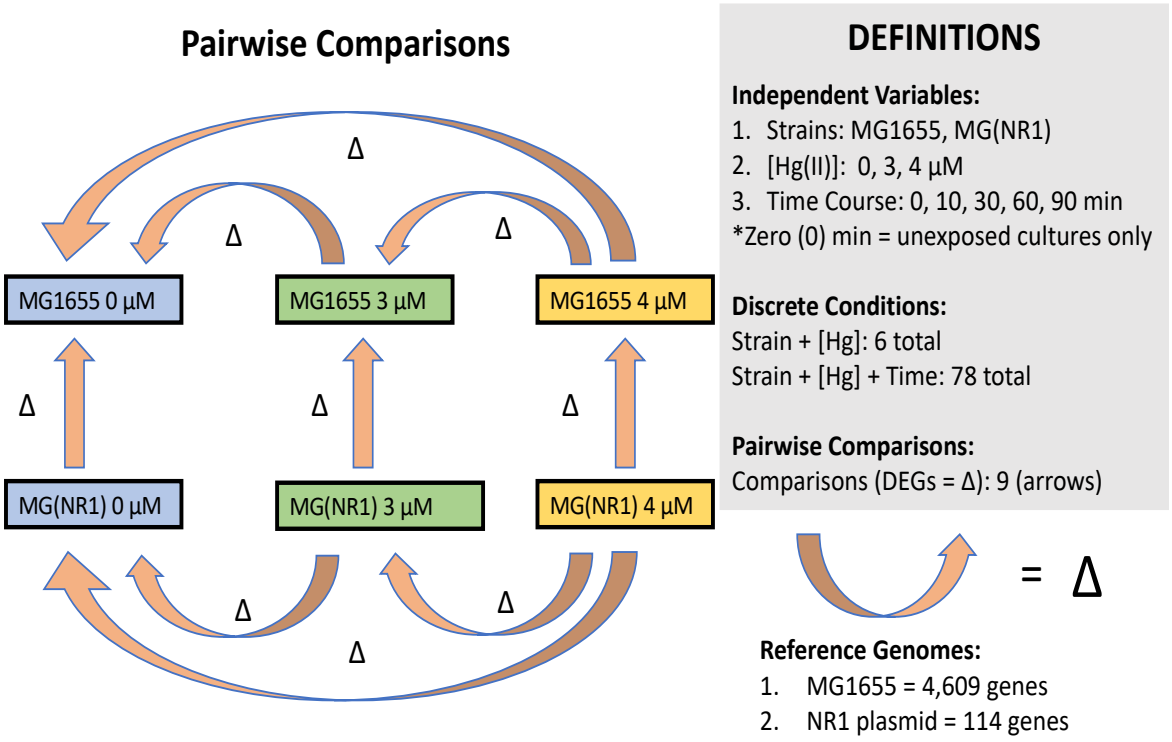

Figure 2.1 Graphical abstract of overview of comparisons defining differentially expressed genes (DEGs). Each arrow shows the direction of the comparison for a given condition. Hg-sensitive (MG1655) and Hg-resistant [MG(NR1)] cultures: (1) unexposed, 0 µM $HgCl_2$ (blue), (2) sub-acute, 3 µM Hg (green), and acute, 4 µM Hg (orange).

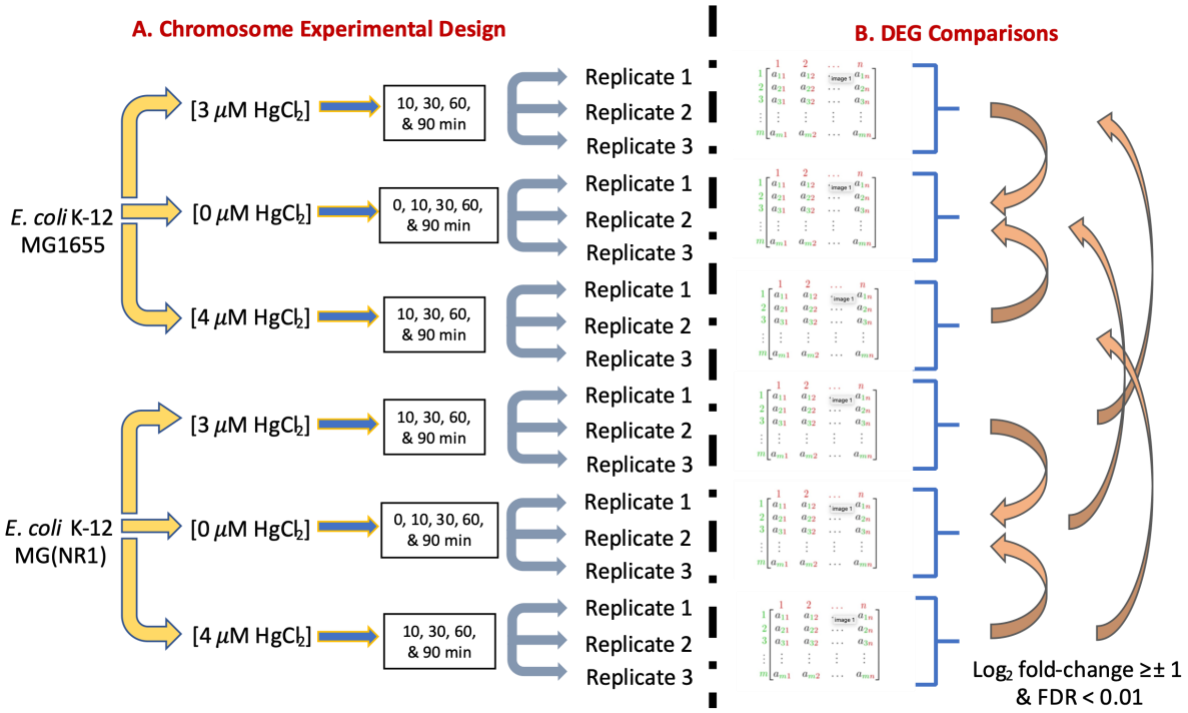

Figure 2.2 Graphical abstract of experimental detail of RNA-Seq study. (A) Schematics of Hg-sensitive (MG1655) and Hg-resistant [MG(NR1)] conditions, time points, and biological replicates. (B) Schematics of bioinformatics comparison for differentially expressed genes (DEGs). Each arrow dictates the direction of comparisons being made for a given condition. See also Figure 2.1.

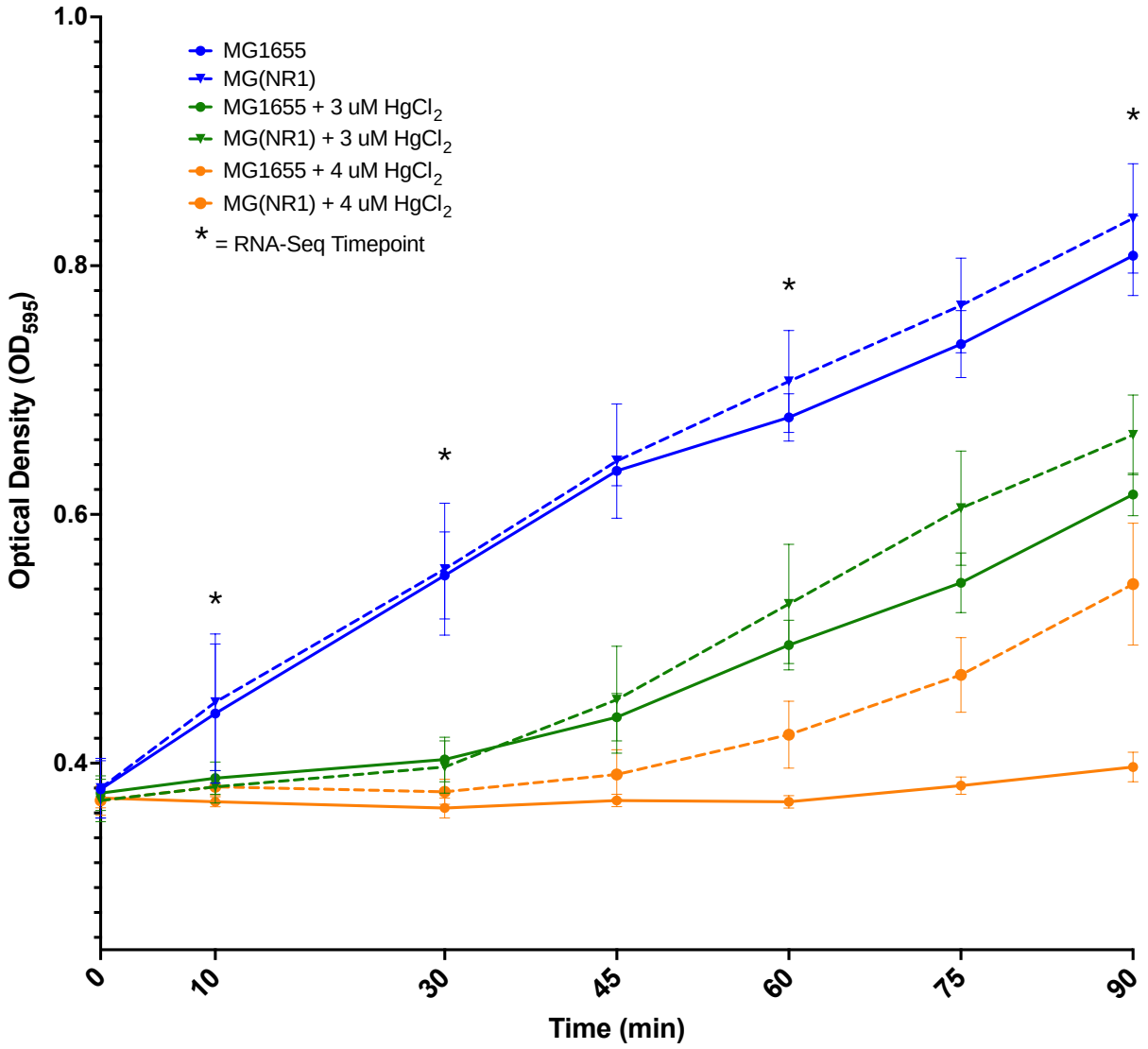

Figure 2.3 Effects of sub-acute and acute mercury exposure on growth of *E. coli* MG1655 and MG1655(NR1). Both strains were grown aerobically in glucose-MOPS minimal medium and exposed (or not) to the indicated [Hg] at mid-exponential phase. No Hg (blue), 3 µM Hg (green), 4 µM Hg (orange). Solid lines for each color indicate the Hg-sensitive (HgS) strain MG1655; dashed lines indicate the Hg-resistant (HgR) strain MG1655(NR1). Standard errors are for 3 biological replicates in each culture condition. Asterisks indicate sampling times for RNA-Seq aliquots.

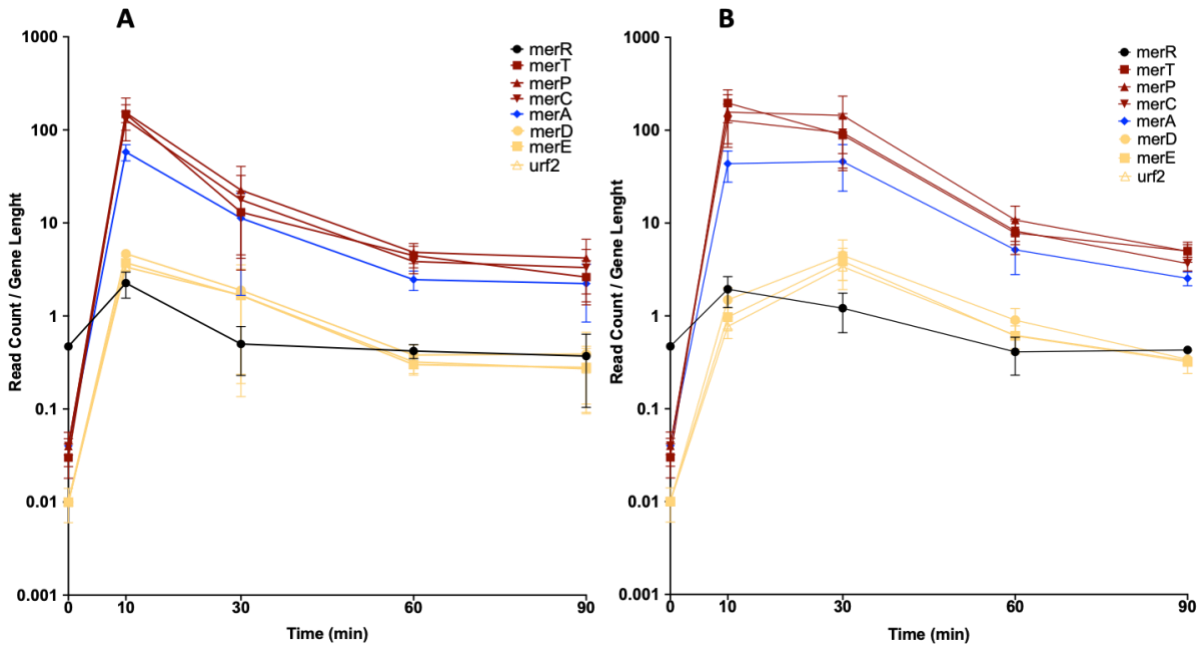

Figure 2.4 Line graph distribution of reads of *mer* operon genes. Expression of each *mer* gene at (A) 3 µM Hg or (B) 4 µM Hg. Each value is the average read count for the indicated *mer* gene divided by the full-length of that gene (bp). Error bars are standard error of 3 biological replicates. *merR* (black), *merTPC* (red) are the promoter-proximal genes, *merA* (blue), and *merDEUrf2* are the promoter-distal genes (yellow). Line graphs show (1) the differences in read abundance per gene, (2) the similarities of trajectories at each [Hg] and (3) the differences between the trajectories at the two [Hg]s. Pearson correlation coefficients were used to assess the strength of linear association between trajectories. We chose the following standards: $r(3) \geq 0.90 – 1.0$, $p < 0.05$ (Two-Tailed) for a very strong positive association; $r(3) \geq 0.70 – 0.89$, $p < 0.05$ (Two-Tailed) for a strong association; $r(3) \geq 0.40 – 0.69$, $p < 0.05$ (Two-Tailed) for a moderate association; $r(3) \geq 0.10 – 0.39$, $p < 0.05$ (Two-Tailed) for a weak association; and $r(3) \geq 0.00 – 0.10$, $p < 0.05$ (Two-Tailed) for a negligible association (Schober et al., 2018)(See Table 2.4).

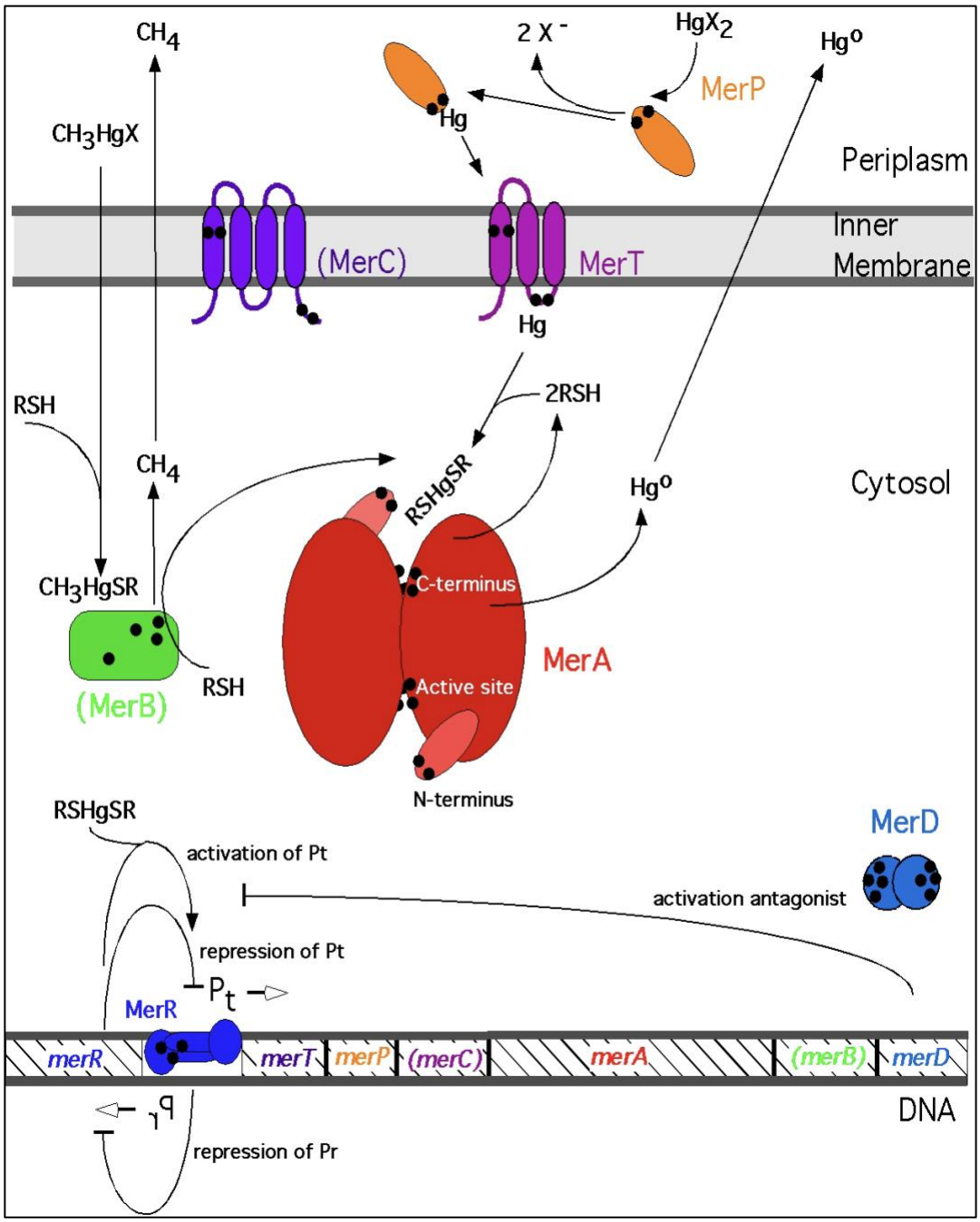

Figure 2.5: Bacterial mercury resistance operon with its promoter regions and associated proteins. The Tn*21*operon consist of *merRTPCADE*. The MerB protein is associated with organomercurial resistance and not encoded on Tn*21* (Barkay et al., 2003).

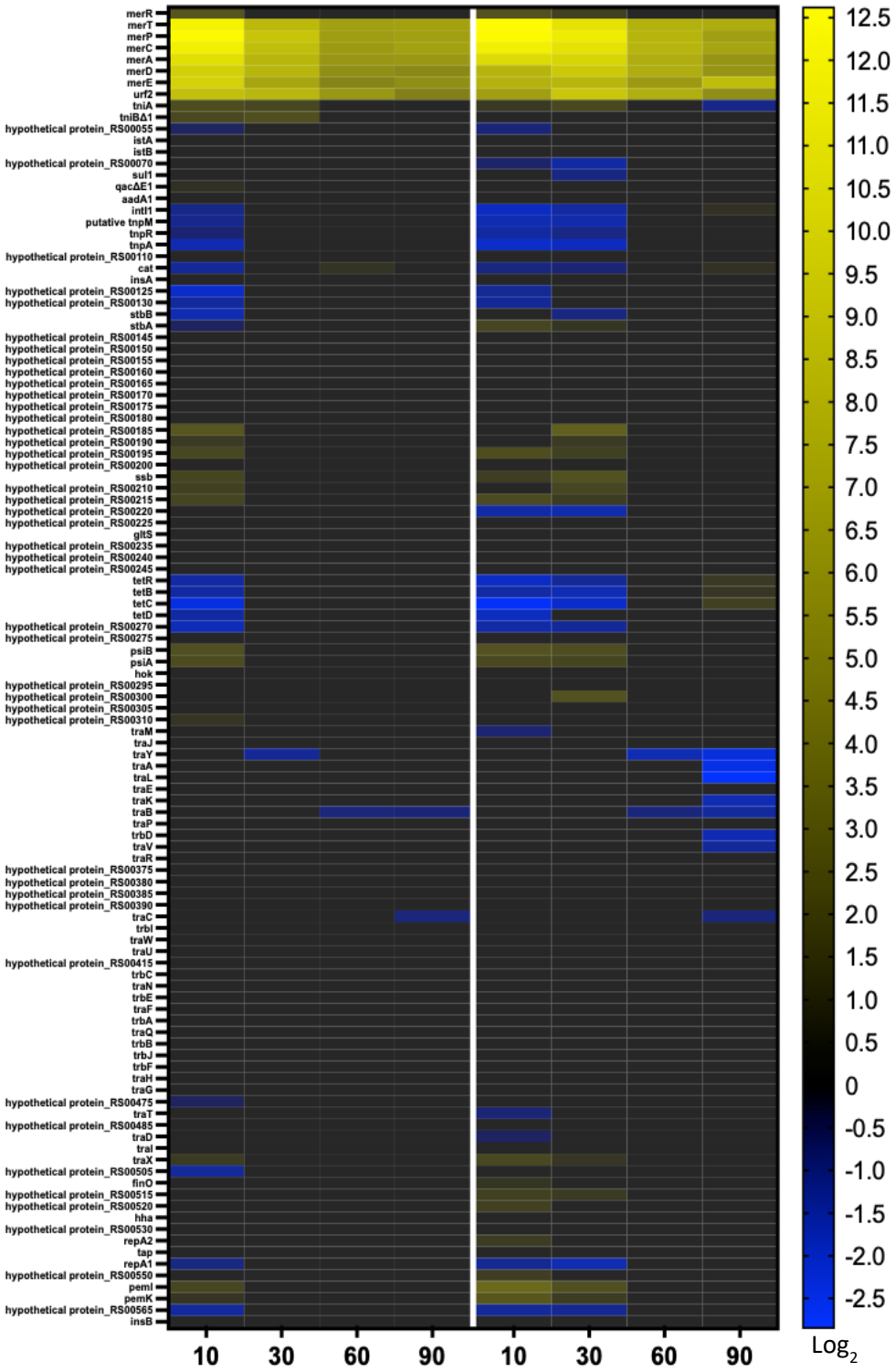

Figure 2.6 A heat map of all 114 genes of the NR1 plasmid. Y-axis lists genes by their order in the plasmid sequence and X-axis shows the time points for each [$HgCl_2$] condition. Left: 3 µM Hg and Right: 4 µM Hg.

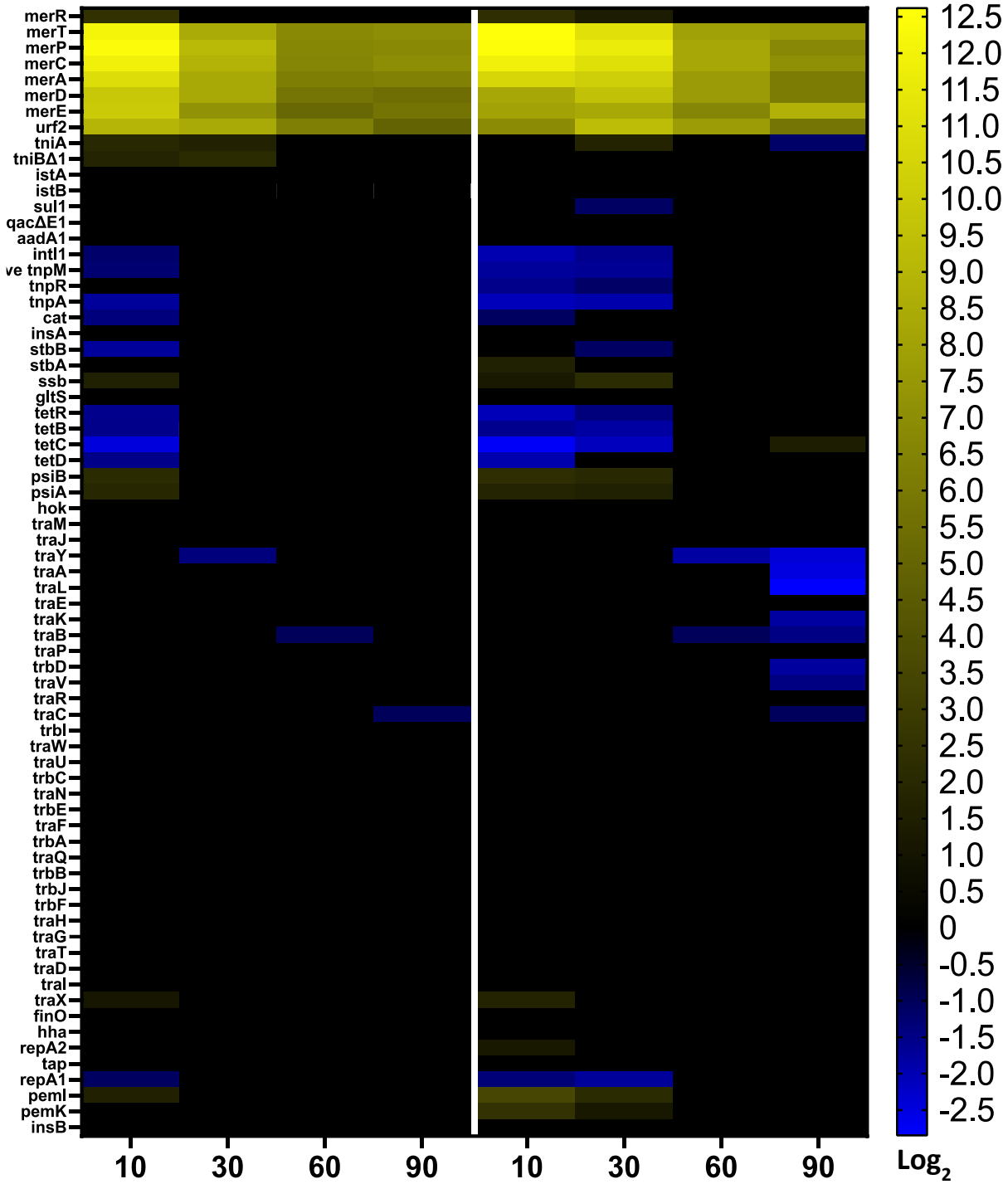

Figure 2.7 A heat map of the 71 genes of known function on the NR1 plasmid. Y-axis lists genes by their order in the plasmid sequence and X-axis shows the time points for each [$HgCl_2$] condition. Left: 3 µM Hg and Right: 4 µM Hg.

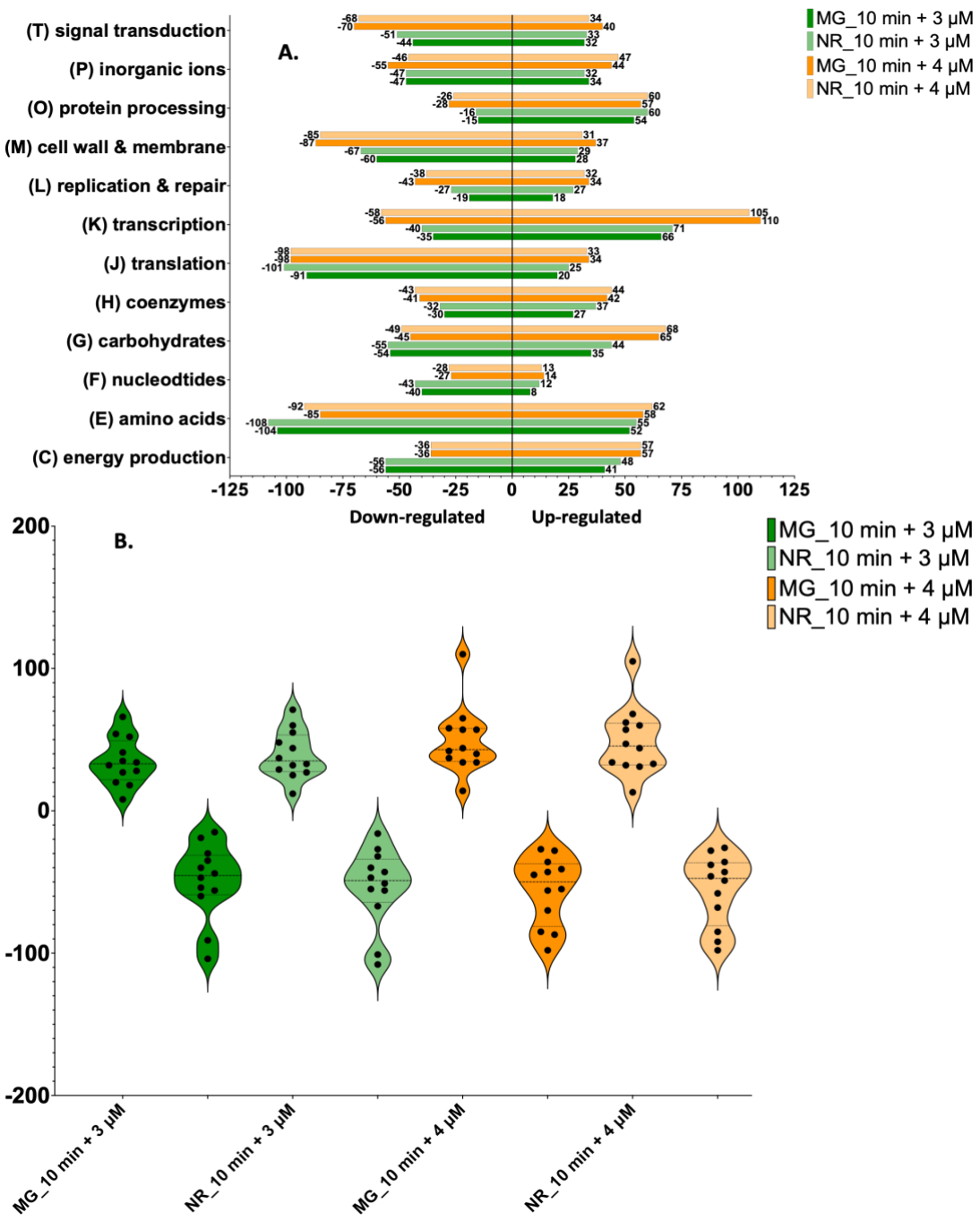

Figure 2.8 Numbers of differentially expressed chromosomal genes at 10 min in the COG categories most affected by $HgCl_2$. COG categories were chosen if there was a sum of more than 50 up- and down-regulated DEGs at 10 min. The color bars identify each [$HgCl_2$] condition: green for 3 µM and orange for 4 µM Hg. Color intensity reflects the strain phenotype: dark shade is HgS, and pale shade is HgR). (A) Counts of DEGs in indicated COG category. On x-axis positive is up-regulated and negative is down-regulate genes. (B) Distributions of filter-passing COG categories at 10 min for each [Hg] condition. Mann Whitney test (Two-tailed; $p < 0.05$) compared each up- and down-regulated COG category (* p-value < 0.05).

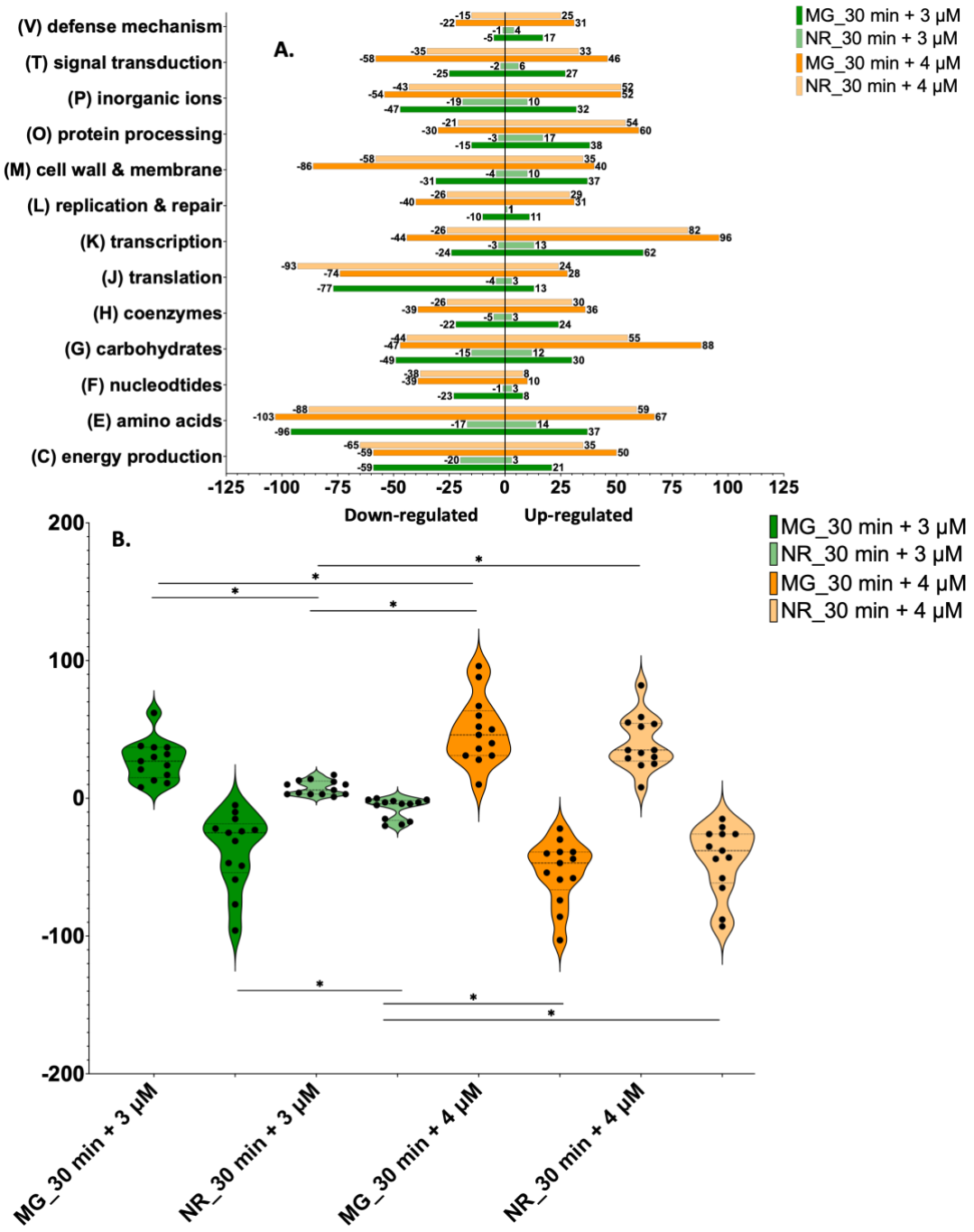

Figure 2.9 Numbers of differentially expressed genes at 30 min in the COG categories most affected by $HgCl_2$. COG categories were chosen if there was a sum of more than 50 up- and down-regulated DEGs at 30 min. The color bars identify each [$HgCl_2$] condition: green for 3 µM and orange for 4 µM Hg. Color intensity reflects the strain phenotype: dark shade is HgS, and pale shade is HgR). (A) Counts of DEGs in indicated COG category. On x-axis positive is up-regulated and negative is down-regulate genes. (B) Distributions of filter-passing COG categories at 10 min for each [Hg] condition. Mann Whitney test (Two-tailed; $p < 0.05$) compared each up- and down-regulated COG category (* p-value < 0.05).

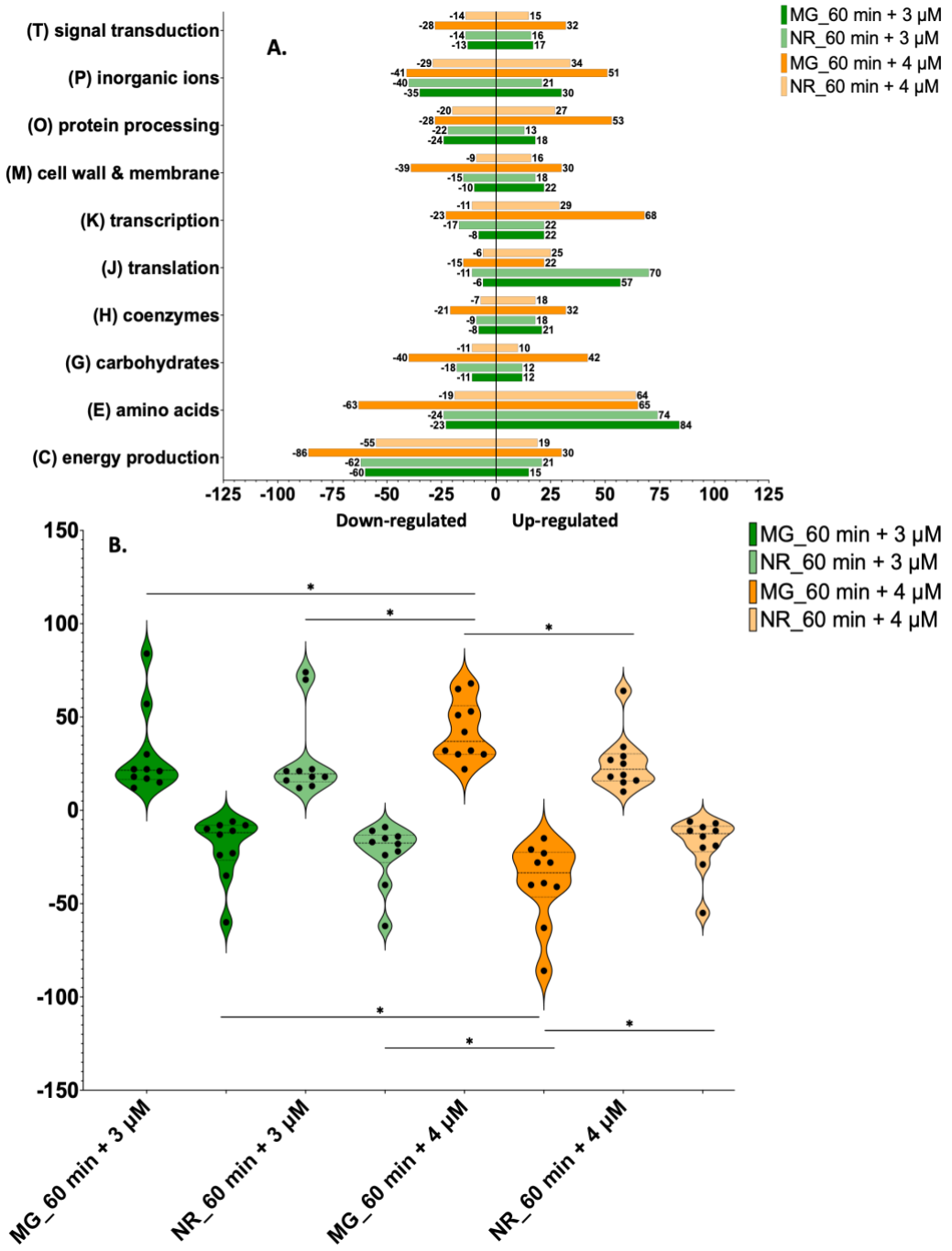

Figure 2.10 Numbers of differentially expressed genes at 60 min in the COG categories most affected by $HgCl_2$. COG categories were chosen if there was a sum of more than 50 up- and down-regulated DEGs at 60 min. The color bars identify each [$HgCl_2$] condition: green for 3 µM and orange for 4 µM Hg. Color intensity reflects the strain phenotype: dark shade is HgS, and pale shade is HgR). (A) Counts of DEGs in indicated COG category. On x-axis positive is up-regulated and negative is down-regulate genes. (B) Distributions of filter-passing COG categories at 10 min for each [Hg] condition. Mann Whitney test (Two-tailed; $p < 0.05$) compared each up- and down-regulated COG category (* p-value < 0.05).

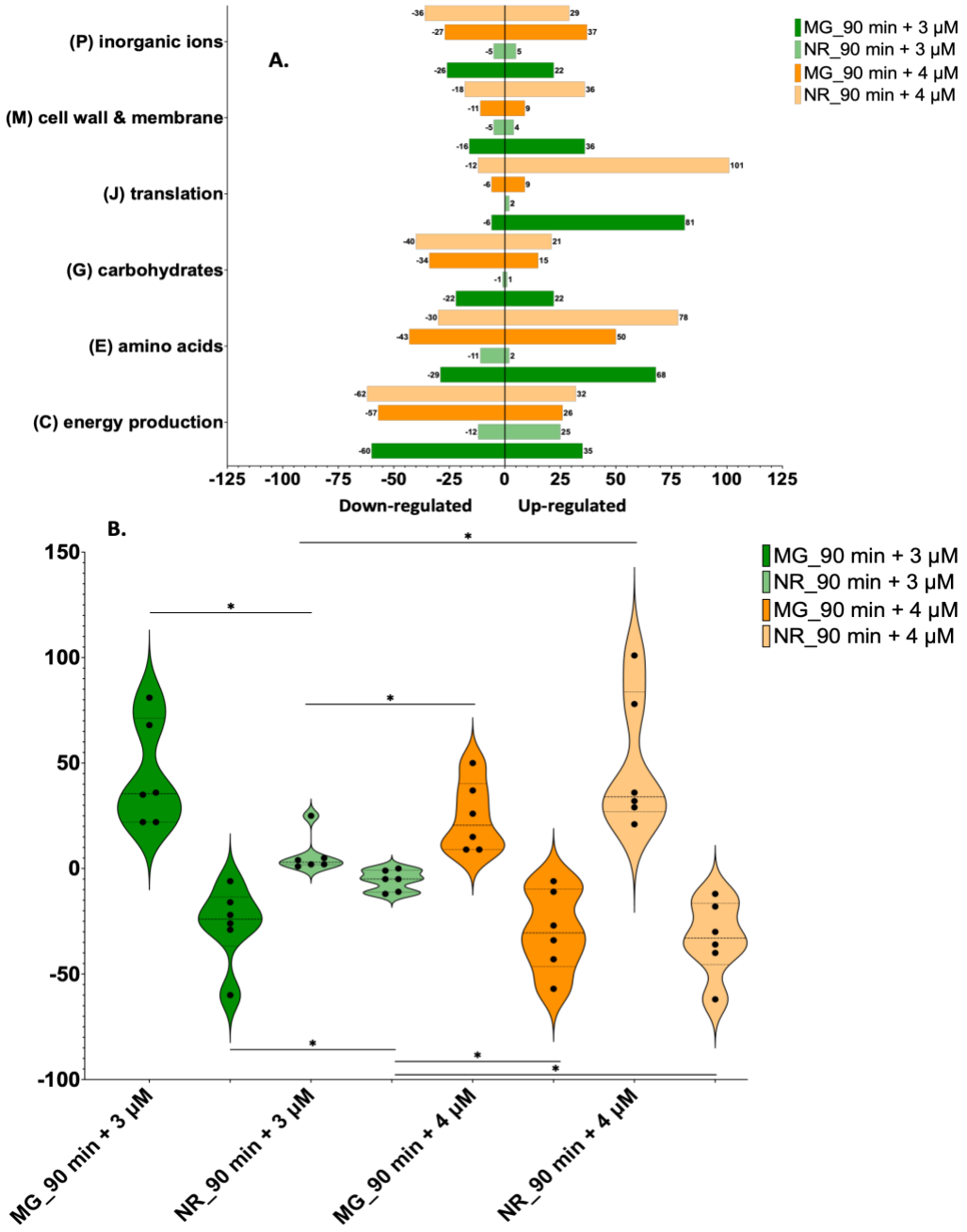

Figure 2.11 Numbers of differentially expressed genes at 90 min in the COG categories most affected by $HgCl_2$. COG categories were chosen if there was a sum of more than 50 up- and down-regulated DEGs at 90 min. The color bars identify each [$HgCl_2$] condition: green for 3 µM and orange for 4 µM Hg. Color intensity reflects the strain phenotype: dark shade is HgS, and pale shade is HgR). (A) Counts of DEGs in indicated COG category. On x-axis positive is up-regulated and negative is down-regulate genes. (B) Distributions of filter-passing COG categories at 10 min for each [Hg] condition. Mann Whitney test (Two-tailed; $p < 0.05$) compared each up- and down-regulated COG category (* p-value < 0.05).

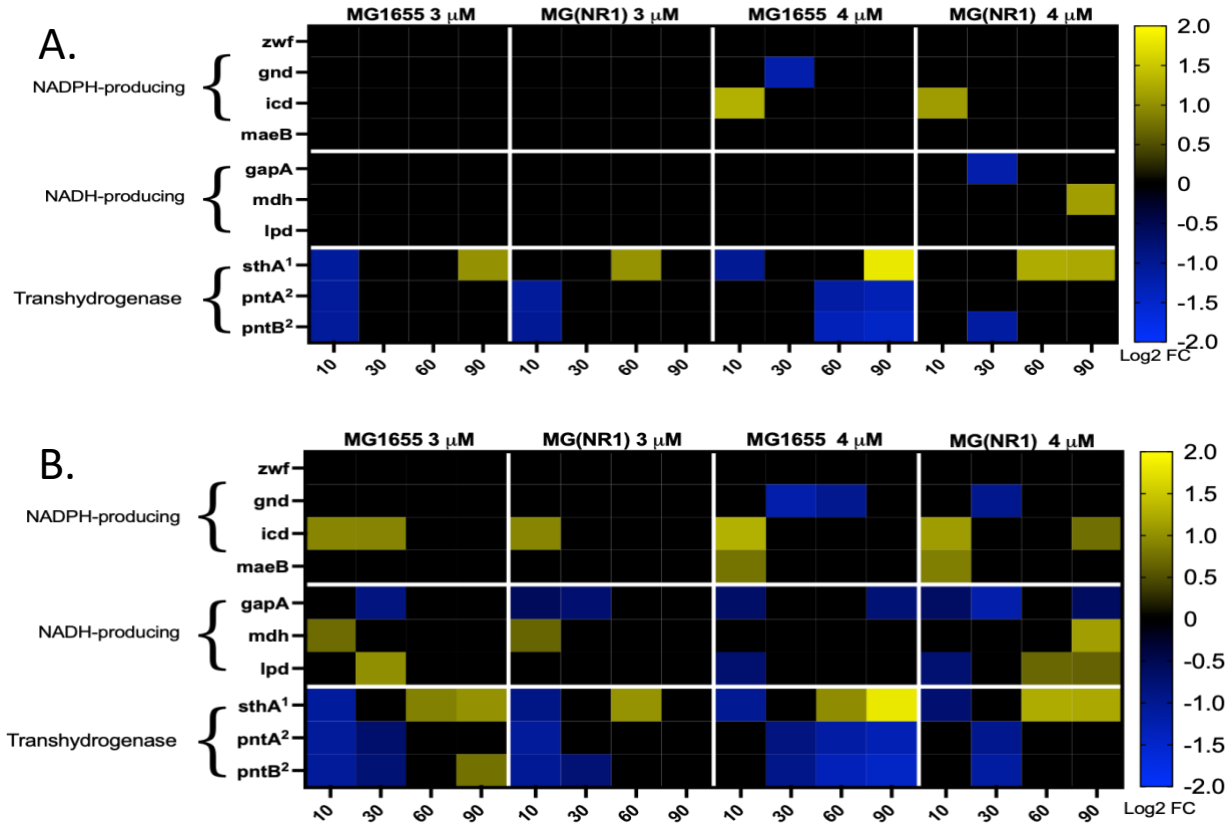

Figure 2.12 A heat map of chromosomal NAD(P)H metabolism genes. (A) DEG criteria $Log_2 \leq \pm 1$ and FDR < 0.01 and (B) $Log_2 \leq \pm 0.5$ and FDR < 0.01.

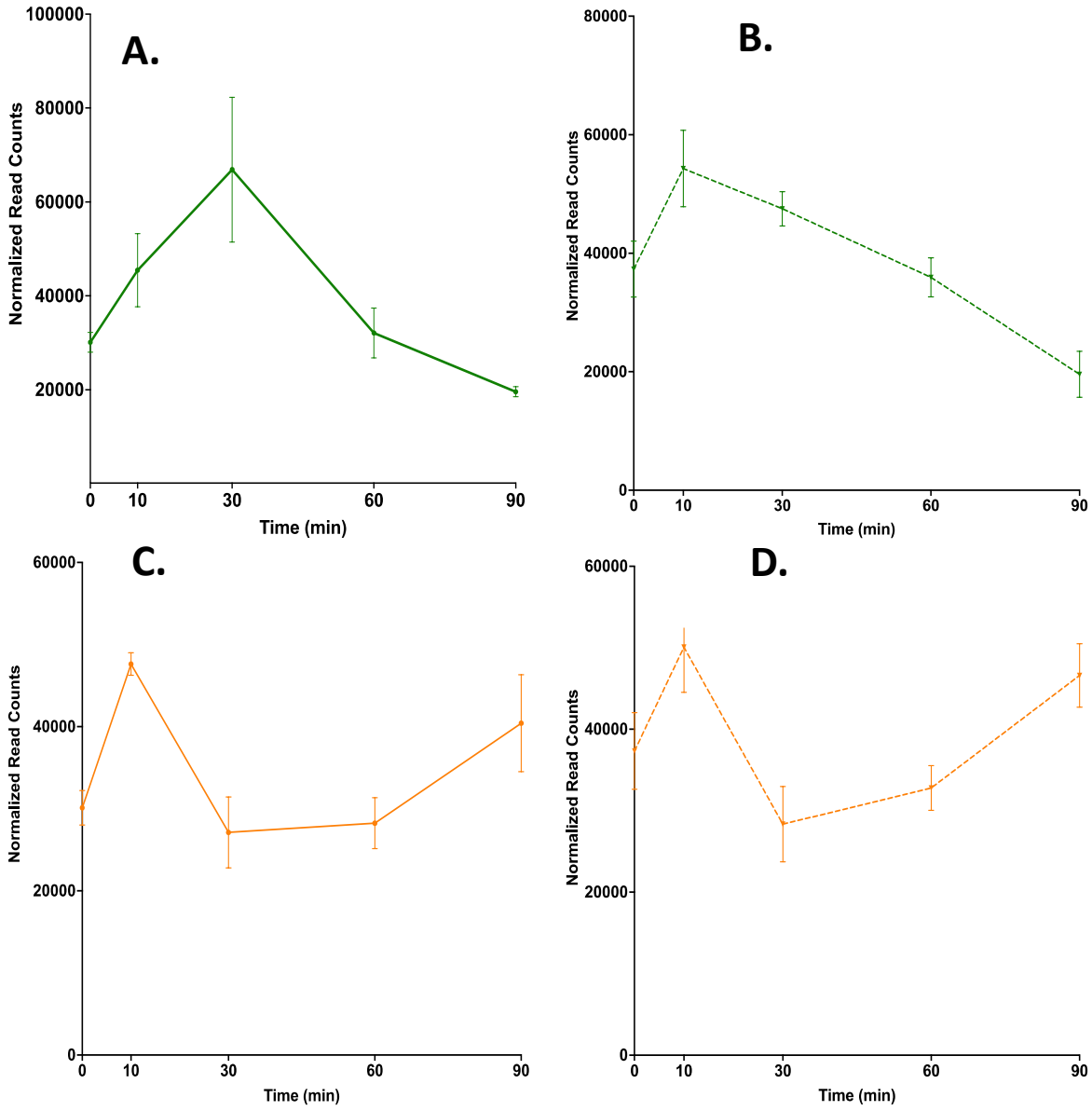

Figure 2.13 Line graphs distribution of isocitrate dehydrogenase reads. Expression of *icd* gene at (A) HgS, 3 µM Hg, (B) HgR 3 µM Hg, (C) HgS, 4 µM Hg, (D) HgR, 4 µM Hg. Each value is the average read count for the indicated *icd* gene. Error bars are standard error of 3 biological replicates. Line graphs show (1) the differences in read and (2) the similarities of trajectories at each [$HgCl_2$]. Pearson correlation coefficients were used to assess the strength of linear association between trajectories. We chose the following standards: $r(3) \geq 0.90 – 1.0$, $p < 0.05$ (Two-Tailed) for a very strong positive association; $r(3) \geq 0.70 – 0.89$, $p < 0.05$ (Two-Tailed) for a strong association; $r(3) \geq 0.40 – 0.69$, $p < 0.05$ (Two-Tailed) for a moderate association; $r(3) \geq 0.10 – 0.39$, $p < 0.05$ (Two-Tailed) for a weak association; and $r(3) \geq 0.00 – 0.10$, $p < 0.05$ (Two-Tailed) for a negligible association (Schober et al., 2018)(See Table 2.4).

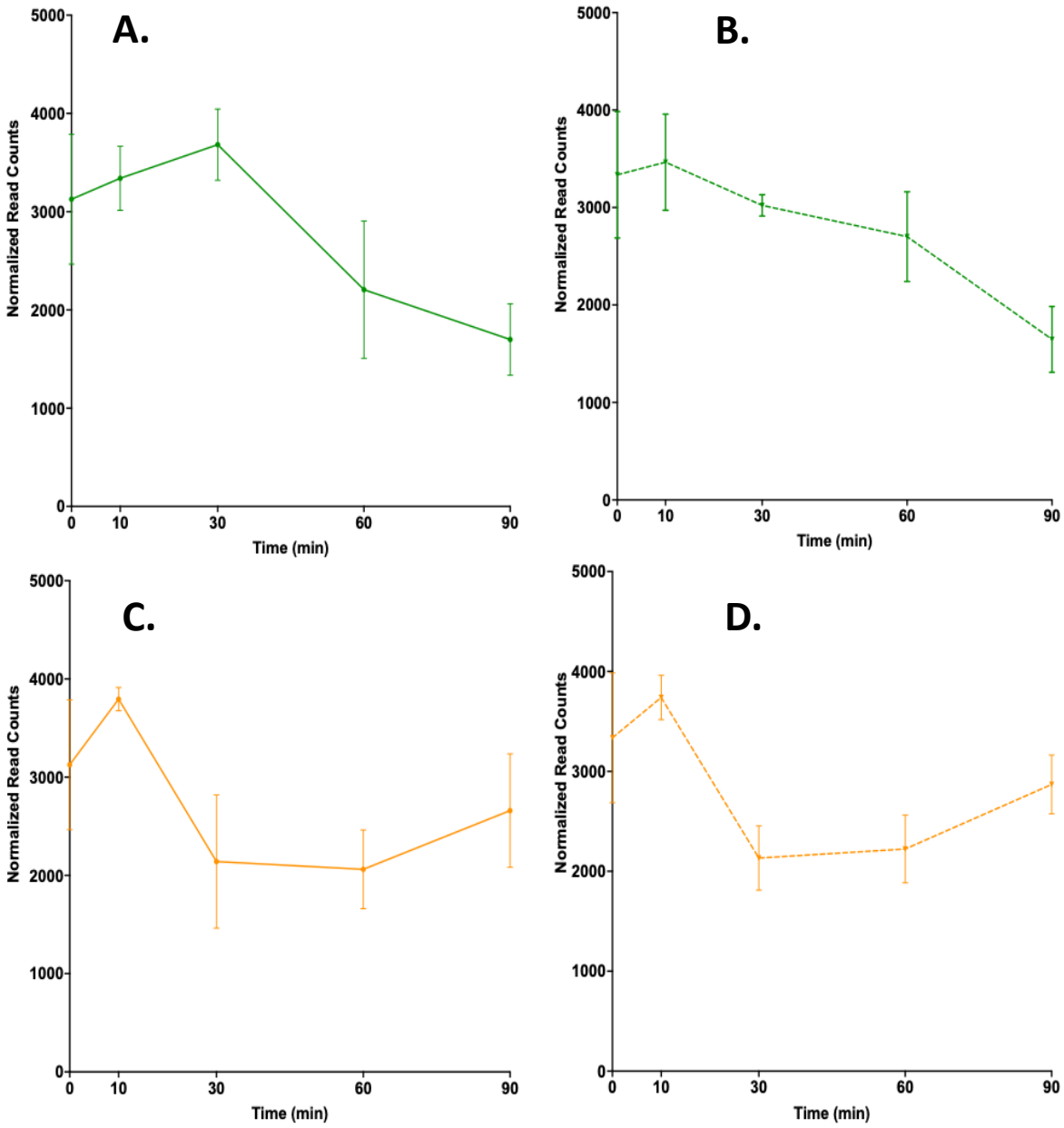

Figure 2.14 Line graphs distribution of malate dehydrogenase reads. Expression of *maeB* gene at (A) HgS, 3 µM Hg, (B) HgR 3 µM Hg, (C) HgS, 4 µM Hg, (D) HgR, 4 µM Hg. Each value is the average read count for the indicated *maeB* gene. Error bars are standard error of 3 biological replicates. Line graphs show (1) the differences in read and (2) the similarities of trajectories at each [$HgCl_2$]. Pearson correlation coefficients were used to assess the strength of linear association between trajectories. We chose the following standards: $r(3) \geq 0.90 – 1.0$, $p < 0.05$ (Two-Tailed) for a very strong positive association; $r(3) \geq 0.70 – 0.89$, $p < 0.05$ (Two-Tailed) for a strong association; $r(3) \geq 0.40 – 0.69$, $p < 0.05$ (Two-Tailed) for a moderate association; $r(3) \geq 0.10 – 0.39$, $p < 0.05$ (Two-Tailed) for a weak association; and $r(3) \geq 0.00 – 0.10$, $p < 0.05$ (Two-Tailed) for a negligible association (Schober et al., 2018)(See Table 2.4).

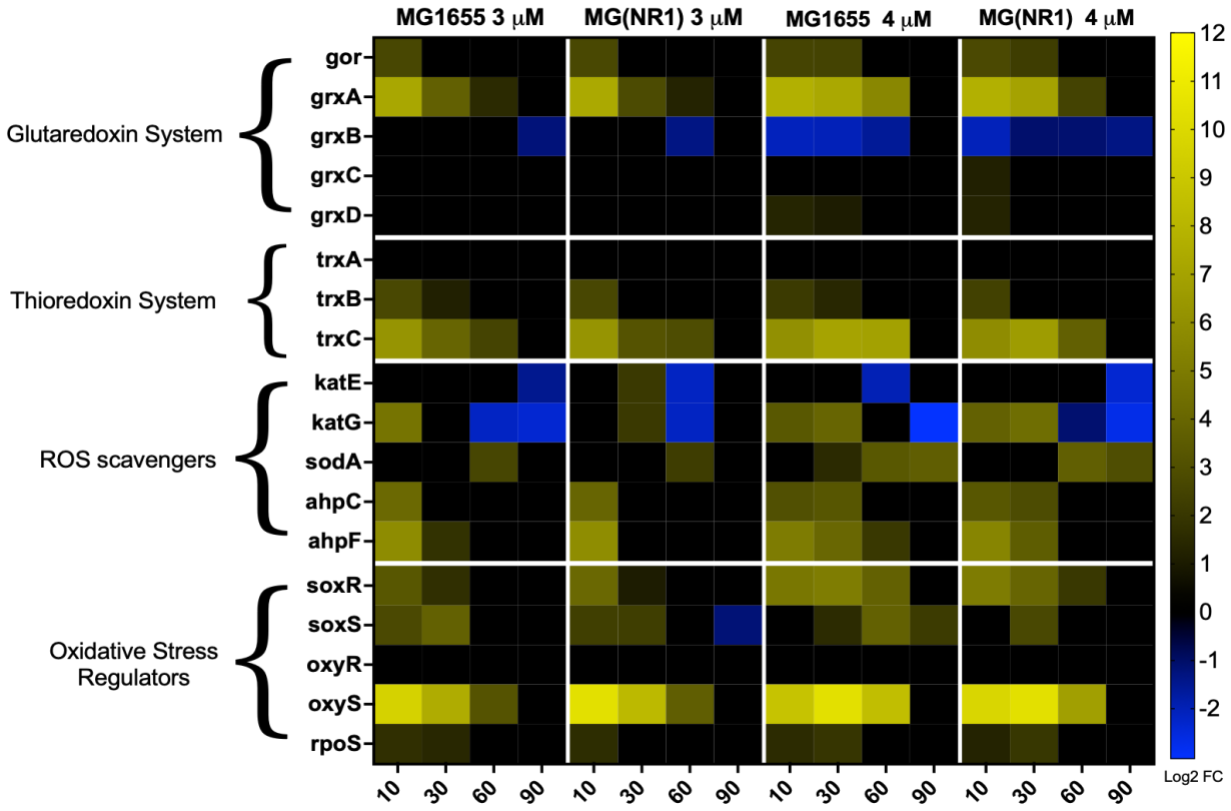

Figure 2.15 A heat map of chromosomal oxidative stress response genes. DEG criteria $Log_2 \leq \pm 1$ and FDR < 0.01.

CHAPTER 3

TRANSCRIPTIONAL RESPONSE OF *ESCHERICHIA COLI* GENES ENCONDING PROTEINS HIGHLY VULNERABLE TO DAMAGE BY MERCURY COMPOUNDS

[1]WIGGINS, A.G., LAVOIE, S.P.; SUMMERS, A.O., To be submitted to *J Biol Inorg Chem.*

Abstract

Mercury (Hg) is a highly reactive toxic metal with both inorganic and organic forms to which aerobic organisms are especially vulnerable. Its avidity for thiols gives it many potential targets including the protein binding sites of benign essential redox active metals such as iron and copper, releasing them to amplify cellular damage via Fenton chemistry production of reactive oxygen species (ROS). To investigate the effects caused by acute inorganic and organic Hg exposure, we implemented proteomics to identify stable Hg-protein binding sites in *Escherichia coli*. Our observation identified 310 proteins that formed stable adducts. Importantly, we found that organic and inorganic mercurial had distinct effects and structural preferences. To reveal the transcriptional response needed for recovery, we applied transcriptomics to our model and exposed *E. coli* without mercury resistance (HgS) to sub-acute Hg concentrations. Proteins observed in energy production and metabolism, ribosomal proteins, and amino acid biosynthesis were highly modified, and their transcriptional response is examined here. The changes in their gene expression were idiosyncratic for each compound, consistent with the idea of distinct biochemical damage requiring alternative transcriptional responses for recovery. This work now serves as a foundation for studying how *E. coli* with mercury resistance (HgR) transcriptionally responds to proteins that formed Hg-adducts.

Introduction

Several common toxic metals are transition elements with incomplete d-orbitals in their electron configuration (Nies, 1999). This provides them the ability to form chemical complexes in biology that may or may not be redox-active. Some heavy-metal cations are essential and

play important roles in biochemical reactions. However, some heavy-metal ions bind too tightly for life to have evolved any physiological functions for their use (e.g., Hg(II), Cd(II), and Ag(I)). Instead, they form non-functional complexes that cause deleterious effects in cells when they encounter them. Once inside the cell, these metals bind to thiol functional groups which can destabilize protein structure, inhibit enzymatic activity, displace essential reactive metals such as iron and copper generating promiscuously toxic reactive oxygen species (ROS) that damage lipids, proteins, and nucleic acids.

Growing recognition of the distinct biochemical effects of inorganic and organic mercurial on living cells is driving changes internationally in industrial and medical uses and disposal of this versatile but dangerous element. There is also increased interest in nutritional and pharmaceutical measures to assist detoxification of humans exposed to mercurial. and related inorganic toxins suspected of contributing to neurological disorders including Parkinsonism and autism. Prokaryotes have evolved an effective way to survive exposure to ionic inorganic mercury, Hg(II), by simply reducing it to volatile monoatomic Hg(0) vapor, a strategy can only applicable for single cell, free living microbes. Multicellular eucaryotic organism systems for defense against toxic metals are related to systems employed in the homeostatic management of essential metals such as copper and zinc. These strategies employ low molecular weight thiol compounds such as glutathione and small proteins such as metallothionein to sequester and discard the deleterious metal by active efflux. Hg's strong bonding to thiols make this thermodynamically ineffective and since thiols are used in many enzymes' active sites and in stabilizing protein folds, Hg has many possible targets it can disable.

Mercury's mobility, chemical reactivity, and bioavailability is due to its specific form, which holds true for its toxic effects inside a cell (LaVoie et al., 2015, Wang et al., 2012, Oram et al., 1996, Cheesman et al., 1988). Both Hg(II) and RHg(I) ions are soft Lewis acids that form stable complexes with high affinity for thiol and selenol groups (Wang et al., 2012). The most stable and abundant complex is in a near-linear, two-coordination between Hg(II) and two thiolate ligands. Despite its high affinity for these ligands, Hg(II) and RHg(I) complexes are kinetically labile, rapidly undergoing ligand exchange with other free thiols or selenols (Wang et al., 2012, Cheesman et al., 1988). Ligand exchange involving a three-coordinate Hg intermediate favors the complex with a higher formation constant (Oram et al., 1996, Cheesman et al., 1988), which also plays a key role in detoxification and resistance (Lian et al., 2014, Hong et al., 2010, Ledwidge et al., 2005, Barkay et al., 2003). There is limited data on the molecular effects different mercury compounds have on model organisms and none have been conducted on cells encoding HgR.

Clear definition of the biochemical and molecular effects of different Hg compounds is fundamental to understanding the damage to cellular processes and how these processes recover. Previously we studied the effects of different mercurial compounds on mercury sensitive (HgS) *Escherichia coli* MG1655 cells growing aerobically and exposed to acute levels of mercurial compounds (LaVoie et al., 2015) in environmentally (Malm, 1998) and clinically relevant concentrations (Summers et al., 1993). We found divalent mercuric chloride ($HgCl_2$) more effectively blocked cellular thiols (on a molar basis) than monovalent organomercurials, i.e., efficacy reflects the valence state. Cells were able to bind Hg(II), but not PMA in several-fold excess over available cellular thiols. X-ray spectroscopy showed that the non-thiol ligands

were in nucleotide bases and histidine of proteins. Using global LC-MS/MS proteomics, we detected protein-mercury adducts in 310 of *E. coli's* proteins when exposed during late exponential phase to 40 µM phenylmercury acetate (PMA). Hg(II)-adducts were also observed likely from breakdown or incomplete synthesis commonly found in all organomercurial products or possibly by dephenylation of PhHg-adducts in random peptides able to provide bis-cysteine coordination and a proton donor similar to the active site of the organomercurial lyase, MerB (Hong et al., 2010, Parks et al., 2009). Of the 310 *E. coli's* proteins showing an adduct, 78 of the 214 chromosomally encoded Fe-binding proteins were observed with multiple PhHg- and/or Hg-adducts, often in proteins with Fe-S clusters and or in proteins doing cluster assembly (LaVoie et al., 2015). Accompanying electron paramagnetic resonance (EPR) spectroscopy revealed massive release of labile Fe from these redox-active clusters. This was the first *in vivo* demonstration of Hg compounds forming stable protein adducts that displaced labile iron. PMA exposure also disrupted cellular electrolyte balance via the KefC antiporter by bis-coordination with glutathione (GSH)-S-conjugates that depleted the free GSH pool. Each organomercurial compound was similar in blocking thiol groups, but Hg(II) displaced more protein-bound iron because of its ability to coordinate two or more cysteines.

We undertook global transcriptomics of *E. coli's* transcriptional response from sub-acute $HgCl_2$ and PMA as it recovered to provide a quantitative system-wide description of *in vivo* effects each mercurial compound had (LaVoie and Summers, 2018). Energy production, intermediary metabolism, and most uptake pathways were down-regulated by both mercurial, but nearly all stress response systems were up-regulated by at least one mercury compound. Motility, biofilm synthesis, phosphate metabolism, certain amino acid biosynthesis pathways,

and several miscellaneous genes were affected differently. We concluded organic and inorganic mercurial had distinct effects on these cellular processes and adduct formation had preferred structural requirements. No previous studies at that time had assessed the molecular underpinnings of distinct effects of mercurial compounds on a global scale in any model system. This work has served as a foundation for understanding how the widely found mobile HgR (mer) locus assists the cell in recovery from Hg exposure.

Here we let proteomic data drive consideration of corresponding transcriptomic data on how bacteria recover with the assistance of plasmid-borne HgR. The strong evolutionary conservation of many of these genes can inform development of diagnostic tools and therapeutic interventions for Hg exposure which remains surprisingly widespread in the developed world (Wiggins et al., 2018, Yin et al., 2016) and nearly universal in the developing world.

Methods

Cell cultures

In both the proteomics (LaVoie et al., 2015) and transcriptomics (LaVoie and Summers, 2018) experiments, *E. coli* K-12 MG1655 was subcultured from cryostorage on lysogeny broth (LB) agar and grown overnight at 37°C. Approximately six well-isolated colonies were inoculated into a 50 ml overnight starter culture of Neidhardt MOPS minimal medium (Neidhardt et al., 1974) supplemented with 20 mg/L uracil and 5 mg/L thiamine and shaken at 250 rpm for 18 h at 37°C.

(a) Peptides were observed by mass spectrometry after fractionation of the global, soluble and insoluble preparations from the standard protocol using a previously described method (Callister et al., 2008). For global proteomics, the saturated overnight cultures were diluted into at 1/40 into 1700 ml of the same medium, divided equally into two 2800 ml Fernbach flasks for optimum aeration and shaken at 250 rpm, 37 °C until achieving an OD_{595} of 0.5 - 0.6. The two cultures were combined for homogeneity and divided again with 800 ml in each Fernbach flask. Phenylmercuric acetate (Fisher) was added to make 40 µM in one flask and the other was untreated. Both cultures incubated at 37C, 250 rpm for 15 min, transferred to 500 ml PE spin bottles and centrifuged at 17,700 x g, for 10 min at 4 °C. Cell pellets were suspended in 8 ml of 50 mM cold ammonium bicarbonate (pH 7.8) at 100X the original culture volume. The cell suspensions were dispensed on ice as 1 ml aliquots for future experiments and iodoacetamide (IAM, Sigma-Aldrich, product # I6125) to 10 mM was added to block reassociation of PMA adducts during proteomic processing. Cell suspensions were stored at -70 °C until shipped on dry ice to the Environmental Molecular Sciences Laboratory at the Pacific-Northwest National Laboratory, Richland, WA, for standard proteomic analysis. See below and also LaVoie *et al*. 2015 for proteomics details.

(b) For RNA-Seq transcriptomics cultures were diluted (1:30) dispensed as 100 ml aliquots in a single flask for each condition (depending on the experiment) into 500-ml Erlenmeyer flasks and incubated shaking at 250 rpm, 37°C to OD_{600} ~0.47 for MG1655 (LaVoie and Summers, 2018) or OD_{595} ~0.4 for MG1655(NR1) (See details in Chapter 2) and then exposed to 3 µM $HgCl_2$ or phenylmercuric acetate (PMA), or untreated and incubation continued for 60 min. Samples for RNA preparation were taken on ice at 0 (pre-exposure) and

at 10, 30, and 60 min after Hg-exposure and immediately centrifuged at 20,800 x g for 3 min at 4 °C. Spent medium was aspirated and cell pellets were frozen at −70 °C within 5 min after collection.

Cell lysis for proteomics

At EMSL, 1 ml cell suspensions were diluted to as necessary in 100 mM ammonium bicarbonate, pH 8.0, with 10 mM IAM which was included through all pre-LC-MS/MS steps. These cell suspensions were then lysed with a PBI Bar Cycler NEP 3229 (Ringham et al., 2007) for ten cycles, holding at 35,000 psi with 20 second intervals. Protein concentrations were determined with the Bradford assay and the cell lysates were immediately fractionated as follows.

Subcellular fractionation for proteomics

Half of each cell lysate was used for the global preparation and the other half was centrifuged to produce the soluble and insoluble fractions. In the latter process, first unbroken cells were removed via centrifugation at 4000 rpm at 4°C for 2 min and the supernatant was removed and further centrifuged at 100,000 rpm for 10 m at 4°C for precipitation of cell walls and ribosomes (aka “insoluble”). The supernatant of the 100K spin (aka “soluble”) was removed and cryoarchived. The insoluble 100K pellet, was suspended in 100 µl of 100 mM ammonium bicarbonate with IAM and centrifuged 100K??? again. The combined supernatants defined the soluble proteins and the proteins remaining in the pellet defined the insoluble proteins. The pellet was solubilized in 50 mM ammonium bicarbonate, pH 7.8 with 1% 3-[3-

(cholamidopropyl)dimethyl-ammonio]-1-proanesulfonate (CHAPS). Protein concentrations insoluble, insoluble, and global fractions were determined by the Bradford assay using BSA as a standard.

Protein denaturation and trypsin lysis of cell fractions for proteomics

Global and soluble fractions were diluted 10-fold with 100 mM ammonium bicarbonate-IAM. The insoluble fractions were diluted with 50 mM ammonium bicarbonate-IAM. Calcium chloride was added to 1 mM and the fractions were digested for 3 h at 37°C with sequencing grade modified trypsin (Promega, Madison WI) at a ratio of 1:50 (wt/wt) trypsin-to-cell protein. Digested proteins were desalted by a C-18 SPE column (Supelco, St. Louis, MO), concentrated by SpeedVac (Thermo Savant, San Jose CA) to 0.1 ml and the peptide content was measured with the BCA assay (Pierce, Rockford IL).

Proteomics peptide detection and identification

Peptides in each fraction were separated by reverse phase liquid chromatography using an established protocol (Kiebel et al., 2006). Triplicate mass spectra of global, soluble and insoluble fractions were obtained on a ThermoScientific Exactive Orbitrap mass spectrometer (Thermo Scientific, San Jose, CA) equipped with a custom built electrospray ionization (ESI) interface (Callister et al., 2008). Peptides in MS/MS spectra identified by SEQUEST based on the Comprehensive Microbial Resource (Peterson et al., 2001) for the genome sequence of *E. coli* K12-MG1655. Cysteine modifications expected were CAM (+57.0215, carbamoyl) or phenylmercury (+278.0019). LC-MS/MS peptide hit lists were generated by SEQUEST using the

E. coli genome sequence (GenBank: U00096.2) and allowing carbamylating by IAM or adducts of phenylHg (PhHg) or Hg (trace contaminant in all organomercurials products) on cysteine. Results for SEQUEST were re-scored by MS-GF (Kim et al., 2010) and SEQUEST matches to Hg and PhHg adducts were additionally re-scored by PeptideProphet (Keller et al., 2005) to maximize true identifications of Hg adducts. Filtering criteria were based on false discovery rates (FDR) computed from searches against a reversed sequence database as decoys. The primary filter for spectral matches was MS-GF's spectral probability, which we required to score less than 1.6e-10 for acceptance of any peptide match. This threshold yielded an FDR of 0.001 over all spectra. To eliminate false discoveries that are singletons, we further improved accuracy by both requiring more than one spectrum for any peptide and, for proteins with only a single observed peptide, requiring a MS-GF spectrum probability less than 1e-11 and at least one tryptic end (semi or fully tryptic). For matches to peptides modified by Hg, we relaxed the MS-GF spectrum probability threshold to 5e-7 but required PeptideProphet's probability to be greater than 0.8 for acceptance. Both thresholds yielded a high FDR when used alone, but when combined and with two additional criteria that peptides be fully tryptic and from proteins passing by the MS-GF spectral probability filter, these criteria produced zero matches to Hg modified decoy sequences (FDR = 0.0). As an alternative estimate of FDR focused on incorrect modifications rather than on incorrect sequences, we used “Hg adducts” detected in the Hg-free samples as a distinct estimate of FDR. This yielded an FDR of 0.009 for spectra identified as Hg-modified.

Purification of mRNA for RNA-Seq

A cell pellet from each condition and sampling time was thawed on ice and total RNA was isolated by RNA*snap*™ (Stead et al., 2012), and stored at -70°C. DNA contamination was removed by two treatments with Turbo-DNase (Ambion; Life Technologies). RNA concentrations and A_{260}/A_{280} ratios were determined using a Nanodrop™ 1000 spectrophotometer (Thermo Scientific). Ribosomal RNA depletion was performed with the Ribo-Zero™ rRNA removal kit for Gram-negative bacteria (Epicentre).

RNA-Seq Library Preparation and Next-generation Sequencing

The quality and quantity of rRNA-depleted RNA was assessed on a 2100 Bioanalyzer RNA pico chip (Agilent Technologies) using manufacturer's recommendations. Next generation sequencing (NGS) libraries were prepared using the Kapa biosystems NGS stranded library prep kit for RNA-Seq with dual indexed Illumina adapters (LaVoie and Summers, 2018) or iTru adapters (Chapter 2). Library insert size was 276 bp, as determined by high sensitivity NGS fragment analysis kit for Fragment Analyzer™ (Advanced Analytical Technologies) using manufacturer's instructions. Quantification of each library was done by qPCR and all 30 libraries were pooled in equal concentrations. The library preparation, quality analysis, and pooling were performed by the Georgia Genomics Facility (http://dna.uga.edu). Paired-end (2 x 50 bp) sequencing of the pooled libraries using the Illumina HiSeq 2000 platform (LaVoie and Summers, 2018) was performed by the HudsonAlpha Institute for Biotechnology Genomic Services Laboratory (http://gsl.hudsonalpha.org) or paired-end (2 x 75 bp) sequencing of pooled libraries using or NextSeq 2500 platform by Georgia Genomics Facility (Chapter 2).

Data processing of transcriptomics samples

Quality control of Illumina data was carried out as describe previously for HgS cultures (LaVoie and Summers, 2018) and HgS and HgR cells (Chapter 2 of Dissertation). Mapped read counts were analyzed for significant differential expression (false discovery rate ≤ 0.01, fold-change ≥ ± 2) using the baySeq package in R for HgS cells and DESeq2 package in R for HgS and HgR cells. All genes that did not meet both the ≤1% FDR and ≥2 fold-change criteria were indicated as no-change in figures, tables, and text. Two-way comparisons were made for all three biological replicates of each condition and time point for $HgCl_2$ exposure or PMA exposure versus their unexposed control.

Results and Discussion

Hg effects on energy metabolism

Many steps in energy generation are reduction or oxidation reactions that depend on redox-active metal ions with sulfur, selenium, and nitrogen ligands that are susceptible to mercury binding (LaVoie and Summers, 2018). Another Group 12 metal, cadmium, repressed aerobic energy metabolism genes in *E. coli*, suggesting a shift towards anaerobic pathways (Wang and Crowley, 2005). However, mercury compounds differentially affected aerobic and anaerobic energy metabolism (LaVoie and Summers, 2018). The oxygen sensors *fnr* (Salmon et al., 2003) and *aer* (Bibikov et al., 2000) that trigger the anaerobic shift were up-regulated by PMA but unchanged with $HgCl_2$ in *E. coli* (LaVoie and Summers, 2018). Expression of glucose metabolism genes declined with PMA and Hg(II) exposure, but twice as many genes were down with PMA exposure (LaVoie and Summers, 2018). We also observed Hg-adducts in three ATP-

synthase subunits, isocitrate dehydrogenase, NADH:quinone oxidoreductase subunit F, and the A and B subunits of succinate:quinone oxidoreductase (Table 3.1)(LaVoie et al., 2015). All these proteins formed multiple adducts with monovalent PMA, except *nuoF* (Table 3.2) but only four formed divalent adducts with Hg(II) (Table 3.2).

Hg-adducts occurred in three of the nine ATP synthase proteins (Table 3.2, Fig. 3.2). The ATPase subunit A formed 86 PMA- and 16 Hg(II)-adducts (Table 3.2). The A subunit is the largest of the 9 subunits (Rao et al., 1988) essential in forming the membrane-intrinsic F_o component and in coupling the F_1 and F_o components (Rao et al., 1988). Potentially, Hg binding could disrupt ATP-synthase complex at many sites. Lrp represses the ATPase operon but was not differentially expressed at any time. Mercury exposure of HgS cells decreased expression of all nine ATP-synthase subunits up to 30 min (LaVoie et al., 2015), but HgR cells restored expression of these Hg-vulnerable proteins roughly 20 min before HgS cells could (Fig. 3.2).

Only the F subunit *(nuoF)* of the 13 NADH dehydrogenase I subunits (Fig. 3.2) exhibited a PhHg adduct. NuoF lies within the inner membrane serving the electron input role in the enzyme via its cysteine rich 4Fe-4S cluster (Braun et al., 1998, Leif et al., 1995), which would have been disrupted by the PhHg adduct. Although NuoF had no stable Hg(II) adduct this compound also resulted in less transcription. The *nuoF* gene is dually controlled by the oxygen-sensing repressor FNR and bacterial histone-like global regulator IHF (Bongaerts et al., 1995). IHF was immediately up-regulated with PMA, but not until 30 min with $HgCl_2$ (LaVoie and Summers, 2018). NuoF was initially down-regulated in both strains but the HgR cells restored normal NADH dehydrogenase I expression by 30 min (Fig. 3.2). Quicker recovery in the HgR cells of both ATP-synthase and the electron transport chain is consistent with their observed

resumption of mid-logarithmic growth at 30 min (Fig. 2.3, green), i.e., the HgS chromosome alone lacks adequate resources to repair or remake these core energy-generating complexes. Since both ATP-synthase and NADPH dehydrogenase are largely inner membrane proteins, it is unlikely that cytosolic MerA could directly remove the offending Hg adducts, so the functions of these two protein complexes are likely restored not by repair, but synthesis of fresh proteins once MerA has eliminated Hg from the cytosol.

The TCA cycle enzymes isocitrate (*icd*) and succinate dehydrogenase (*sdhABCD*) both contained mercury adducts: PhHg-adducts in the catalytic [3Fe-4S] complex of subunits *sdhAB* (Yankovskaya et al., 2003) and Hg(II)-adducts in *icd* both of which would likely have rendered the enzymes non-functional (Table 3.2, Fig. 3.2). Cra and Nac activate transcription of *icd* (Chao et al., 1997), but neither were differentially expressed (LaVoie and Summers, 2018). PMA did not alter *icd* expression, but Hg(II) immediately increased *icd* transcription in the HgS strain (Fig. 3.2). It is noteworthy that Icd is always very highly expressed so although the ~ 30% increase in reads did not meet the typical standard for a DEG it resulted in considerably more reads than for many other glycolysis and TCA cycle proteins and the increase persisted over several time points in both levels of Hg (Fig. 2.11B). Thus, we consider it a physiologically relevant response to mercuric Hg(II) but not to PMA. However, that these two responses diverge suggests that damage to the protein does not control its transcription; rather PMA and Hg likely affect differentially the proteins that control transcription of the operon, which are Cra and Nac.

PMA exposure decreased expression of succinate dehydrogenase, but $HgCl_2$ did not (LaVoie and Summers, 2018), although the HgR strain strongly increases both SdhAB subunits very late in the experiment, perhaps reflecting continued post-repair growth when the

unexposed control has already used all its glucose and achieved saturation. The *sdhABCD* operon is repressed by the oxygen-sensing FNR activator in response to anaerobic shift, which *fnr* was up-regulated in HgS cells in PMA exposure but not by Hg (LaVoie and Summers, 2018). This suggests that FNR might be responding to Hg(II) as if it were oxidative damage. Hg can form disulfides of vicinal protein thiols which would mimic an early event in oxidative stress.

Hg-adducts of ribosomal proteins

Fourteen ribosomal proteins formed Hg-adducts (Table 3.3), so it is plausible that ribosome structure, assembly, and/or function could be affected (LaVoie et al., 2015). Many of these proteins are known to bind zinc and are a major tightly regulated reservoir of Zn(II) in *E. coli*. Inorganic mercury exposure repressed expression of up to 85% of ribosomal proteins and 74% at 10 min and 30 min in HgS cells (LaVoie and Summers, 2018). Transcription of ribosomal proteins is regulated by the nutritional stress-induced nucleotide (ppGpp) and binding of DksA to RNA polymerase. Together ppGpp and DksA inhibit ribosomal protein expression and transcription of rRNA operons, which encode rRNAs and some tRNAs (Lemke et al., 2011). Although ppGpp synthase genes, *spoT* and *relA*, are down-regulated or unchanged, *dksA* is up-regulated for both Hg and PMA (LaVoie and Summers, 2018). Ribosomal protein expression can also be inhibited by translational feedback due to excess ribosomal proteins binding their own mRNA and inhibiting its translation (Nomura et al., 1984, Wilson and Nierhaus, 2007). Hg(II) will readily displace Zn(II) in these largely cysteine and histidine Zn(II) binding sites in these proteins. Large scale release of Zn(II) from those that are part of that reservoir would engage the Zn(II) homeostasis apparatus controlled by ZntR which controls the ZntA efflux pump under

excess Zn(II) and the Zn(II) uptake pump, Znu which is repressed by Zur under replete Zn(II) conditions. The HgR strain restored transcription of a few Hg-adducted r-proteins by 30 min and 53% of those genes by 60 min (Fig. 3.3) when the HgR strain was growing at a rate similar unexposed cells (Fig. 2.3, green).

Leader peptides of histidine and leucine

Hg-adducts occurred in 54 proteins associated with amino acid biosynthesis (Table 3.4). Several require a precursor leader peptide to direct biosynthesis (Oman and Van Der Donk, 2010). Several biosynthetic pathways respond uniquely to each mercury compound (LaVoie and Summers, 2018) (Fig. 3.3). In particular, the leader peptide and genes associated with biosynthesis of histidine and leucine were transcriptionally expressed differently depending on exposure to a given mercury compounds (Fig. 3.4).

The histidine operon (*hisLGDCBHAFI*) is controlled normally by transcriptional attenuation (Alifano et al., 1996)6) mediated by timely translation of a leader peptide (*hisL*) that contains seven histidine residues (Barnes, 1978, Blasi et al., 1973). The pace of the ribosome depends on availability of histidyl-charged tRNAs and controls which of two alternative loops can form in the mRNA between the ribosome and RNA polymerase, one of which would terminate transcription. The bis-coordination formation constants of Hg(II) with the histidine imidazole is 10^{15} M^{-1} (Brooks and Davidson, 1960), with the imino nitrogen-3 of the thymine ring (Brooks – Davidson, 1959) and uracil in RNA of 10^{20} M^{-1} (Olliff, manuscript in preparation) offering several points at which Hg(II) (but not monovalent PMA) could simulate histidine starvation leading to higher expression than any other amino acid pathway. The *his* operon can

also be activated by *dksA* and *dnaJ* which are also upregulated by Hg(II) (LaVoie and Summers, 2018), (Fig. 3.3 and 3.4).

Leucine biosynthesis (*leuLABCD*) is also regulated by attenuation (Wessler and Calvo, 1981). PMA exposure increased transcription of operon, but Hg(II) exposure did not (Fig. 3.3 and 3.4) (LaVoie and Summers, 2018). Translation of the leader peptide controls four of five enzymes for synthesis of isoleucine and valine; LeuL has 32 amino acids including multiple isoleucine, valine, and leucine resides (and thus many uracil-rich codons in the mRNA) but no cysteines or histidine residues (Wessler and Calvo, 1981). In HgR cells, $HgCl_2$ decreased expression for isoleucine, valine, and leucine but PMA increased their expression (LaVoie and Summers, 2018). (Fig. 3.3 and 3.4).

Small RNAs also figure in a distinct COG category (oxidative stress) as manifest by the strong up-regulation of which controls a protein and another small RNA involved in formation and repair of Fe-S centers which are prime targets of Hg(II) damage (LaVoie 2015 and 2018).

Conclusion

We approached this descriptive study without specific preconceived ideas about what correspondence there might be between a protein's binding PhHg or Hg and a transcriptional response, up, down, or none. Since global bottom-up proteomics is not quantitative, we did not expect to see precise quantitative correspondence of observed spectra and observed mRNA reads. However, it was satisfying that the distribution of proteins vulnerable to mercurial damage corresponded generally with the numbers of proteins in the various COG categories as did the statistically significant transcriptional responses. We provisionally interpret these results to

reflect the pervasiveness and versatility of mercury as a toxicant, not limited to a narrow subset of biological systems or even to thiol or selenol targets. That said, within several COG categories there are specific processes that are more vulnerable as reflected by either proteomics or transcriptomics and often by both. Of special interest are pathways regulated by leader and/or small RNAs. Hg(II) binding *in vitro* to imino nitrogen of thymine and histidine has long been regarded as a curiosity without biological relevance because millimolar thiol buffering in all aerobic or facultative organisms would compete as ligands for any mercurial. However, LaVoie, 2015 and 2018 Hg(II) showed, and Wiggins confirmed and extended (Chapters 2 and 3) that redox shock by even sub-acute Hg exposure depletes thiols to the extent that Hg(II) will take nitrogen ligands. Once formed within a larger DNA molecule the thymine-Hg-thymine crosslink is stable to a 3-fold molar excess of thiol (Olliff, manuscript in preparation), so we are continuing examination of Hg(II) as an azophilic toxicant under a DOE award with collaborators in Canada. These datasets contain many other promising leads for understanding the cell biology of recovery.

References

ALIFANO, P., FANI, R., LIÒ, P., LAZCANO, A., BAZZICALUPO, M., CARLOMAGNO, M. S. & BRUNI, C. B. 1996. Histidine biosynthetic pathway and genes: structure, regulation, and evolution. *Microbiological reviews,* 60**,** 44-69.

BARKAY, T., MILLER, S. M. & SUMMERS, A. O. 2003. Bacterial mercury resistance from atoms to ecosystems. *FEMS microbiology reviews,* 27**,** 355-384.

BARNES, W. M. 1978. DNA sequence from the histidine operon control region: seven histidine codons in a row. *Proceedings of the National Academy of Sciences,* 75**,** 4281-4285.

BIBIKOV, S. I., BARNES, L. A., GITIN, Y. & PARKINSON, J. S. 2000. Domain organization and flavin adenine dinucleotide-binding determinants in the aerotaxis signal transducer Aer of Escherichia coli. *Proceedings of the National Academy of Sciences,* 97**,** 5830-5835.

BLASI, F., BRUNI, C. B., AVITABILE, A., DEELEY, R. G., GOLDBERGER, R. F. & MEYERS, M. M. 1973. Inhibition of transcription of the histidine operon in vitro by the first enzyme of the histidine pathway. *Proceedings of the National Academy of Sciences,* 70**,** 2692-2696.

BONGAERTS, J., ZOSKE, S., WEIDNER, U. & LINDEN, G. 1995. Transcriptional regulation of the proton translocating NADH dehydrogenase (nuoA-N) of Escherichia coli by electron acceptors, electron donors and gene regulators. *Molecular microbiology,* 16**,** 521-534.

BRAUN, M., BUNGERT, S. & FRIEDRICH, T. 1998. Characterization of the overproduced NADH dehydrogenase fragment of the NADH: ubiquinone oxidoreductase (complex I) from Escherichia coli. *Biochemistry,* 37**,** 1861-1867.

BROOKS, P. & DAVIDSON, N. 1960. Mercury (II) complexes of imidazole and histidine. *Journal of the American Chemical Society,* 82**,** 2118-2123.

CALLISTER, S. J., MCCUE, L. A., TURSE, J. E., MONROE, M. E., AUBERRY, K. J., SMITH, R. D., ADKINS, J. N. & LIPTON, M. S. 2008. Comparative bacterial proteomics: analysis of the core genome concept. *PloS one,* 3**,** e1542.

CHAO, G., SHEN, J., TSENG, C. P., PARK, S.-J. & GUNSALUS, R. P. 1997. Aerobic regulation of isocitrate dehydrogenase gene (icd) expression in Escherichia coli by the arcA and fnr gene products. *Journal of bacteriology,* 179**,** 4299-4304.

CHEESMAN, B. V., ARNOLD, A. P. & RABENSTEIN, D. L. 1988. Nuclear magnetic resonance studies of the solution chemistry of metal complexes. 25. Hg (thiol) 3 complexes and Hg (II)-thiol ligand exchange kinetics. *Journal of the American Chemical Society,* 110**,** 6359-6364.

HONG, B., NAUSS, R., HARWOOD, I. M. & MILLER, S. M. 2010. Direct measurement of mercury (II) removal from organomercurial lyase (MerB) by tryptophan fluorescence: NmerA domain of coevolved γ-proteobacterial mercuric ion reductase (MerA) is more efficient than MerA catalytic core or glutathione. *Biochemistry,* 49**,** 8187-8196.

KELLER, A., ENG, J., ZHANG, N., LI, X. J. & AEBERSOLD, R. 2005. A uniform proteomics MS/MS analysis platform utilizing open XML file formats. *Molecular systems biology,* 1**,** 2005.0017.

KIEBEL, G. R., AUBERRY, K. J., JAITLY, N., CLARK, D. A., MONROE, M. E., PETERSON, E. S., TOLIĆ, N., ANDERSON, G. A. & SMITH, R. D. 2006. PRISM: a data management system for high-throughput proteomics. *Proteomics,* 6**,** 1783-1790.

KIM, S., MISCHERIKOW, N., BANDEIRA, N., NAVARRO, J. D., WICH, L., MOHAMMED, S., HECK, A. J. & PEVZNER, P. A. 2010. The generating function of CID, ETD, and CID/ETD pairs of tandem mass spectra: applications to database search. *Molecular & Cellular Proteomics,* 9**,** 2840-2852.

LAVOIE, S. P., MAPOLELO, D. T., COWART, D. M., POLACCO, B. J., JOHNSON, M. K., SCOTT, R. A., MILLER, S. M. & SUMMERS, A. O. 2015. Organic and inorganic mercurials have distinct effects on cellular thiols, metal homeostasis, and Fe-binding proteins in Escherichia coli. *JBIC Journal of Biological Inorganic Chemistry,* 20**,** 1239-1251.

LAVOIE, S. P. & SUMMERS, A. O. 2018. Transcriptional responses of Escherichia coli during recovery from inorganic or organic mercury exposure. *BMC genomics,* 19**,** 1-24.

LEDWIDGE, R., PATEL, B., DONG, A., FIEDLER, D., FALKOWSKI, M., ZELIKOVA, J., SUMMERS, A. O., PAI, E. F. & MILLER, S. M. 2005. NmerA, the metal binding domain of mercuric ion reductase, removes Hg2+ from proteins, delivers it to the catalytic core, and protects cells under glutathione-depleted conditions. *Biochemistry,* 44**,** 11402-11416.

LEIF, H., SLED, V. D., OHNISHI, T., WEISS, H. & FRIEDRICH, T. 1995. Isolation and characterization of the proton-translocating NADH: ubiquinone oxidoreductase from Escherichia coli. *European journal of biochemistry,* 230**,** 538-548.

LIAN, P., GUO, H.-B., RICCARDI, D., DONG, A., PARKS, J. M., XU, Q., PAI, E. F., MILLER, S. M., WEI, D.-Q. & SMITH, J. C. 2014. X-ray structure of a Hg2+ complex of mercuric reductase (MerA) and quantum mechanical/molecular mechanical study of Hg2+ transfer between the C-terminal and buried catalytic site cysteine pairs. *Biochemistry,* 53**,** 7211-7222.

MALM, O. 1998. Gold mining as a source of mercury exposure in the Brazilian Amazon. *Environmental research,* 77**,** 73-78.

NEIDHARDT, F. C., BLOCH, P. L. & SMITH, D. F. 1974. Culture medium for enterobacteria. *Journal of bacteriology,* 119**,** 736-747.

NIES, D. H. 1999. Microbial heavy-metal resistance. *Applied microbiology and biotechnology,* 51**,** 730-750.

OMAN, T. J. & VAN DER DONK, W. A. 2010. Follow the leader: the use of leader peptides to guide natural product biosynthesis. *Nature chemical biology,* 6**,** 9-18.

ORAM, P. D., FANG, X., FERNANDO, Q., LETKEMAN, P. & LETKEMAN, D. 1996. The formation constants of mercury (II)− glutathione complexes. *Chemical research in toxicology,* 9**,** 709-712.

PARKS, J. M., GUO, H., MOMANY, C., LIANG, L., MILLER, S. M., SUMMERS, A. O. & SMITH, J. C. 2009. Mechanism of Hg− C protonolysis in the organomercurial lyase MerB. *Journal of the American Chemical Society,* 131**,** 13278-13285.

PETERSON, J. D., UMAYAM, L. A., DICKINSON, T., HICKEY, E. K. & WHITE, O. 2001. The comprehensive microbial resource. *Nucleic acids research,* 29**,** 123-125.

RAO, R., PAGAN, J. & SENIOR, A. 1988. Directed mutagenesis of the strongly conserved lysine 175 in the proposed nucleotide-binding domain of alpha-subunit from Escherichia coli F1-ATPase. *Journal of Biological Chemistry,* 263**,** 15957-15963.

SALMON, K., HUNG, S.-P., MEKJIAN, K., BALDI, P., HATFIELD, G. W. & GUNSALUS, R. P. 2003. Global gene expression profiling in Escherichia coli K12: the effects of oxygen availability and FNR. *Journal of Biological Chemistry,* 278**,** 29837-29855.

STEAD, M. B., AGRAWAL, A., BOWDEN, K. E., NASIR, R., MOHANTY, B. K., MEAGHER, R. B. & KUSHNER, S. R. 2012. RNA snap™: a rapid, quantitative and inexpensive, method for isolating total RNA from bacteria. *Nucleic acids research,* 40**,** e156-e156.

SUMMERS, A., WIREMAN, J., VIMY, M., LORSCHEIDER, F., MARSHALL, B., LEVY, S., BENNETT, S. & BILLARD, L. 1993. Mercury released from dental" silver" fillings provokes an increase in mercury-and antibiotic-resistant bacteria in oral and intestinal floras of primates. *Antimicrobial agents and chemotherapy,* 37**,** 825-834.

WANG, A. & CROWLEY, D. E. 2005. Global gene expression responses to cadmium toxicity in Escherichia coli. *Journal of bacteriology,* 187**,** 3259-3266.

WANG, F., LEMES, M. & KHAN, M. A. 2012. Metallomics of mercury: Role of thiol-and selenol-containing biomolecules. *Environmental Chemistry and Toxicology of Mercury,* 517.

WESSLER, S. R. & CALVO, J. M. 1981. Control of leu operon expression in Escherichia coli by a transcription attenuation mechanism. *Journal of molecular biology,* 149**,** 579-597.

YANKOVSKAYA, V., HORSEFIELD, R., TORNROTH, S., LUNA-CHAVEZ, C., MIYOSHI, H., LÉGER, C., BYRNE, B., CECCHINI, G. & IWATA, S. 2003. Architecture of succinate dehydrogenase and reactive oxygen species generation. *Science,* 299**,** 700-704.

Table 3.1: Differential expression of genes for proteins that formed stable mercury adducts during in vivo exposure. Using global LC-MS/MS proteomics 310 proteins were found to form stable mercury adducts upon exposure of late exponential phase *E. coli* cultures to acute levels of PMA or Merthiolate (LaVoie et al., 2015). Fold-change expression of these genes are from two RNA-Seq global expression analyses: (A) PMA, (B) Hg(II) (LaVoie and Summers, 2018, and (C) NR1 plasmid + Hg(II) (Wiggins, Chapter 2). Genes (Column B) with proteins (D) yielding stable PhHg (E, pink) or Hg (I, orange). For RNA-seq data (F-H, J-O) yellow** means positive fold-change and blue means negative fold-change upon indicated mercury exposure compared to the unexposed culture at indicated time point.

gene_id	gene_name	PMA_t10	PMA_t30	PMA_t60	Hg_t10	Hg_t30	Hg_t60	NR1_t10	NR1_t30	NR1_t60
b2316	accD	2.84	2.73	n.s.	n.s.	n.s.	n.s.	n.s.	n.s.	n.s.
b4015	aceA	-10.09	-7.26	n.s.	n.s.	n.s.	n.s.	n.s.	n.s.	n.s.
b4014	aceB	-2.83	n.s.	n.s.	n.s.	n.s.	n.s.	n.s.	n.s.	n.s.
b0114	aceE	n.s.	-2.16	n.s.	n.s.	-2.31	n.s.	n.s.	n.s.	n.s.
b0115	aceF	-3.13	-4.20	n.s.	n.s.	-3.28	n.s.	n.s.	n.s.	n.s.
b2296	ackA	n.s.	n.s.	n.s.	n.s.	-2.61	-3.49	n.s.	n.s.	-2.47
b0118	acnB	-6.22	-7.23	n.s.	2.49	2.32	n.s.	2.364	n.s.	n.s.
b1241	adhE	-19.68	-33.05	n.s.	-4.88	-8.64	-8.58	-2.63	n.s.	-2.13
b0605	ahpC	3.14	2.49	n.s.	14.69	2.79	n.s.	15.362	n.s.	n.s.
b2697	alaS	n.s.	n.s.	n.s.	-2.81	-2.98	n.s.	-2.43	n.s.	n.s.
b1415	aldA	-14.97	-6.91	n.s.	-5.02	-2.46	n.s.	-5.48	n.s.	5.40
b3959	argB	-9.50	-5.29	n.s.	-5.66	n.s.	n.s.	-6.57	n.s.	11.23
b3359	argD	-10.89	-4.00	n.s.	-3.33	n.s.	n.s.	-4.02	n.s.	10.31
b3957	argE	n.s.	n.s.	n.s.	n.s.	2.50	n.s.	n.s.	n.s.	2.12
b0273	argF	-12.18	-6.27	n.s.	-3.72	n.s.	n.s.	-4.49	n.s.	12.66
b3172	argG	-5.60	-5.17	n.s.	-4.35	-2.69	n.s.	-4.78	n.s.	7.55
b3960	argH	-6.66	-5.63	n.s.	-4.90	-2.49	n.s.	-4.50	n.s.	9.48
b4254	argI	n.s.	n.s.	n.s.	n.s.	-2.49	n.s.	n.s.	n.s.	5.44
b2310	argT	n.s.	2.29	n.s.	2.49	2.32	n.s.	n.s.	n.s.	n.s.
b2255	arnA	-16.89	-12.21	n.s.	-7.10	-4.73	n.s.	-5.89	n.s.	n.s.
b0754	aroG	n.s.	n.s.	n.s.	n.s.	n.s.	n.s.	n.s.	n.s.	n.s.
b3433	asd	n.s.	-2.06	n.s.	n.s.	n.s.	n.s.	n.s.	n.s.	n.s.
b0674	asnB	n.s.	n.s.	n.s.	-2.16	n.s.	n.s.	n.s.	n.s.	n.s.
b0930	asnS	2.05	2.62	n.s.	n.s.	n.s.	n.s.	n.s.	n.s.	n.s.
b3734	atpA	-3.61	-3.65	n.s.	-3.56	-4.09	n.s.	-2.63	n.s.	n.s.
b3732	atpD	-2.13	-5.16	n.s.	-3.27	-4.28	n.s.	-2.53	n.s.	n.s.
b3735	atpH	-3.47	-2.96	n.s.	-4.28	-4.13	n.s.	-3.49	n.s.	n.s.
b2480	bcp	4.33	4.22	n.s.	n.s.	3.67	n.s.	n.s.	n.s.	n.s.
b0126	can	n.s.	n.s.	n.s.	2.29	3.57	2.58	n.s.	n.s.	n.s.
b0032	carA	-34.58	-15.75	n.s.	-4.64	n.s.	n.s.	-5.44	n.s.	4.77
b1888	cheA	-3.04	-2.94	n.s.	n.s.	n.s.	-2.64	n.s.	n.s.	n.s.
b2592	clpB	n.s.	n.s.	n.s.	19.05	4.13	n.s.	14.449	n.s.	n.s.
b3032	cpdA	n.s.	n.s.	n.s.	n.s.	n.s.	n.s.	n.s.	n.s.	n.s.
b0123	cueO	5.49	n.s.	-5.88	20.73	17.82	n.s.	8.113	n.s.	-3.64
b1275	cysB	-3.65	-2.42	n.s.	-2.15	-3.17	n.s.	-2.19	n.s.	n.s.
b2752	cysD	-51.39	-47.15	n.s.	n.s.	-11.78	n.s.	n.s.	n.s.	3.60
b2763	cysI	-39.87	-165.83	n.s.	-2.47	-13.88	n.s.	-2.15	n.s.	3.17
b4214	cysQ	4.46	2.74	n.s.	3.04	2.97	n.s.	2.584	n.s.	n.s.
b0632	dacA	n.s.	n.s.	n.s.	-3.37	n.s.	n.s.	-2.75	n.s.	n.s.
b2478	dapA	3.85	2.78	n.s.	n.s.	n.s.	n.s.	n.s.	n.s.	n.s.
b0031	dapB	-2.01	n.s.	n.s.	-2.43	-2.05	n.s.	-2.68	n.s.	n.s.
b0166	dapD	n.s.	n.s.	n.s.	n.s.	n.s.	n.s.	n.s.	n.s.	n.s.
b1919	dcyD	-3.40	-2.73	n.s.	n.s.	-3.21	n.s.	n.s.	n.s.	n.s.
b3162	deaD	n.s.	n.s.	n.s.	n.s.	n.s.	n.s.	n.s.	n.s.	2.74
b3287	def	3.25	2.48	n.s.	8.32	2.02	n.s.	6.782	n.s.	n.s.
b4381	deoC	-2.43	-2.68	n.s.	n.s.	n.s.	n.s.	n.s.	n.s.	n.s.
b0160	dgt	3.10	n.s.	n.s.	n.s.	n.s.	n.s.	n.s.	n.s.	n.s.
b1198	dhaM	-4.33	-4.29	n.s.	-2.98	-4.36	n.s.	-2.20	n.s.	n.s.
b0145	dksA	3.69	4.98	n.s.	2.40	3.77	n.s.	n.s.	n.s.	n.s.

b1591	dmsD	2.34	n.s.	n.s.	n.s.	n.s.	n.s.	n.s.	n.s.	n.s.
b0015	dnaJ	n.s.	n.s.	n.s.	5.62	n.s.	n.s.	4.377	n.s.	n.s.
b3860	dsbA	n.s.	n.s.	n.s.	n.s.	n.s.	n.s.	n.s.	n.s.	n.s.
b3640	dut	2.44	2.27	n.s.	n.s.	2.31	n.s.	n.s.	n.s.	n.s.
b1850	eda	n.s.	n.s.	n.s.	n.s.	n.s.	n.s.	n.s.	n.s.	n.s.
b3209	elbB	n.s.	-2.05	n.s.	2.05	n.s.	n.s.	2.218	n.s.	n.s.
b2779	eno	-3.75	-2.61	n.s.	-2.74	-4.27	n.s.	-2.19	n.s.	n.s.
b4391	ettA	n.s.	n.s.	n.s.	n.s.	n.s.	n.s.	n.s.	n.s.	n.s.
b1092	fabD	n.s.	n.s.	n.s.	n.s.	n.s.	n.s.	n.s.	n.s.	n.s.
b1288	fabI	-3.22	-3.23	n.s.	n.s.	n.s.	n.s.	n.s.	n.s.	n.s.
b0180	fabZ	n.s.	n.s.	n.s.	n.s.	n.s.	n.s.	n.s.	n.s.	n.s.
b2925	fbaA	-2.58	-5.33	n.s.	n.s.	-4.66	n.s.	n.s.	n.s.	n.s.
b4232	fbp	2.98	2.16	n.s.	3.82	2.31	n.s.	3.036	n.s.	n.s.
b2525	fdx	n.s.	n.s.	n.s.	2.38	n.s.	n.s.	n.s.	n.s.	n.s.
b0684	fldA	2.07	n.s.	n.s.	3.16	n.s.	n.s.	2.524	n.s.	n.s.
b3288	fmt	n.s.	2.00	n.s.	6.54	n.s.	n.s.	4.735	n.s.	n.s.
b0529	folD	n.s.	2.08	n.s.	n.s.	n.s.	n.s.	n.s.	n.s.	n.s.
b3178	ftsH	n.s.	n.s.	n.s.	5.76	n.s.	n.s.	4.661	n.s.	n.s.
b1612	fumA	n.s.	n.s.	n.s.	n.s.	n.s.	n.s.	n.s.	n.s.	2.33
b0683	fur	n.s.	n.s.	n.s.	12.75	8.71	n.s.	10.118	n.s.	n.s.
b3340	fusA	n.s.	n.s.	n.s.	-2.45	-3.02	n.s.	-2.16	n.s.	n.s.
b0756	galM	2.60	2.27	n.s.	2.83	2.11	n.s.	2.389	n.s.	n.s.
b1236	galU	n.s.	n.s.	n.s.	n.s.	n.s.	n.s.	n.s.	n.s.	n.s.
b1779	gapA	-2.00	-2.82	n.s.	-2.15	-4.47	-3.71	n.s.	n.s.	n.s.
b2094	gatA	-18.78	-46.42	n.s.	-13.35	-25.82	n.s.	-8.94	-2.08	n.s.
b2093	gatB	-13.16	-76.02	n.s.	-13.23	-20.89	n.s.	-8.40	-2.13	n.s.
b2096	gatY	-7.65	-9.55	n.s.	-5.24	-9.75	-13.14	-3.21	n.s.	n.s.
b2095	gatZ	-12.71	-14.87	n.s.	-11.92	-18.42	n.s.	-7.86	n.s.	n.s.
b2905	gcvT	n.s.	n.s.	4.75	n.s.	n.s.	n.s.	n.s.	-2.91	3.67
b1761	gdhA	-4.91	-5.11	n.s.	n.s.	-2.80	n.s.	n.s.	n.s.	n.s.
b3553	ghrB	n.s.	n.s.	n.s.	2.16	n.s.	n.s.	n.s.	n.s.	n.s.
b3429	glgA	-2.62	-3.17	n.s.	-2.06	-3.08	n.s.	n.s.	n.s.	n.s.
b3176	glmM	n.s.	n.s.	n.s.	2.16	n.s.	n.s.	n.s.	n.s.	n.s.
b3729	glmS	n.s.	n.s.	n.s.	-2.21	n.s.	n.s.	n.s.	n.s.	n.s.
b3870	glnA	-13.97	-27.05	n.s.	-9.36	-9.75	n.s.	-7.05	n.s.	3.14
b2553	glnB	n.s.	n.s.	n.s.	n.s.	n.s.	n.s.	n.s.	n.s.	n.s.
b3426	glpD	n.s.	n.s.	n.s.	5.60	2.36	n.s.	5.314	n.s.	n.s.
b3926	glpK	-6.65	-7.50	n.s.	-4.40	-4.26	n.s.	-3.16	n.s.	n.s.
b0720	gltA	-2.74	n.s.	n.s.	n.s.	n.s.	n.s.	n.s.	n.s.	2.24
b3212	gltB	-4.46	-4.44	n.s.	-2.42	-3.24	n.s.	n.s.	n.s.	n.s.
b3213	gltD	-5.00	-24.85	n.s.	n.s.	-5.09	n.s.	n.s.	n.s.	n.s.
b2400	gltX	n.s.	n.s.	n.s.	-2.22	n.s.	n.s.	n.s.	n.s.	n.s.
b2551	glyA	n.s.	n.s.	n.s.	n.s.	n.s.	n.s.	n.s.	n.s.	n.s.
b3559	glyS	n.s.	n.s.	n.s.	-3.14	n.s.	n.s.	n.s.	n.s.	n.s.
b0222	gmhA	n.s.	n.s.	n.s.	2.17	n.s.	n.s.	2.087	n.s.	n.s.
b2029	gnd	n.s.	n.s.	n.s.	n.s.	n.s.	n.s.	n.s.	n.s.	n.s.
b3612	gpmM	-2.93	-4.76	n.s.	-2.05	-4.65	-5.14	n.s.	n.s.	n.s.
b3608	gpsA	-3.35	-4.43	n.s.	-4.41	-3.92	n.s.	-3.65	n.s.	n.s.
b4143	groL	n.s.	n.s.	n.s.	3.02	n.s.	n.s.	3.262	n.s.	n.s.
b3610	grxC	2.17	n.s.	n.s.	n.s.	n.s.	n.s.	n.s.	n.s.	n.s.
b1654	grxD	2.85	2.71	n.s.	n.s.	n.s.	n.s.	n.s.	n.s.	n.s.
b2688	gshA	n.s.	n.s.	n.s.	n.s.	n.s.	n.s.	n.s.	n.s.	n.s.
b0838	gstB	2.75	n.s.	n.s.	3.11	2.12	n.s.	2.212	n.s.	n.s.
b2507	guaA	-3.00	-3.50	n.s.	-2.20	-4.72	n.s.	-2.15	n.s.	n.s.
b2508	guaB	-11.36	-10.75	n.s.	-2.71	-2.87	n.s.	-2.95	n.s.	n.s.
b0369	hemB	n.s.	n.s.	n.s.	2.81	n.s.	n.s.	2.267	n.s.	n.s.
b0154	hemL	3.05	2.99	n.s.	3.34	n.s.	n.s.	2.710	n.s.	n.s.
b2022	hisB	-3.31	-3.11	n.s.	n.s.	12.93	13.15	n.s.	n.s.	n.s.
b2021	hisC	-6.01	-11.63	n.s.	2.28	18.74	16.49	n.s.	n.s.	2.25
b2020	hisD	-5.58	-14.54	n.s.	3.56	22.43	n.s.	6.130	n.s.	2.33
b2025	hisF	-6.84	-9.35	n.s.	n.s.	5.50	13.52	n.s.	n.s.	n.s.
b2019	hisG	-4.83	-13.20	n.s.	6.04	11.74	n.s.	8.325	n.s.	2.27
b2023	hisH	-7.51	-6.93	n.s.	n.s.	8.25	13.41	n.s.	n.s.	n.s.
b2026	hisI	-3.59	-10.09	n.s.	n.s.	5.64	13.30	n.s.	4.73	n.s.
b2309	hisJ	-4.86	-3.43	2.32	-2.87	n.s.	n.s.	-2.54	n.s.	3.79
b1237	hns	2.58	4.85	n.s.	n.s.	n.s.	n.s.	n.s.	n.s.	n.s.
b4349	hsdM	-4.07	-2.89	n.s.	-2.87	n.s.	n.s.	-2.23	n.s.	n.s.
b3401	hslO	2.14	3.79	n.s.	3.92	n.s.	n.s.	2.866	n.s.	n.s.
b3931	hslU	n.s.	n.s.	n.s.	4.83	n.s.	n.s.	4.531	n.s.	n.s.
b1136	icd	n.s.	n.s.	n.s.	2.08	n.s.	n.s.	n.s.	n.s.	n.s.
b0026	ileS	n.s.	n.s.	n.s.	n.s.	n.s.	n.s.	n.s.	n.s.	n.s.
b3671	ilvB	n.s.	2.49	n.s.	-5.11	-6.10	n.s.	-4.42	n.s.	2.68
b3774	ilvC	-17.04	-30.27	n.s.	-6.66	-7.34	n.s.	-6.07	n.s.	2.42
b0077	ilvI	n.s.	n.s.	n.s.	-2.43	-2.20	-2.30	n.s.	n.s.	n.s.
b3670	ilvN	n.s.	2.88	n.s.	-4.15	-6.32	n.s.	-2.87	n.s.	2.39
b3168	infB	n.s.	n.s.	n.s.	n.s.	n.s.	n.s.	n.s.	n.s.	n.s.
b1718	infC	n.s.	n.s.	n.s.	n.s.	n.s.	n.s.	n.s.	n.s.	n.s.
b0382	iraP	8.54	8.22	n.s.	2.48	n.s.	n.s.	2.181	n.s.	-2.65
b2528	iscA	4.41	7.31	n.s.	14.33	5.45	3.42	7.916	n.s.	n.s.
b2529	iscU	4.32	7.68	n.s.	14.29	6.15	3.54	7.92	2.07	n.s.
b2524	iscX	n.s.	n.s.	n.s.	2.32	n.s.	n.s.	n.s.	n.s.	n.s.
b2515	ispG	n.s.	n.s.	n.s.	n.s.	n.s.	n.s.	n.s.	n.s.	n.s.
b1215	kdsA	2.33	2.46	n.s.	n.s.	n.s.	n.s.	n.s.	n.s.	n.s.
b0074	leuA	6.67	6.91	n.s.	-2.34	n.s.	n.s.	n.s.	n.s.	n.s.
b0073	leuB	2.18	3.39	n.s.	-2.78	-2.98	n.s.	n.s.	n.s.	n.s.
b0072	leuC	n.s.	3.11	n.s.	-2.54	-4.86	n.s.	n.s.	n.s.	n.s.
b0071	leuD	n.s.	3.21	n.s.	-2.17	-5.67	n.s.	n.s.	n.s.	n.s.
b0642	leuS	n.s.	n.s.	n.s.	n.s.	n.s.	n.s.	n.s.	n.s.	n.s.
b3454	livF	-6.37	-7.11	n.s.	-5.11	-2.42	n.s.	-3.56	n.s.	n.s.
b3460	livJ	-30.00	-20.92	n.s.	-9.75	-6.21	n.s.	-4.40	n.s.	n.s.
b0439	lon	2.73	2.71	n.s.	5.91	2.89	n.s.	4.652	n.s.	n.s.
b0116	lpd	n.s.	n.s.	n.s.	n.s.	2.34	n.s.	n.s.	n.s.	n.s.
b0889	lrp	n.s.	n.s.	n.s.	n.s.	n.s.	n.s.	n.s.	n.s.	n.s.
b2687	luxS	2.07	n.s.	n.s.	n.s.	n.s.	n.s.	2.034	n.s.	-2.10
b4024	lysC	-4.54	-7.76	n.s.	-2.31	-3.92	n.s.	n.s.	n.s.	n.s.
b2463	maeB	n.s.	n.s.	n.s.	n.s.	n.s.	n.s.	n.s.	n.s.	n.s.
b3236	mdh	-3.22	-3.46	n.s.	n.s.	n.s.	n.s.	n.s.	n.s.	n.s.
b1686	menI	-3.10	-5.68	n.s.	n.s.	n.s.	n.s.	n.s.	n.s.	n.s.
b3939	metB	-2.01	2.02	n.s.	6.75	10.55	7.15	n.s.	n.s.	3.37
b3829	metE	-10.41	-187.04	10.82	n.s.	-5.66	n.s.	n.s.	-2.11	3.99

b3941	metF	-13.51	n.s.	n.s.	5.27	n.s.	n.s.	n.s.	n.s.	6.43
b4019	metH	n.s.	n.s.	n.s.	n.s.	n.s.	n.s.	n.s.	n.s.	n.s.
b3938	metJ	n.s.	n.s.	n.s.	4.03	2.53	n.s.	n.s.	n.s.	n.s.
b2942	metK	-16.73	-4.71	n.s.	n.s.	n.s.	n.s.	n.s.	n.s.	n.s.
b3940	metL	-2.90	n.s.	n.s.	2.16	n.s.	3.74	n.s.	n.s.	2.56
b0199	metN	-5.51	n.s.	n.s.	4.77	6.03	n.s.	n.s.	n.s.	2.26
b1176	minC	n.s.	n.s.	n.s.	n.s.	n.s.	n.s.	n.s.	n.s.	n.s.
b3742	mioC	n.s.	n.s.	n.s.	n.s.	n.s.	2.20	n.s.	n.s.	n.s.
b3195	mlaF	3.90	3.51	n.s.	3.87	4.02	n.s.	2.400	n.s.	n.s.
b2684	mprA	2.98	2.53	n.s.	2.99	2.00	n.s.	2.049	n.s.	n.s.
b3251	mreB	n.s.	n.s.	n.s.	n.s.	n.s.	n.s.	n.s.	n.s.	n.s.
b1778	msrB	n.s.	2.09	n.s.	2.97	3.36	n.s.	3.153	n.s.	n.s.
b1832	msrC	2.82	2.77	n.s.	n.s.	n.s.	n.s.	n.s.	n.s.	n.s.
b0159	mtn	n.s.	n.s.	n.s.	n.s.	n.s.	n.s.	n.s.	n.s.	n.s.
b0750	nadA	n.s.	-5.34	n.s.	n.s.	-2.57	-3.74	n.s.	-2.28	n.s.
b0639	nadD	-4.38	-2.71	n.s.	n.s.	n.s.	n.s.	n.s.	n.s.	n.s.
b1740	nadE	n.s.	n.s.	n.s.	n.s.	n.s.	n.s.	n.s.	n.s.	n.s.
b2518	ndk	n.s.	2.38	4.46	-2.51	n.s.	n.s.	-3.50	n.s.	5.45
b0578	nfsB	n.s.	n.s.	n.s.	n.s.	n.s.	n.s.	n.s.	n.s.	n.s.
b2235	nrdB	n.s.	n.s.	n.s.	n.s.	n.s.	n.s.	n.s.	n.s.	n.s.
b2284	nuoF	-10.34	-3.31	n.s.	-2.58	-7.83	n.s.	-2.28	n.s.	n.s.
b3169	nusA	n.s.	n.s.	n.s.	-2.23	n.s.	n.s.	-2.04	n.s.	n.s.
b0957	ompA	n.s.	n.s.	n.s.	n.s.	n.s.	n.s.	n.s.	n.s.	n.s.
b1243	oppA	-12.81	-14.93	n.s.	n.s.	-6.60	n.s.	n.s.	n.s.	n.s.
b1247	oppF	-4.75	-36.02	n.s.	-2.24	-8.73	n.s.	-2.12	n.s.	n.s.
b0134	panB	n.s.	n.s.	n.s.	n.s.	n.s.	n.s.	n.s.	n.s.	n.s.
b0133	panC	n.s.	n.s.	n.s.	n.s.	n.s.	n.s.	n.s.	n.s.	n.s.
b0131	panD	2.71	2.61	n.s.	n.s.	2.61	n.s.	n.s.	n.s.	n.s.
b3403	pck	n.s.	n.s.	n.s.	n.s.	n.s.	n.s.	n.s.	n.s.	n.s.
b2564	pdxJ	2.92	2.08	n.s.	2.00	n.s.	n.s.	2.147	n.s.	n.s.
b2418	pdxK	n.s.	n.s.	n.s.	2.06	n.s.	n.s.	2.031	n.s.	n.s.
b1636	pdxY	-3.41	-4.61	n.s.	-2.85	n.s.	n.s.	-3.14	n.s.	n.s.
b4260	pepA	n.s.	n.s.	n.s.	n.s.	n.s.	n.s.	n.s.	n.s.	n.s.
b0932	pepN	n.s.	n.s.	n.s.	n.s.	n.s.	n.s.	n.s.	n.s.	n.s.
b3916	pfkA	n.s.	-2.12	n.s.	n.s.	n.s.	n.s.	2.253	n.s.	n.s.
b0903	pflB	-4.79	-21.56	-2.49	-2.26	-7.45	-7.14	n.s.	n.s.	-3.78
b2926	pgk	-4.81	-5.34	n.s.	n.s.	-2.12	n.s.	n.s.	n.s.	n.s.
b0767	pgl	2.89	n.s.	n.s.	3.71	n.s.	n.s.	3.327	n.s.	n.s.
b0688	pgm	2.49	2.27	n.s.	n.s.	2.52	n.s.	n.s.	n.s.	n.s.
b1714	pheS	-4.88	-3.32	n.s.	-3.52	-3.46	n.s.	-3.43	n.s.	n.s.
b1713	pheT	-2.25	n.s.	n.s.	n.s.	-3.65	n.s.	n.s.	n.s.	n.s.
b4041	plsB	n.s.	n.s.	n.s.	n.s.	n.s.	n.s.	n.s.	n.s.	n.s.
b4235	pmbA	n.s.	n.s.	n.s.	n.s.	n.s.	n.s.	n.s.	n.s.	n.s.
b3164	pnp	-2.55	-2.02	n.s.	n.s.	n.s.	n.s.	n.s.	n.s.	n.s.
b1603	pntA	-2.43	-2.59	n.s.	-2.03	n.s.	n.s.	-2.11	n.s.	n.s.
b3956	ppc	-4.17	-5.96	n.s.	-2.33	-2.36	n.s.	n.s.	n.s.	n.s.
b0525	ppiB	n.s.	n.s.	n.s.	n.s.	-3.04	n.s.	n.s.	n.s.	n.s.
b1702	ppsA	n.s.	n.s.	n.s.	2.50	5.38	n.s.	2.059	n.s.	n.s.
b4375	prfC	-2.62	n.s.	n.s.	-3.04	n.s.	n.s.	-2.86	n.s.	2.67
b3498	prlC	n.s.	n.s.	n.s.	3.59	2.37	n.s.	3.627	n.s.	n.s.
b0243	proA	n.s.	n.s.	n.s.	n.s.	n.s.	n.s.	n.s.	n.s.	n.s.
b0386	proC	n.s.	n.s.	n.s.	n.s.	n.s.	n.s.	n.s.	n.s.	n.s.
b1207	prs	-3.78	-2.16	n.s.	n.s.	n.s.	n.s.	-2.16	n.s.	n.s.
b2297	pta	n.s.	-2.67	n.s.	n.s.	-2.52	n.s.	n.s.	n.s.	n.s.
b1101	ptsG	-2.74	-11.80	n.s.	-6.37	-13.06	n.s.	-4.54	-2.11	n.s.
b2416	ptsI	-2.91	-3.44	n.s.	-3.32	-2.54	n.s.	-2.41	n.s.	n.s.
b4177	purA	-3.57	-3.49	n.s.	n.s.	-2.20	n.s.	n.s.	n.s.	n.s.
b1131	purB	-11.66	-8.07	n.s.	-7.47	n.s.	n.s.	-4.94	n.s.	n.s.
b2476	purC	n.s.	n.s.	n.s.	-2.65	n.s.	n.s.	-3.43	n.s.	n.s.
b2312	purF	-6.91	-4.42	n.s.	-9.77	n.s.	n.s.	-6.88	n.s.	2.94
b4006	purH	-5.90	-2.31	n.s.	-4.16	n.s.	n.s.	-4.60	n.s.	n.s.
b2557	purL	-23.79	-13.57	n.s.	-4.11	n.s.	n.s.	-4.51	n.s.	n.s.
b2499	purM	-6.53	n.s.	n.s.	-4.77	n.s.	3.39	-5.61	n.s.	n.s.
b1658	purR	n.s.	2.95	n.s.	n.s.	n.s.	n.s.	n.s.	n.s.	n.s.
b1676	pykF	-5.20	-3.05	n.s.	-5.08	-4.42	n.s.	-3.78	n.s.	n.s.
b1062	pyrC	-2.29	n.s.	n.s.	n.s.	n.s.	n.s.	-2.29	n.s.	n.s.
b2780	pyrG	-2.82	-2.04	n.s.	-2.60	n.s.	n.s.	n.s.	n.s.	n.s.
b2699	recA	2.47	2.46	n.s.	10.11	3.18	n.s.	5.911	n.s.	n.s.
b2039	rfbA	-2.19	n.s.	n.s.	n.s.	n.s.	n.s.	n.s.	n.s.	n.s.
b2040	rfbD	-2.07	n.s.	n.s.	-2.56	n.s.	n.s.	-2.20	n.s.	n.s.
b3780	rhlB	n.s.	n.s.	n.s.	n.s.	n.s.	n.s.	n.s.	n.s.	n.s.
b3783	rho	-6.05	-3.67	n.s.	n.s.	n.s.	n.s.	n.s.	n.s.	n.s.
b3041	ribB	n.s.	n.s.	n.s.	n.s.	-2.54	n.s.	n.s.	n.s.	n.s.
b1286	rnb	-25.38	-15.37	n.s.	-5.63	-3.54	n.s.	-3.99	n.s.	2.49
b2914	rpiA	n.s.	n.s.	n.s.	n.s.	n.s.	n.s.	n.s.	n.s.	n.s.
b3317	rplB	n.s.	-3.16	n.s.	-11.56	-5.50	n.s.	-6.76	n.s.	2.33
b3305	rplF	n.s.	n.s.	n.s.	-2.54	-2.51	n.s.	-2.31	n.s.	2.21
b3985	rplJ	n.s.	n.s.	n.s.	-3.34	-3.87	n.s.	-2.67	n.s.	2.03
b3310	rplN	n.s.	n.s.	n.s.	-2.04	-2.21	n.s.	-2.10	n.s.	n.s.
b3185	rpmA	n.s.	n.s.	n.s.	n.s.	n.s.	n.s.	n.s.	n.s.	2.51
b3936	rpmE	n.s.	n.s.	n.s.	n.s.	n.s.	n.s.	n.s.	n.s.	4.78
b1717	rpmI	n.s.	n.s.	n.s.	-2.42	-2.19	n.s.	-2.29	n.s.	n.s.
b3295	rpoA	n.s.	-2.26	n.s.	n.s.	-2.64	n.s.	n.s.	n.s.	2.00
b3987	rpoB	-2.78	-2.00	n.s.	n.s.	n.s.	n.s.	n.s.	n.s.	n.s.
b3988	rpoC	-3.05	-3.51	n.s.	n.s.	n.s.	n.s.	n.s.	n.s.	n.s.
b3067	rpoD	n.s.	n.s.	n.s.	2.51	n.s.	n.s.	2.302	n.s.	n.s.
b0911	rpsA	-5.40	-3.32	n.s.	-6.90	-3.57	n.s.	-5.37	n.s.	2.20
b0169	rpsB	n.s.	n.s.	n.s.	n.s.	n.s.	n.s.	n.s.	n.s.	n.s.
b3296	rpsD	n.s.	n.s.	n.s.	n.s.	-2.43	n.s.	n.s.	n.s.	2.16
b3306	rpsH	n.s.	n.s.	n.s.	-2.66	-2.96	n.s.	-2.54	n.s.	2.21
b3297	rpsK	n.s.	n.s.	n.s.	n.s.	-2.35	n.s.	n.s.	n.s.	2.28
b3342	rpsL	n.s.	n.s.	n.s.	-3.18	-2.34	n.s.	-2.63	n.s.	n.s.
b3311	rpsQ	n.s.	-2.81	n.s.	-3.86	-4.44	n.s.	-2.69	n.s.	n.s.
b3929	rraA	2.18	n.s.	n.s.	2.53	n.s.	n.s.	2.811	n.s.	n.s.
b1540	rspR	n.s.	n.s.	n.s.	n.s.	n.s.	n.s.	n.s.	n.s.	n.s.
b0723	sdhA	-7.63	-4.99	n.s.	n.s.	n.s.	n.s.	n.s.	n.s.	4.69
b0724	sdhB	-5.85	-8.92	n.s.	n.s.	n.s.	n.s.	n.s.	n.s.	3.80
b2897	sdhE	2.46	n.s.	n.s.	n.s.	n.s.	n.s.	n.s.	n.s.	n.s.
b1764	selD	n.s.	n.s.	n.s.	n.s.	n.s.	n.s.	n.s.	n.s.	n.s.
b2913	serA	n.s.	n.s.	n.s.	n.s.	n.s.	n.s.	n.s.	n.s.	n.s.

b1656	sodB	-8.39	-17.43	n.s.	n.s.	-2.95	-5.86	n.s.	-2.04	n.s.
b2938	speA	n.s.	n.s.	n.s.	n.s.	2.30	n.s.	n.s.	n.s.	n.s.
b0726	sucA	-5.71	-5.22	n.s.	-3.17	n.s.	n.s.	-2.56	n.s.	2.82
b0728	sucC	-4.64	-8.99	n.s.	-3.58	-4.19	n.s.	-2.67	n.s.	2.61
b0729	sucD	-3.21	-9.53	n.s.	-2.79	-4.28	n.s.	-2.22	n.s.	2.24
b2464	talA	n.s.	n.s.	n.s.	3.89	n.s.	4.85	2.84	4.33	-4.77
b0008	talB	n.s.	n.s.	n.s.	2.10	n.s.	n.s.	n.s.	n.s.	n.s.
b0406	tgt	n.s.	n.s.	n.s.	-2.62	n.s.	n.s.	-2.53	n.s.	n.s.
b0002	thrA	-11.23	-24.90	n.s.	-4.92	-7.55	n.s.	-4.23	-2.23	2.26
b0003	thrB	-8.27	-23.87	n.s.	-3.70	-8.04	n.s.	-3.20	-2.24	2.29
b0004	thrC	-5.61	-15.91	n.s.	-3.41	-7.84	n.s.	-3.06	-2.41	2.27
b1719	thrS	n.s.	n.s.	n.s.	n.s.	n.s.	n.s.	n.s.	n.s.	n.s.
b3919	tpiA	n.s.	-2.84	n.s.	-3.13	-7.27	n.s.	-2.39	n.s.	n.s.
b1324	tpx	2.14	2.28	n.s.	n.s.	n.s.	n.s.	n.s.	n.s.	n.s.
b1260	trpA	n.s.	n.s.	n.s.	n.s.	-2.91	n.s.	n.s.	n.s.	n.s.
b1261	trpB	-2.05	n.s.	n.s.	n.s.	-2.72	n.s.	n.s.	n.s.	n.s.
b1262	trpC	n.s.	n.s.	n.s.	n.s.	n.s.	n.s.	n.s.	n.s.	n.s.
b1263	trpD	-10.27	-10.57	n.s.	-5.21	-7.14	n.s.	-4.47	n.s.	n.s.
b1264	trpE	-19.64	-28.20	n.s.	-5.94	-7.69	n.s.	-5.22	n.s.	n.s.
b3781	trxA	2.45	n.s.	n.s.	n.s.	n.s.	n.s.	n.s.	n.s.	n.s.
b0888	trxB	n.s.	2.12	n.s.	7.53	3.61	n.s.	6.085	n.s.	n.s.
b1807	tsaB	n.s.	n.s.	n.s.	-3.51	n.s.	n.s.	-3.77	n.s.	2.55
b1344	ttcA	3.25	3.43	n.s.	n.s.	n.s.	n.s.	n.s.	n.s.	n.s.
b3339	tufA	-2.40	-3.57	n.s.	n.s.	-3.28	n.s.	n.s.	n.s.	n.s.
b1637	tyrS	n.s.	n.s.	n.s.	n.s.	n.s.	n.s.	n.s.	n.s.	n.s.
b2232	ubiG	2.63	2.13	n.s.	n.s.	n.s.	n.s.	n.s.	n.s.	n.s.
b3831	udp	n.s.	-3.22	n.s.	n.s.	-2.90	-3.65	2.178	n.s.	-2.72
b0675	umpH	n.s.	n.s.	n.s.	n.s.	n.s.	n.s.	n.s.	n.s.	n.s.
b3495	uspA	2.64	n.s.	n.s.	5.08	2.78	n.s.	5.240	n.s.	-2.62
b2042	wcaN	n.s.	n.s.	n.s.	n.s.	n.s.	n.s.	n.s.	n.s.	n.s.
b3787	wecC	-9.16	-5.67	n.s.	-4.41	n.s.	n.s.	-3.00	n.s.	n.s.
b0101	yacG	-2.83	-2.15	n.s.	n.s.	-2.40	n.s.	n.s.	n.s.	n.s.
b0163	yaeH	6.30	3.99	n.s.	4.92	3.14	n.s.	6.097	n.s.	-2.74
b4406	yaeP	9.05	5.18	n.s.	4.71	3.61	n.s.	5.624	n.s.	-2.05
b0287	yagU	2.47	3.82	-2.20	-2.70	n.s.	n.s.	-2.03	n.s.	-2.01
b0471	ybaB	-2.84	-2.50	n.s.	-2.25	-2.37	n.s.	-2.01	n.s.	n.s.
b0528	ybcJ	n.s.	n.s.	n.s.	n.s.	n.s.	n.s.	n.s.	n.s.	n.s.
b0711	ybgJ	2.95	2.05	n.s.	2.49	2.09	n.s.	2.040	n.s.	n.s.
b0773	ybhB	n.s.	n.s.	n.s.	n.s.	n.s.	n.s.	n.s.	n.s.	n.s.
b0801	ybiC	n.s.	n.s.	n.s.	n.s.	-3.04	n.s.	n.s.	n.s.	n.s.
b0917	ycaR	n.s.	n.s.	n.s.	n.s.	n.s.	n.s.	n.s.	n.s.	n.s.
b1180	ycgM	10.42	6.55	n.s.	4.62	3.13	n.s.	3.721	n.s.	n.s.
b1203	ychF	n.s.	n.s.	n.s.	n.s.	n.s.	n.s.	n.s.	n.s.	n.s.
b1287	yciW	-30.06	-20.18	n.s.	-4.22	-10.94	n.s.	-3.79	n.s.	3.80
b1539	ydfG	n.s.	n.s.	n.s.	n.s.	n.s.	-2.10	n.s.	n.s.	n.s.
b1687	ydiJ	-5.61	-4.69	n.s.	-2.23	n.s.	n.s.	-2.49	n.s.	n.s.
b1864	yebC	-2.76	n.s.	n.s.	-2.74	-3.61	n.s.	-2.41	n.s.	n.s.
b1930	yedF	n.s.	n.s.	n.s.	-2.27	-4.63	n.s.	n.s.	n.s.	n.s.
b2012	yeeD	-5.90	-15.77	n.s.	4.92	-4.56	n.s.	2.462	n.s.	2.51
b2300	yfcE	6.09	4.68	n.s.	2.44	2.32	n.s.	2.030	n.s.	n.s.
b2471	yffB	2.36	2.43	n.s.	2.45	n.s.	n.s.	2.548	n.s.	-2.64
b2898	ygfZ	2.10	n.s.	n.s.	2.57	n.s.	n.s.	2.267	n.s.	n.s.
b2959	yggL	n.s.	n.s.	n.s.	n.s.	n.s.	n.s.	n.s.	n.s.	n.s.
b2962	yggX	3.88	3.29	n.s.	n.s.	2.02	n.s.	n.s.	n.s.	n.s.
b3205	yhbJ	-4.23	-4.06	n.s.	n.s.	n.s.	n.s.	n.s.	n.s.	n.s.
b3346	yheO	n.s.	n.s.	n.s.	n.s.	n.s.	n.s.	n.s.	n.s.	n.s.
b3764	yifE	n.s.	n.s.	n.s.	n.s.	n.s.	n.s.	n.s.	n.s.	n.s.
b1727	yniC	3.50	4.15	n.s.	2.47	2.33	n.s.	n.s.	n.s.	n.s.
b3070	yqjH	n.s.	n.s.	n.s.	n.s.	3.54	10.81	n.s.	n.s.	n.s.
b1857	znuA	n.s.	n.s.	n.s.	-1.99	n.s.	3.67	n.s.	-10.23	n.s.
b1852	zwf	n.s.	n.s.	n.s.	n.s.	n.s.	n.s.	n.s.	n.s.	n.s.

Table 3.2: Relationship of Protein-Hg Damage and Transcriptional Response: Energy Production and Central Carbon Metabolism. Proteins were found with phenylmercury (PhHg) adducts (pink) and/or inorganic mercury (Hg) adducts (orange). Their mRNA was higher (yellow), lower (blue) or no different (n.s.) compared to unexposed cultures at the same time. (10, 30, and 60 min) See also Figure 3.1.

Gene Name	PhHg_spectra_count	PMA_t10	PMA_t30	PMA_t60	Hg_spectra_count	Hg_t10	Hg_t30	Hg_t60	NR1_t10	NR1_t30	NR1_t60
atpA	86	-3.61	-3.65	n.s.	16	-3.56	-4.09	n.s.	-2.63	n.s.	n.s.
atpD	5	-2.13	-5.16	n.s.	8	-3.27	-4.28	n.s.	-2.53	n.s.	n.s.
atpH	5	-3.47	-2.96	n.s.	0	-4.28	-4.13	n.s.	-3.49	n.s.	n.s.
icd	2	n.s.	n.s.	n.s.	5	2.08	n.s.	n.s.	n.s.	n.s.	n.s.
nuoF	1	-10.34	-3.31	n.s.	0	-2.58	-7.83	n.s.	-2.28	n.s.	n.s.
sdhA	145	-7.63	-4.99	n.s.	1	n.s.	n.s.	n.s.	n.s.	n.s.	4.69
sdhB	2	-5.85	-8.92	n.s.	0	n.s.	n.s.	n.s.	n.s.	n.s.	3.80

Table 3.3: Relationship of Protein-Hg Damage and Transcriptional Response: Ribosome Structure or Modification. Proteins were found with phenylmercury acetate (PhHg) adducts (pink) and/or inorganic mercury (Hg) adducts (orange). Their mRNA was higher (yellow), lower (blue) or no different (n.s.) compared to unexposed cultures at the same time. (10, 30, and 60 min). See also Figure 3.2.

Gene Name	PhHg_spectra_count	PMA_t10	PMA_t30	PMA_t60	Hg_spectra_count	Hg_t10	Hg_t30	Hg_t60	NR1_t10	NR1_t30	NR1_t60
rplB	0	n.s.	-3.16	n.s.	1	-11.56	-5.50	n.s.	-6.76	n.s.	2.33
rpsQ	40	n.s.	-2.81	n.s.	0	-3.86	-4.44	n.s.	-2.69	n.s.	n.s.
rplN	34	n.s.	n.s.	n.s.	0	-2.04	-2.21	n.s.	-2.10	n.s.	n.s.
rpsH	0	n.s.	n.s.	n.s.	1	-2.66	-2.96	n.s.	-2.54	n.s.	2.21
rplF	57	n.s.	n.s.	n.s.	1	-2.54	-2.51	n.s.	-2.31	n.s.	2.21
rpsK	40	n.s.	n.s.	n.s.	0	n.s.	-2.35	n.s.	n.s.	n.s.	2.28
rpsD	0	n.s.	n.s.	n.s.	14	n.s.	-2.43	n.s.	n.s.	n.s.	2.16
rpsL	18	n.s.	n.s.	n.s.	0	-3.18	-2.34	n.s.	-2.63	n.s.	n.s.
rpsA	26	-5.40	-3.32	n.s.	5	-6.90	-3.57	n.s.	-5.37	n.s.	2.20
rpmI	5	n.s.	n.s.	n.s.	0	-2.42	-2.19	n.s.	-2.29	n.s.	n.s.
rplJ	146	n.s.	n.s.	n.s.	0	-3.34	-3.87	n.s.	-2.67	n.s.	2.03
rpsB	127	n.s.	n.s.	n.s.	0	n.s.	n.s.	n.s.	n.s.	n.s.	n.s.
rpmA	4	n.s.	n.s.	n.s.	0	n.s.	n.s.	n.s.	n.s.	n.s.	2.51
rpmE	1	n.s.	n.s.	n.s.	99	n.s.	n.s.	n.s.	n.s.	n.s.	4.78

Table 3.4: Relationship of Protein-Hg Damage and Transcriptional Response: Amino Acid Biosynthesis. Proteins were found with phenylmercury acetate (PhHg) adducts (pink) and/or inorganic mercury (Hg) adducts (orange). Their mRNA was higher (yellow), lower (blue) or no different (n.s.) compared to unexposed cultures at the same time. (10, 30, and 60 min). See also Fig. 3.3.

Gene Name	PhHg_spectra_count	PMA_t10	PMA_t30	PMA_t60	Hg_spectra_count	Hg_t10	Hg_t30	Hg_t60	NR1_t10	NR1_t30	NR1_t60
argB	3	-9.50	-5.29	n.s.	0	-5.66	n.s.	n.s.	-6.57	n.s.	11.23
argD	22	-10.89	-4.00	n.s.	0	-3.33	n.s.	n.s.	-4.02	n.s.	10.31
argE	5	n.s.	n.s.	n.s.	0	n.s.	2.50	n.s.	n.s.	n.s.	2.12
argF	11	-12.18	-6.27	n.s.	0	-3.72	n.s.	n.s.	-4.49	n.s.	12.66
argG	4	-5.60	-5.17	n.s.	0	-4.35	-2.69	n.s.	-4.78	n.s.	7.55
argH	50	-6.66	-5.63	n.s.	0	-4.90	-2.49	n.s.	-4.50	n.s.	9.48
argI	12	n.s.	n.s.	n.s.	11	n.s.	-2.49	n.s.	n.s.	n.s.	5.44
asd	60	n.s.	-2.06	n.s.	0	n.s.	n.s.	n.s.	n.s.	n.s.	n.s.
asnB	5	n.s.	n.s.	n.s.	5	-2.16	n.s.	n.s.	n.s.	n.s.	n.s.
cysB	10	-3.65	-2.42	n.s.	5	-2.15	-3.17	n.s.	-2.19	n.s.	n.s.
cysD	14	-51.39	-47.15	n.s.	1	n.s.	-11.78	n.s.	n.s.	n.s.	3.60
cysI	0	-39.87	-165.83	n.s.	6	-2.47	-13.88	n.s.	-2.15	n.s.	3.17
dapA	5	3.85	2.78	n.s.	0	n.s.	n.s.	n.s.	n.s.	n.s.	n.s.
dapB	21	-2.01	n.s.	n.s.	1	-2.43	-2.05	n.s.	-2.68	n.s.	n.s.
dapD	34	n.s.	n.s.	n.s.	0	n.s.	n.s.	n.s.	n.s.	n.s.	n.s.
glnA	25	-13.97	-27.05	n.s.	1	-9.36	-9.75	n.s.	-7.05	n.s.	3.14
gltB	38	-4.46	-4.44	n.s.	0	-2.42	-3.24	n.s.	n.s.	n.s.	n.s.
gltD	51	-5.00	-24.85	n.s.	1	n.s.	-5.09	n.s.	n.s.	n.s.	n.s.
glyA	108	n.s.	n.s.	n.s.	0	n.s.	n.s.	n.s.	n.s.	n.s.	n.s.
hisB	3	-3.31	-3.11	n.s.	0	n.s.	12.93	13.15	n.s.	n.s.	n.s.
hisC	2	-6.01	-11.63	n.s.	0	2.28	18.74	16.49	n.s.	n.s.	2.25
hisD	1	-5.58	-14.54	n.s.	0	3.56	22.43	n.s.	6.13	n.s.	2.33
hisF	32	-6.84	-9.35	n.s.	0	n.s.	5.50	13.52	n.s.	n.s.	n.s.
hisG	3	-4.83	-13.20	n.s.	0	6.04	11.74	n.s.	8.32	n.s.	2.27
hisH	4	-7.51	-6.93	n.s.	2	n.s.	8.25	13.41	n.s.	n.s.	n.s.
hisI	7	-3.59	-10.09	n.s.	0	n.s.	5.64	13.30	n.s.	4.73	n.s.
ilvB	1	n.s.	2.49	n.s.	1	-5.11	-6.10	n.s.	-4.42	n.s.	2.68
ilvC	121	-17.04	-30.27	n.s.	147	-6.66	-7.34	n.s.	-6.07	n.s.	2.42
ilvI	3	n.s.	n.s.	n.s.	0	-2.43	-2.20	-2.30	n.s.	n.s.	n.s.
ilvN	6	n.s.	2.88	n.s.	0	-4.15	-6.32	n.s.	-2.87	n.s.	2.39
leuA	4	6.67	6.91	n.s.	0	-2.34	n.s.	n.s.	n.s.	n.s.	n.s.
leuB	6	2.18	3.39	n.s.	0	-2.78	-2.98	n.s.	n.s.	n.s.	n.s.
leuC	37	n.s.	3.11	n.s.	0	-2.54	-4.86	n.s.	n.s.	n.s.	n.s.
leuD	4	n.s.	3.21	n.s.	0	-2.17	-5.67	n.s.	n.s.	n.s.	n.s.
luxS	40	2.07	n.s.	n.s.	0	n.s.	n.s.	n.s.	2.03	n.s.	-2.10
lysC	0	-4.54	-7.76	n.s.	1	-2.31	-3.92	n.s.	n.s.	n.s.	n.s.
metB	6	-2.01	2.02	n.s.	0	6.75	10.55	7.15	n.s.	n.s.	3.37
metE	215	-10.41	-187.04	10.82	70	n.s.	-5.66	n.s.	n.s.	-2.11	3.99
metF	8	-13.51	n.s.	n.s.	0	5.27	n.s.	n.s.	n.s.	n.s.	6.43
metH	1	n.s.	n.s.	n.s.	0	n.s.	n.s.	n.s.	n.s.	n.s.	n.s.
metJ	52	n.s.	n.s.	n.s.	0	4.03	2.53	n.s.	n.s.	n.s.	n.s.
metK	8	-16.73	-4.71	n.s.	0	n.s.	n.s.	n.s.	n.s.	n.s.	n.s.
metL	3	-2.90	n.s.	n.s.	0	2.16	n.s.	3.74	n.s.	n.s.	2.56
mtn	13	n.s.	n.s.	n.s.	0	n.s.	n.s.	n.s.	n.s.	n.s.	n.s.
proA	1	n.s.	n.s.	n.s.	0	n.s.	n.s.	n.s.	n.s.	n.s.	n.s.
proC	1	n.s.	n.s.	n.s.	0	n.s.	n.s.	n.s.	n.s.	n.s.	n.s.
serA	32	n.s.	n.s.	n.s.	2	n.s.	n.s.	n.s.	n.s.	n.s.	n.s.
thrB	33	-8.27	-23.87	n.s.	17	-3.70	-8.04	n.s.	-3.20	-2.24	2.29
thrC	37	-5.61	-15.91	n.s.	0	-3.41	-7.84	n.s.	-3.06	-2.41	2.27
trpA	155	n.s.	n.s.	n.s.	11	n.s.	-2.91	n.s.	n.s.	n.s.	n.s.
trpB	1	-2.05	n.s.	n.s.	0	n.s.	-2.72	n.s.	n.s.	n.s.	n.s.
trpC	9	n.s.	n.s.	n.s.	0	n.s.	n.s.	n.s.	n.s.	n.s.	n.s.
trpD	16	-10.27	-10.57	n.s.	0	-5.21	-7.14	n.s.	-4.47	n.s.	n.s.
trpE	1	-19.64	-28.20	n.s.	0	-5.94	-7.69	n.s.	-5.22	n.s.	n.s.

Table 3.5: Transcriptional Response to Mercury Exposure of Attenuation-controlled mRNAs. Color indicates mRNAs was higher (yellow), lower (blue) or no different (n.s.) compared to unexposed cultures at the same time. (10, 30, and 60 min). See also Figure 3.4.

Gene Name	PMA_t10	PMA_t30	PMA_t60	Hg_t10	Hg_t30	Hg_t60	NR1_t10	NR1_t30	NR1_t60
thrL	n.s.	n.s.	n.s.	-2.08	-2.13	n.s.	n.s.	n.s.	n.s.
leuL	3.80	3.25	n.s.	n.s	n.s.	n.s.	n.s.	n.s.	n.s.
trpL	n.s.	-4.22	-2.90	-2.14	-3.80	n.s.	-2.07	n.s.	n.s.
pheM	n.s.	n.s.	n.s.	-2.26	-2.09	n.s.	-2.62	n.s.	n.s.
hisL	n.s.	n.s.	n.s.	2.87	2.28	n.s.	2.04	n.s.	n.s.
pheL	n.s.	n.s.	n.s.	n.s	n.s.	n.s.	n.s.	n.s.	n.s.
ivbL	2.06	n.s.	n.s.	-2.02	-2.06	n.s.	-2.30	n.s.	n.s.
tnaC	-7.67	-6.33	n.s.	-7.90	-4.62	n.s.	-6.58	n.s.	n.s.
ilvL	2.41	n.s.	n.s.	n.s	n.s.	n.s.	n.s.	n.s.	n.s.
rhoL	n.s	n.s.	n.s.	n.s	n.s.	n.s.	n.s.	n.s.	n.s.
pyrL	n.s	n.s.	n.s.	n.s	n.s.	n.s.	2.94	n.s.	2.56
uof	2.16	2.37	n.s.	7.44	2.53	n.s.	7.33	n.s.	n.s.
mgtL	2.35	2.11	n.s.	2.64	n.s.	n.s.	3.12	n.s.	n.s.
idlP	n.s	n.s.	n.s.	n.s	n.s.	n.s.	3.94	n.s.	n.s.
rseD	n.s	n.s.	n.s.	n.s	n.s.	n.s.	n.s.	n.s.	n.s.
speFL	n.s	n.s.	n.s.	n.s	n.s.	n.s.	n.s.	n.s.	n.s.

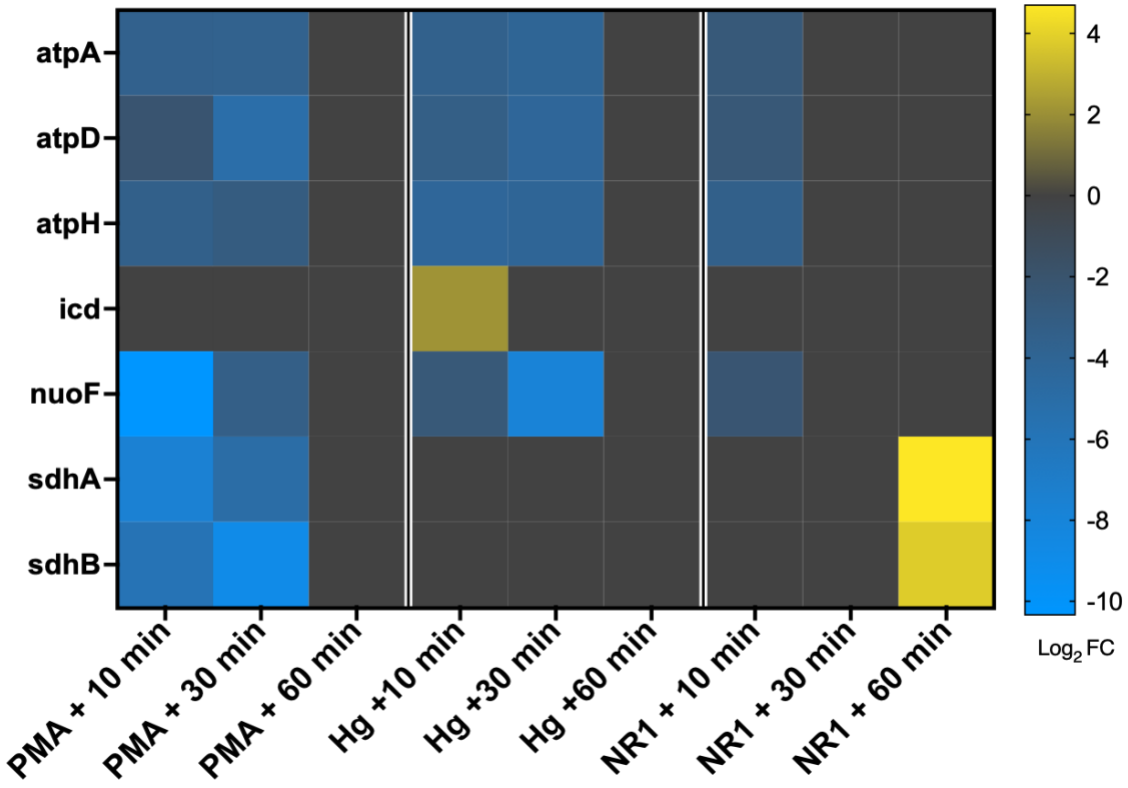

Figure 3.1: Heat map of RNA-Seq data in Table 3.2. Fold-changes for Hg-sensitive (PMA and Hg) and Hg-resistant (NR1) cells compared to their unexposed condition. Up- (yellow), down- (blue), and not significantly changed (black) genes at 10-, 30-, and 60-min post Hg-challenge.

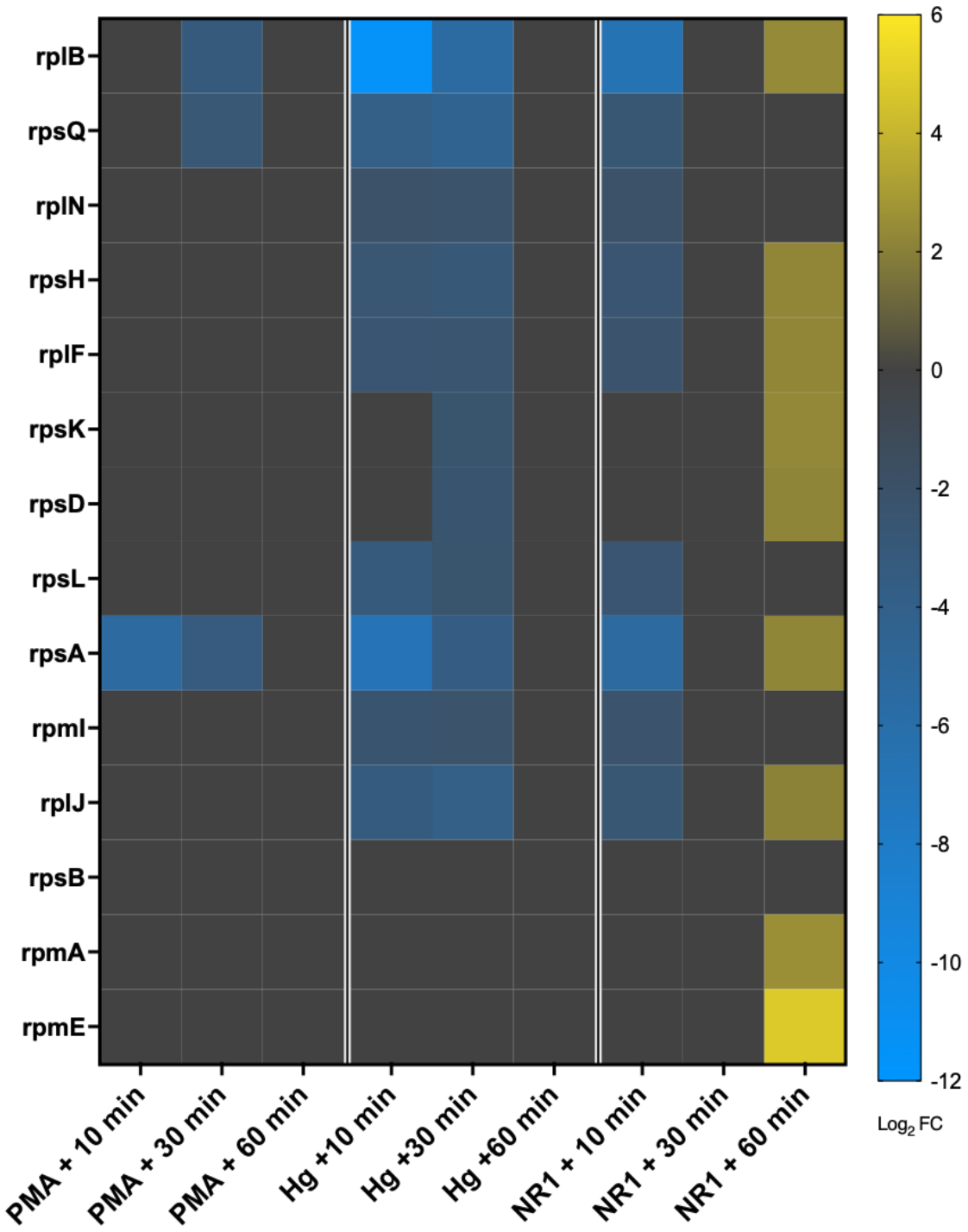

Figure 3.2: Heat map of RNA-Seq data in Table 3.3. Fold-changes for Hg-sensitive (PMA and Hg) and Hg-resistant (NR1) cells compared to their unexposed condition. Up- (yellow), down- (blue), and not significantly changed (black) genes at 10-, 30-, and 60-min post Hg-challenge.

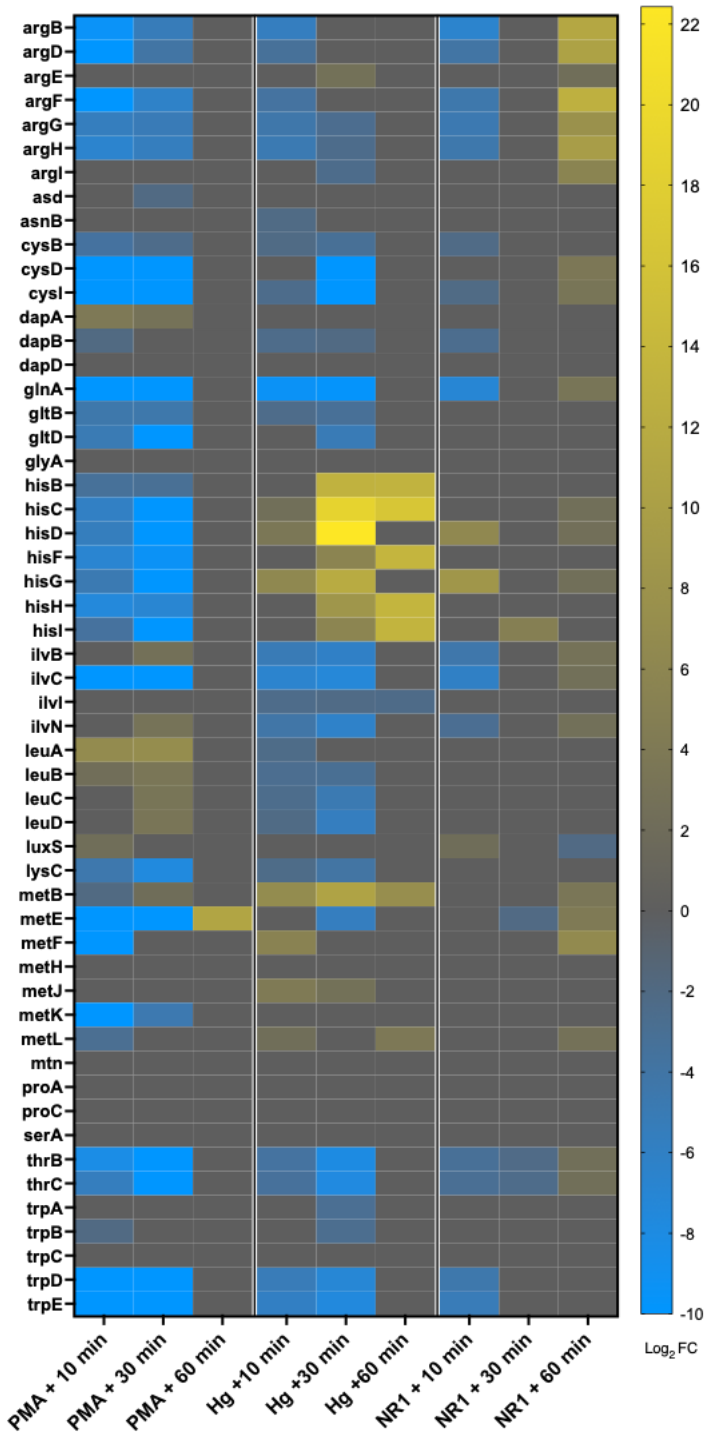

Figure 3.3: Heat map of RNA-Seq data in Table 3.4. Fold-changes for Hg-sensitive (PMA and Hg) and Hg-resistant (NR1) cells compared to their unexposed condition. Up- (yellow), down- (blue), and not significantly changed (black) genes at 10-, 30-, and 60-min post Hg-challenge.

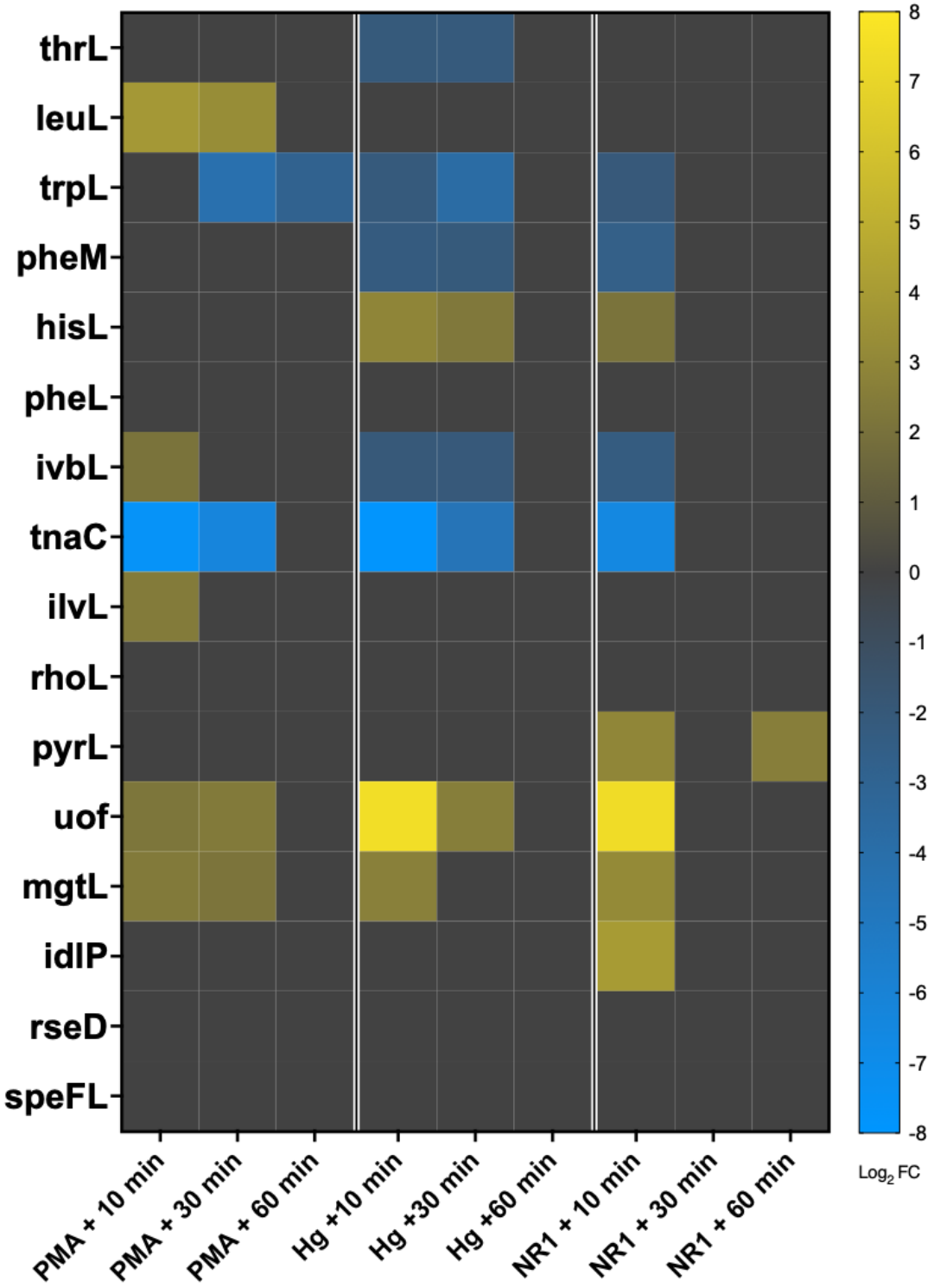

Figure 3.4: Heat map of RNA-Seq data in Table 3.5. Fold-changes for Hg-sensitive (PMA and Hg) and Hg-resistant (NR1) cells compared to their unexposed condition. Up- (yellow), down- (blue), and not significantly changed (black) genes at 10-, 30-, and 60-min post Hg-challenge.

CHAPTER 4

SUMMARY

In the preceding chapters of this dissertation, I documented my use of biochemical and molecular methods to compare the transcriptional response to inorganic mercury exposure in a model microbe harboring a model plasmid-born mercury resistance locus. I also took advantage of previously acquired proteomic data set for this same microbe to assess the correlation between the vulnerability of a protein to binding mercury during in vivo exposure and the changes in transcription of that gene upon mercury exposure.

In chapter 2, I quantified global transcriptional (aka RNA-Seq) changes after exposure to sub-acute or acute inorganic mercury in actively growing wild-type *E. coli* and *E. coli* with plasmid-born mercury resistance. In sub-acute exposure, the *mer* locus allowed for faster recovery than the plasmid-free strain at the same mercury exposure concentration. My RNA-Seq data revealed plasmid-encoded genes were the most highly expressed genes during mercury exposure. Identification of a low number of other plasmid genes increased expression and other key antibiotic resistance transposons decreases expression, which implies mercury exposure does not place selective pressure on antibiotic genes. However, integrases and other transposition genes increased expression, which for the first-time hints at why evolution might have frequently associated this metal resistance with multiple antibiotic resistance genes. As growth in the plasmid cultures recovered, so do the affected plasmid processes. We also identified key metabolic sources of NADPH being enhanced or restrained by mercury exposure.

Key sources that increased expression in mercury resistance cultures were isocitrate dehydrogenase and malate dehydrogenase, which are enzymes associated with the TCA cycle. This work is the first high resolution, longitudinal examination of the collaboration between a microbe's chromosome with a salient resistance locus on a naturally isolated plasmid. Apart from the specific genes on this plasmid and this resistance system, this work exemplifies the power of RNA-Seq to go to the heart of cellular processes that underpin plasmid persistence and spread, and the basis in real time of their awesome promiscuity of not just the plasmids, but the individual mobile elements they carry as they go about their days in our commensal gastrointestinal microbiota.

In chapter 3, the *in vivo* protein targets identified by acute PMA exposure using LC-MS/MS proteomics was combined with transcript data to see how the chromosome responds transcriptionally to mercury-damaged proteins. Key cysteine peptides were identified *in vivo* as mercury binding sites in 310 proteins which represented most of the COG categories. For example, ribosomal proteins were significantly more affected by $HgCl_2$ exposure than monovalent PMA and we know that a large subset of ribosomal proteins play a significant role as a reservoir of Zn(II), an essential metal that uses both cysteines and histidine for holding stocks of Zn(II) atoms. Such sites would not be so hospitable to monovalent PMA. Energy production proteins are rich in cysteines in Fe-S redox centers as are other central players including the ATP-synthase subunits whose expression was inhibited for a longer interval by monovalent PMA. Glucose metabolism pathways were affected both mercurial compounds, but mostly PMA. Three amino acid biosynthetic pathways were affected in opposite directions by PMA and $HgCl_2$ exposure. Expression of all ribosomal proteins, ATP-synthase, glucose

metabolism, and amino acid biosynthesis genes were returned to normal levels after mercury exposure in mercury resistance cells, coinciding with recovery of a normal growth rate. This work shows that although Hg(II) was known to be a very promiscuous toxicant, being able to see its damage at a very granular molecular level reveals that there are more vulnerable protein and pathway targets. This information can inform design of nutritional and/or pharmaceutical interventions against episodic and chronic mercury exposure in microbes and larger organisms.

Future Direction

The *in vivo* effects of mercury have long been recognized to involve binding to thiol ligands such as cysteines in proteins. Mercury toxicity is regarded as primarily disruption of thiol homeostasis by direct interactions with cysteines involved in catalysis and/or structure of proteins as well as the indirect generation of reactive oxygen species (ROS) by releasing redox active beneficial metals such as iron and copper from their redox active host proteins. However, it is also known that *in vitro* inorganic Hg(II) studies have shown that mercuric ion reacts with imino nitrogen in amino acids such as histidine and tryptophan and nucleotide bases such as adenosine, uridine, and thymidine (Nehzati et al., 2021, Ngu-Schwemlein et al., 2020, Birgersson et al., 1973, Leslie, 1967, Brooks and Davidson, 1960). However, Hg-N binding has not been imagined to occur *in vivo* because the formation constant of an Hg-N bond is much weaker than the Hg-S bond and the common cytosolic thiol buffer, glutathione, present at 10-15 mM in aerobic organisms would sequester all Hg(II) at normal low levels of exposure. As Hg(II) displaces labile iron from redox active proteins it generates ROS oxidizing the small thiol buffers like glutathione to become disulfides and cystic acid, no longer able to bind Hg(II). The

next most reactive ligands for Hg(II) are imino nitrogen of nucleotide bases and histidine. In my RNA-Seq work, the most intense up-regulated signals were for the genes of histidine biosynthesis – the strength of the signal looked like the cell was starving for histidine. *In vitro* studies indicate Hg(II) has a high affinity for nitrogen on nucleotide bases and can shift coordination from the oxygen donors to the N3, N3' groups of adjacent nucleotides (Nehzati et al., 2021). In November of 2021, I prepared several batches of Hg(II)-exposed MG1655 cells which we sent to biophysics collaborator Graham George at University of Saskatchewan for high resolution X-ray spectroscopy. The XAS run showed strong Hg-nitrogen signals and we've also learned the Department of Energy will fund more instrument time at Stanford for the next two years for our project to use mass spectrometry identify small non-coding RNAs from MG1655 that stably bind Hg(II) in *E.coli* and in intestinal epithelial Caco cells. The goal of the Summers' lab remains to define the biochemical domain of mercury as an azophilic, not just thiophilic, toxicant. We will thereby have more precise biochemical ways of understanding how metazoans recover and what are the most efficacious nutritional or pharmaceutical ways to assist that process in humans and ecosystems that have been and continue to be exposed to mercury.

References

AHN, S., JUNG, J., JANG, I.-A., MADSEN, E. L. & PARK, W. 2016. Role of glyoxylate shunt in oxidative stress response. *Journal of Biological Chemistry,* 291**,** 11928-11938.

ALIFANO, P., FANI, R., LIÒ, P., LAZCANO, A., BAZZICALUPO, M., CARLOMAGNO, M. S. & BRUNI, C. B. 1996. Histidine biosynthetic pathway and genes: structure, regulation, and evolution. *Microbiological reviews,* 60**,** 44-69.

ANDERS, S., PYL, P. T. & HUBER, W. 2015. HTSeq—a Python framework to work with high-throughput sequencing data. *bioinformatics,* 31**,** 166-169.

ANDREINI, C., BERTINI, I., CAVALLARO, G., HOLLIDAY, G. L. & THORNTON, J. M. 2008. Metal ions in biological catalysis: from enzyme databases to general principles. *JBIC Journal of Biological Inorganic Chemistry,* 13**,** 1205-1218.

BARKAY, T., KRITEE, K., BOYD, E. & GEESEY, G. 2010. A thermophilic bacterial origin and subsequent constraints by redox, light and salinity on the evolution of the microbial mercuric reductase. *Environmental Microbiology,* 12**,** 2904-2917.

BARKAY, T., MILLER, S. M. & SUMMERS, A. O. 2003. Bacterial mercury resistance from atoms to ecosystems. *FEMS microbiology reviews,* 27**,** 355-384.

BARNES, H. L. 1997. *Geochemistry of hydrothermal ore deposits,* John Wiley & Sons.

BARNES, W. M. 1978. DNA sequence from the histidine operon control region: seven histidine codons in a row. *Proceedings of the National Academy of Sciences,* 75**,** 4281-4285.

BEAUVAIS-FLÜCK, R., SLAVEYKOVA, V. I. & COSIO, C. 2016. Transcriptomic and physiological responses of the green microalga Chlamydomonas reinhardtii during short-term exposure to subnanomolar methylmercury concentrations. *Environmental science & technology,* 50**,** 7126-7134.

BENNETT, B. D., KIMBALL, E. H., GAO, M., OSTERHOUT, R., VAN DIEN, S. J. & RABINOWITZ, J. D. 2009. Absolute metabolite concentrations and implied enzyme active site occupancy in Escherichia coli. *Nature chemical biology,* 5**,** 593-599.

BERNHOFT, R. A. 2012. Mercury toxicity and treatment: a review of the literature. *Journal of environmental and public health,* 2012.

BIBIKOV, S. I., BARNES, L. A., GITIN, Y. & PARKINSON, J. S. 2000. Domain organization and flavin adenine dinucleotide-binding determinants in the aerotaxis signal transducer Aer of Escherichia coli. *Proceedings of the National Academy of Sciences,* 97**,** 5830-5835.

BIRGERSSON, B., DRAKENBERG, T., NEVILLE, G. A., RUDÉN, U. & NIMMICH, W. 1973. Mercury (II) complexes of methionine. *Acta Chemica Scandinavica,* 27**,** 3953-3960.

BJØRKLUND, G., LINDH, U., AASETH, J., MUTTER, J. & CHIRUMBOLO, S. 2018. Mercury in dental amalgams: a great concern for clinical toxicology in developing countries? *Journal of Trace Elements in Medicine and Biology: Organ of the Society for Minerals and Trace Elements (GMS),* 51**,** 9-11.

BLASI, F., BRUNI, C. B., AVITABILE, A., DEELEY, R. G., GOLDBERGER, R. F. & MEYERS, M. M. 1973. Inhibition of transcription of the histidine operon in vitro by the

first enzyme of the histidine pathway. *Proceedings of the National Academy of Sciences,* 70**,** 2692-2696.
BLATTNER, F. R., PLUNKETT III, G., BLOCH, C. A., PERNA, N. T., BURLAND, V., RILEY, M., COLLADO-VIDES, J., GLASNER, J. D., RODE, C. K. & MAYHEW, G. F. 1997. The complete genome sequence of Escherichia coli K-12. *science,* 277**,** 1453-1462.
BONGAERTS, J., ZOSKE, S., WEIDNER, U. & LINDEN, G. 1995. Transcriptional regulation of the proton translocating NADH dehydrogenase (nuoA-N) of Escherichia coli by electron acceptors, electron donors and gene regulators. *Molecular microbiology,* 16**,** 521-534.
BRANCO, V. & CARVALHO, C. 2019. The thioredoxin system as a target for mercury compounds. *Biochimica et Biophysica Acta (BBA)-General Subjects,* 1863**,** 129255.
BRAUN, M., BUNGERT, S. & FRIEDRICH, T. 1998. Characterization of the overproduced NADH dehydrogenase fragment of the NADH: ubiquinone oxidoreductase (complex I) from Escherichia coli. *Biochemistry,* 37**,** 1861-1867.
BROOKS, P. & DAVIDSON, N. 1960. Mercury (II) complexes of imidazole and histidine. *Journal of the American Chemical Society,* 82**,** 2118-2123.
BROWN, H. J., STOKES, H. & HALL, R. M. 1996. The integrons In0, In2, and In5 are defective transposon derivatives. *Journal of Bacteriology,* 178**,** 4429-4437.
CAGUIAT, J. J., WATSON, A. L. & SUMMERS, A. O. 1999. Cd (II)-responsive and constitutive mutants implicate a novel domain in MerR. *Journal of bacteriology,* 181**,** 3462-3471.
CALLISTER, S. J., MCCUE, L. A., TURSE, J. E., MONROE, M. E., AUBERRY, K. J., SMITH, R. D., ADKINS, J. N. & LIPTON, M. S. 2008. Comparative bacterial proteomics: analysis of the core genome concept. *PloS one,* 3**,** e1542.
CARROLL, A. C. & WONG, A. 2018. Plasmid persistence: costs, benefits, and the plasmid paradox. *Canadian journal of microbiology,* 64**,** 293-304.
CHAMPIER, L., DUARTE, V., MICHAUD-SORET, I. & COVÈS, J. 2004. Characterization of the MerD protein from Ralstonia metallidurans CH34: a possible role in bacterial mercury resistance by switching off the induction of the mer operon. *Molecular microbiology,* 52**,** 1475-1485.
CHAO, G., SHEN, J., TSENG, C. P., PARK, S.-J. & GUNSALUS, R. P. 1997. Aerobic regulation of isocitrate dehydrogenase gene (icd) expression in Escherichia coli by the arcA and fnr gene products. *Journal of bacteriology,* 179**,** 4299-4304.
CHEESMAN, B. V., ARNOLD, A. P. & RABENSTEIN, D. L. 1988. Nuclear magnetic resonance studies of the solution chemistry of metal complexes. 25. Hg (thiol) 3 complexes and Hg (II)-thiol ligand exchange kinetics. *Journal of the American Chemical Society,* 110**,** 6359-6364.
CHEN, S., ZHOU, Y., CHEN, Y. & GU, J. 2018. fastp: an ultra-fast all-in-one FASTQ preprocessor. *Bioinformatics,* 34**,** i884-i890.
CHOU, H.-H., MARX, C. J. & SAUER, U. 2015. Transhydrogenase promotes the robustness and evolvability of E. coli deficient in NADPH production. *PLoS genetics,* 11**,** e1005007.
CHRISTAKIS, C. A., BARKAY, T. & BOYD, E. S. 2021. Expanded diversity and phylogeny of mer genes broadens mercury resistance paradigms and reveals an origin for MerA among thermophilic Archaea. *Frontiers in microbiology,* 12.

CHRISTODOULOU, D., LINK, H., FUHRER, T., KOCHANOWSKI, K., GEROSA, L. & SAUER, U. 2018. Reserve flux capacity in the pentose phosphate pathway enables Escherichia coli's rapid response to oxidative stress. *Cell systems,* 6**,** 569-578. e7.
CLARKSON, T. W. 2002. The three modern faces of mercury. *Environ Health Perspect,* 110 Suppl 1**,** 11-23.
CLARKSON, T. W. & MAGOS, L. 2006. The toxicology of mercury and its chemical compounds. *Critical reviews in toxicology,* 36**,** 609-662.
COLOMBO, M. J., HA, J., REINFELDER, J. R., BARKAY, T. & YEE, N. 2013. Anaerobic oxidation of Hg (0) and methylmercury formation by Desulfovibrio desulfuricans ND132. *Geochimica et Cosmochimica Acta,* 112**,** 166-177.
COUNCIL, N. R. 2000. Toxicological effects of methylmercury.
ENGST, S. & MILLER, S. M. 1998. Rapid reduction of Hg (II) by mercuric ion reductase does not require the conserved C-terminal cysteine pair using HgBr2 as the substrate. *Biochemistry,* 37**,** 11496-11507.
FARRAR, W. & WILLIAMS, A. 1977. A history of mercury. *The chemistry of mercury.* Springer.
FOX, B. & WALSH, C. T. 1982. Mercuric reductase. Purification and characterization of a transposon-encoded flavoprotein containing an oxidation-reduction-active disulfide. *Journal of Biological Chemistry,* 257**,** 2498-2503.
FOX, B. S. & WALSH, C. T. 1983. Mercuric reductase: homology to glutathione reductase and lipoamide dehydrogenase. Iodoacetamide alkylation and sequence of the active site peptide. *Biochemistry,* 22**,** 4082-4088.
FRASSINETTI, S., BRONZETTI, G. L., CALTAVUTURO, L., CINI, M. & DELLA CROCE, C. 2006. The role of zinc in life: a review. *Journal of environmental pathology, toxicology and oncology,* 25.
FUHRER, T. & SAUER, U. 2009. Different biochemical mechanisms ensure network-wide balancing of reducing equivalents in microbial metabolism. *Journal of bacteriology,* 191**,** 2112-2121.
GALPERIN, M. Y., WOLF, Y. I., MAKAROVA, K. S., VERA ALVAREZ, R., LANDSMAN, D. & KOONIN, E. V. 2021. COG database update: focus on microbial diversity, model organisms, and widespread pathogens. *Nucleic acids research,* 49**,** D274-D281.
GAMBILL, B. D. & SUMMERS, A. O. 1992. Synthesis and degradation of the mRNA of the Tn21 mer operon. *Journal of molecular biology,* 225**,** 251-259.
GENTÈS, S., TAUPIAC, J., COLIN, Y., ANDRÉ, J.-M. & GUYONEAUD, R. 2017. Bacterial periphytic communities related to mercury methylation within aquatic plant roots from a temperate freshwater lake (South-Western France). *Environmental Science and Pollution Research,* 24**,** 19223-19233.
GERDES, K., GULTYAEV, A. P., FRANCH, T., PEDERSEN, K. & MIKKELSEN, N. D. 1997. Antisense RNA-regulated programmed cell death. *Annual review of genetics,* 31**,** 1-31.
GIONFRIDDO, C. M., TATE, M. T., WICK, R. R., SCHULTZ, M. B., ZEMLA, A., THELEN, M. P., SCHOFIELD, R., KRABBENHOFT, D. P., HOLT, K. E. & MOREAU, J. W. 2016. Microbial mercury methylation in Antarctic sea ice. *Nature microbiology,* 1**,** 1-12.
GLENN, T. C., NILSEN, R. A., KIERAN, T. J., FINGER, J. W., PIERSON, T. W., BENTLEY, K. E., HOFFBERG, S. L., LOUHA, S., GARCÍA-DE LEÓN, F. J. & DEL RIO

PORTILLA, M. A. 2016. Adapterama I: universal stubs and primers for thousands of dual-indexed Illumina libraries (iTru & iNext). *BioRxiv*, 049114.
GOREN, Y., GORING-MORRIS, A. N. & SEGAL, I. 2001. The technology of skull modelling in the Pre-Pottery Neolithic B (PPNB): regional variability, the relation of technology and iconography and their archaeological implications. *Journal of Archaeological Science,* 28**,** 671-690.
GRÉGOIRE, D., LAVOIE, N. & POULAIN, A. 2018. Heliobacteria reveal fermentation as a key pathway for mercury reduction in anoxic environments. *Environmental science & technology,* 52**,** 4145-4153.
GRÉGOIRE, D. S. & POULAIN, A. 2014. A little bit of light goes a long way: the role of phototrophs on mercury cycling. *Metallomics,* 6**,** 396-407.
GRÉGOIRE, D. S. & POULAIN, A. J. 2018. Shining light on recent advances in microbial mercury cycling. *Facets,* 3**,** 858-879.
HAMELIN, S., AMYOT, M., BARKAY, T., WANG, Y. & PLANAS, D. 2011. Methanogens: principal methylators of mercury in lake periphyton. *Environmental science & technology,* 45**,** 7693-7700.
HAMLETT, N., LANDALE, E., DAVIS, B. & SUMMERS, A. 1992. Roles of the Tn21 merT, merP, and merC gene products in mercury resistance and mercury binding. *Journal of bacteriology,* 174**,** 6377-6385.
HELBIG, K., BLEUEL, C., KRAUSS, G. J. & NIES, D. H. 2008. Glutathione and transition-metal homeostasis in Escherichia coli. *Journal of bacteriology,* 190**,** 5431-5438.
HONG, B., NAUSS, R., HARWOOD, I. M. & MILLER, S. M. 2010. Direct measurement of mercury (II) removal from organomercurial lyase (MerB) by tryptophan fluorescence: NmerA domain of coevolved γ-proteobacterial mercuric ion reductase (MerA) is more efficient than MerA catalytic core or glutathione. *Biochemistry,* 49**,** 8187-8196.
HSU-KIM, H., KUCHARZYK, K. H., ZHANG, T. & DESHUSSES, M. A. 2013. Mechanisms regulating mercury bioavailability for methylating microorganisms in the aquatic environment: a critical review. *Environmental science & technology,* 47**,** 2441-2456.
HUANG, J., CHANG, F.-C., WANG, S., HAN, Y.-J., CASTRO, M., MILLER, E. & HOLSEN, T. M. 2013. Mercury wet deposition in the eastern United States: characteristics and scavenging ratios. *Environmental Science: Processes & Impacts,* 15**,** 2321-2328.
IANEVA, O. 2009. Mechanisms of bacteria resistance to heavy metals. *Mikrobiolohichnyi zhurnal (Kiev, Ukraine: 1993),* 71**,** 54-65.
JENSEN, R. B. & GERDES, K. 1995. Programmed cell death in bacteria: proteic plasmid stabilization systems. *Molecular microbiology,* 17**,** 205-210.
JIN, Y. H., DUNLAP, P. E., MCBRIDE, S. J., AL-REFAI, H., BUSHEL, P. R. & FREEDMAN, J. H. 2008. Global transcriptome and deletome profiles of yeast exposed to transition metals. *PLoS genetics,* 4**,** e1000053.
JOY, A. & QURESHI, A. 2020. Mercury in dental amalgam, online retail, and the Minamata convention on mercury. *Environmental Science & Technology,* 54**,** 14139-14142.
KAPOOR, R., DOUGHTY, G. & GORIN, G. 1965. The reaction and assay of glutathione with Hg2+ and alkali. *Biochimica et Biophysica Acta (BBA)-General Subjects,* 100**,** 376-383.
KAWAKAMI, S. K., GLEDHILL, M. & ACHTERBERG, E. P. 2006. Production of phytochelatins and glutathione by marine phytoplankton in response to metal stress 1. *Journal of phycology,* 42**,** 975-989.

KELLER, A., ENG, J., ZHANG, N., LI, X. J. & AEBERSOLD, R. 2005. A uniform proteomics MS/MS analysis platform utilizing open XML file formats. *Molecular systems biology,* 1**,** 2005.0017.

KELLY, D. J., BUDD, K. & LEFEBVRE, D. D. 2007. Biotransformation of mercury in pH-stat cultures of eukaryotic freshwater algae. *Archives of microbiology,* 187**,** 45-53.

KHOLODII, G., GORLENKO, Z., MINDLIN, S., HOBMAN, J. & NIKIFOROV, V. 2002. Tn5041-like transposons: molecular diversity, evolutionary relationships and distribution of distinct variants in environmental bacteriabbThe accession numbers for the nucleotide sequences reported in this work are given in the legends for Figs 1F1 and 2. ccA comparison of the sequence of INT5041C with other proteins is available as supplementary data on Microbiology Online (http://mic. sgmjournals. org). *Microbiology,* 148**,** 3569-3582.

KIEBEL, G. R., AUBERRY, K. J., JAITLY, N., CLARK, D. A., MONROE, M. E., PETERSON, E. S., TOLIĆ, N., ANDERSON, G. A. & SMITH, R. D. 2006. PRISM: a data management system for high-throughput proteomics. *Proteomics,* 6**,** 1783-1790.

KIM, S., MISCHERIKOW, N., BANDEIRA, N., NAVARRO, J. D., WICH, L., MOHAMMED, S., HECK, A. J. & PEVZNER, P. A. 2010. The generating function of CID, ETD, and CID/ETD pairs of tandem mass spectra: applications to database search. *Molecular & Cellular Proteomics,* 9**,** 2840-2852.

KING, J. K., KOSTKA, J. E., FRISCHER, M. E. & SAUNDERS, F. M. 2000. Sulfate-reducing bacteria methylate mercury at variable rates in pure culture and in marine sediments. *Applied and environmental microbiology,* 66**,** 2430-2437.

KIYONO, M. & PAN-HOU, H. 1999. The merG gene product is involved in phenylmercury resistance in Pseudomonas strain K-62. *Journal of bacteriology,* 181**,** 726-730.

KIYONO, M., SONE, Y., NAKAMURA, R., PAN-HOU, H. & SAKABE, K. 2009. The MerE protein encoded by transposon Tn21 is a broad mercury transporter in Escherichia coli. *FEBS letters,* 583**,** 1127-1131.

KRUPP, E. M., MILNE, B. F., MESTROT, A., MEHARG, A. A. & FELDMANN, J. 2008. Investigation into mercury bound to biothiols: structural identification using ESI–ion-trap MS and introduction of a method for their HPLC separation with simultaneous detection by ICP-MS and ESI-MS. *Analytical and Bioanalytical Chemistry,* 390**,** 1753-1764.

KUSANO, T., JI, G., INOUE, C. & SILVER, S. 1990. Constitutive synthesis of a transport function encoded by the Thiobacillus ferrooxidans merC gene cloned in Escherichia coli. *Journal of bacteriology,* 172**,** 2688-2692.

LANGMEAD, B. & SALZBERG, S. L. 2012. Fast gapped-read alignment with Bowtie 2. *Nature methods,* 9**,** 357-359.

LAVOIE, S. P., MAPOLELO, D. T., COWART, D. M., POLACCO, B. J., JOHNSON, M. K., SCOTT, R. A., MILLER, S. M. & SUMMERS, A. O. 2015. Organic and inorganic mercurials have distinct effects on cellular thiols, metal homeostasis, and Fe-binding proteins in Escherichia coli. *JBIC Journal of Biological Inorganic Chemistry,* 20**,** 1239-1251.

LAVOIE, S. P. & SUMMERS, A. O. 2018. Transcriptional responses of Escherichia coli during recovery from inorganic or organic mercury exposure. *BMC genomics,* 19**,** 1-24.

LEDWIDGE, R., PATEL, B., DONG, A., FIEDLER, D., FALKOWSKI, M., ZELIKOVA, J., SUMMERS, A. O., PAI, E. F. & MILLER, S. M. 2005. NmerA, the metal binding domain of mercuric ion reductase, removes Hg2+ from proteins, delivers it to the

catalytic core, and protects cells under glutathione-depleted conditions. *Biochemistry,* 44**,** 11402-11416.
LEIF, H., SLED, V. D., OHNISHI, T., WEISS, H. & FRIEDRICH, T. 1995. Isolation and characterization of the proton-translocating NADH: ubiquinone oxidoreductase from Escherichia coli. *European journal of biochemistry,* 230**,** 538-548.
LESLIE, J. 1967. Effect of mercuric salts on the ultraviolet spectra of aromatic amino acids and proteins. *Archives of Biochemistry and Biophysics,* 121**,** 463-469.
LI, G.-W., BURKHARDT, D., GROSS, C. & WEISSMAN, J. S. 2014. Quantifying absolute protein synthesis rates reveals principles underlying allocation of cellular resources. *Cell,* 157**,** 624-635.
LIAN, P., GUO, H.-B., RICCARDI, D., DONG, A., PARKS, J. M., XU, Q., PAI, E. F., MILLER, S. M., WEI, D.-Q. & SMITH, J. C. 2014. X-ray structure of a Hg2+ complex of mercuric reductase (MerA) and quantum mechanical/molecular mechanical study of Hg2+ transfer between the C-terminal and buried catalytic site cysteine pairs. *Biochemistry,* 53**,** 7211-7222.
LIEBERT, C. A., HALL, R. M. & SUMMERS, A. O. 1999. Transposon Tn 21, flagship of the floating genome. *Microbiology and molecular biology reviews,* 63**,** 507-522.
LIEBERT, C. A., WIREMAN, J., SMITH, T. & SUMMERS, A. O. 1997. Phylogeny of mercury resistance (mer) operons of gram-negative bacteria isolated from the fecal flora of primates. *Applied and Environmental Microbiology,* 63**,** 1066-1076.
LIN, H., MORRELL-FALVEY, J. L., RAO, B., LIANG, L. & GU, B. 2014. Coupled mercury–cell sorption, reduction, and oxidation on methylmercury production by Geobacter sulfurreducens PCA. *Environmental science & technology,* 48**,** 11969-11976.
LIU, G., CAI, Y., O'DRISCOLL, N., FENG, X. & JIANG, G. 2012. Overview of mercury in the environment. *Environmental chemistry and toxicology of mercury***,** 1-12.
LIU, S. & WIATROWSKI, H. A. 2018. Reduction of Hg (II) to Hg (0) by biogenic magnetite from two magnetotactic bacteria. *Geomicrobiology Journal,* 35**,** 198-208.
LOVE, M. I., HUBER, W. & ANDERS, S. 2014. Moderated estimation of fold change and dispersion for RNA-seq data with DESeq2. *Genome biology,* 15**,** 1-21.
LU, X., LIU, Y., JOHS, A., ZHAO, L., WANG, T., YANG, Z., LIN, H., ELIAS, D. A., PIERCE, E. M. & LIANG, L. 2016. Anaerobic mercury methylation and demethylation by Geobacter bemidjiensis Bem. *Environmental science & technology,* 50**,** 4366-4373.
LÁZARO, W. L., DÍEZ, S., DA SILVA, C. J., IGNÁCIO, Á. R. & GUIMARÃES, J. R. 2018. Seasonal changes in peryphytic microbial metabolism determining mercury methylation in a tropical wetland. *Science of the Total Environment,* 627**,** 1345-1352.
MALM, O. 1998. Gold mining as a source of mercury exposure in the Brazilian Amazon. *Environmental research,* 77**,** 73-78.
MASON, R. P., FITZGERALD, W. F. & MOREL, F. M. 1994. The biogeochemical cycling of elemental mercury: anthropogenic influences. *Geochimica et cosmochimica acta,* 58**,** 3191-3198.
MEAGHER, R. B., SUMMERS, A. O. & RUGH, C. L. 1999. Metal resistance sequences and transgenic plants.
MISHRA, S. & IMLAY, J. 2012. Why do bacteria use so many enzymes to scavenge hydrogen peroxide? *Archives of biochemistry and biophysics,* 525**,** 145-160.
MOREL, F. M., KRAEPIEL, A. M. & AMYOT, M. 1998. The chemical cycle and bioaccumulation of mercury. *Annual review of ecology and systematics,* 29**,** 543-566.

MUSLIN, E. H., LI, D., STEVENS, F. J., DONNELLY, M., SCHIFFER, M. & ANDERSON, L. E. 1995. Engineering a domain-locking disulfide into a bacterial malate dehydrogenase produces a redox-sensitive enzyme. *Biophysical journal,* 68**,** 2218-2223.

NATH, K. A., CROATT, A. J., LIKELY, S., BEHRENS, T. W. & WARDEN, D. 1996. Renal oxidant injury and oxidant response induced by mercury. *Kidney international,* 50**,** 1032-1043.

NEHZATI, S., SUMMERS, A. O., DOLGOVA, N. V., ZHU, J., SOKARAS, D., KROLL, T., PICKERING, I. J. & GEORGE, G. N. 2021. Hg (II) Binding to Thymine Bases in DNA. *Inorganic Chemistry,* 60**,** 7442-7452.

NEIDHARDT, F. C., BLOCH, P. L. & SMITH, D. F. 1974. Culture medium for enterobacteria. *Journal of bacteriology,* 119**,** 736-747.

NGU-SCHWEMLEIN, M., MERLE, J., MEEKER, W., RISDON-LANGDON, K. & NIXON, T. 2020. Evaluating the involvement of tryptophan on thiolated peptide-mercury (II) complexes: cation-pi interactions. *Inorganica Chimica Acta,* 506**,** 119552.

NIES, D. H. 1999. Microbial heavy-metal resistance. *Applied microbiology and biotechnology,* 51**,** 730-750.

NIKEL, P. I., FUHRER, T., CHAVARRÍA, M., SÁNCHEZ-PASCUALA, A., SAUER, U. & DE LORENZO, V. 2021. Reconfiguration of metabolic fluxes in Pseudomonas putida as a response to sub-lethal oxidative stress. *The ISME journal,* 15**,** 1751-1766.

OLSEN, T. A., BRANDT, C. C. & BROOKS, S. C. 2016. Periphyton biofilms influence net methylmercury production in an industrially contaminated system. *Environmental Science & Technology,* 50**,** 10843-10850.

OMAN, T. J. & VAN DER DONK, W. A. 2010. Follow the leader: the use of leader peptides to guide natural product biosynthesis. *Nature chemical biology,* 6**,** 9-18.

ORAM, P. D., FANG, X., FERNANDO, Q., LETKEMAN, P. & LETKEMAN, D. 1996. The formation constants of mercury (II)− glutathione complexes. *Chemical research in toxicology,* 9**,** 709-712.

PAL, C., BENGTSSON-PALME, J., KRISTIANSSON, E. & LARSSON, D. J. 2015. Co-occurrence of resistance genes to antibiotics, biocides and metals reveals novel insights into their co-selection potential. *BMC genomics,* 16**,** 1-14.

PARK, S.-J., WIREMAN, J. & SUMMERS, A. 1992. Genetic analysis of the Tn21 mer operator-promoter. *Journal of bacteriology,* 174**,** 2160-2171.

PARKS, J. M., GUO, H., MOMANY, C., LIANG, L., MILLER, S. M., SUMMERS, A. O. & SMITH, J. C. 2009. Mechanism of Hg− C protonolysis in the organomercurial lyase MerB. *Journal of the American Chemical Society,* 131**,** 13278-13285.

PARKS, J. M., JOHS, A., PODAR, M., BRIDOU, R., HURT JR, R. A., SMITH, S. D., TOMANICEK, S. J., QIAN, Y., BROWN, S. D. & BRANDT, C. C. 2013. The genetic basis for bacterial mercury methylation. *Science,* 339**,** 1332-1335.

PARTRIDGE, S. R. & HALL, R. M. 2004. Complex multiple antibiotic and mercury resistance region derived from the r-det of NR1 (R100). *Antimicrobial agents and chemotherapy,* 48**,** 4250-4255.

PETERSON, J. D., UMAYAM, L. A., DICKINSON, T., HICKEY, E. K. & WHITE, O. 2001. The comprehensive microbial resource. *Nucleic acids research,* 29**,** 123-125.

PITTS, K. E. & SUMMERS, A. O. 2002. The roles of thiols in the bacterial organomercurial lyase (MerB). *Biochemistry,* 41**,** 10287-10296.

POLACCO, B. J., PURVINE, S. O., ZINK, E. M., LAVOIE, S. P., LIPTON, M. S., SUMMERS, A. O. & MILLER, S. M. 2011. Discovering mercury protein modifications in whole proteomes using natural isotope distributions observed in liquid chromatography-tandem mass spectrometry. *Molecular & cellular proteomics,* 10.

RAO, R., PAGAN, J. & SENIOR, A. 1988. Directed mutagenesis of the strongly conserved lysine 175 in the proposed nucleotide-binding domain of alpha-subunit from Escherichia coli F1-ATPase. *Journal of Biological Chemistry,* 263**,** 15957-15963.

RAO, Y., MCCOOEYE, M., WINDUST, A., BRAMANTI, E., D'ULIVO, A. & MESTER, Z. N. 2010. Mapping of selenium metabolic pathway in yeast by Liquid Chromatography− Orbitrap Mass Spectrometry. *Analytical chemistry,* 82**,** 8121-8130.

RICCARDI, D., GUO, H.-B., PARKS, J. M., GU, B., SUMMERS, A. O., MILLER, S. M., LIANG, L. & SMITH, J. C. 2013. Why mercury prefers soft ligands. *The Journal of Physical Chemistry Letters,* 4**,** 2317-2322.

ROSS, W., PARK, S. & SUMMERS, A. 1989. Genetic analysis of transcriptional activation and repression in the Tn21 mer operon. *Journal of bacteriology,* 171**,** 4009-4018.

RUI, B., SHEN, T., ZHOU, H., LIU, J., CHEN, J., PAN, X., LIU, H., WU, J., ZHENG, H. & SHI, Y. 2010. A systematic investigation of Escherichia coli central carbon metabolism in response to superoxide stress. *BMC systems biology,* 4**,** 1-12.

RYTUBA, J. Genozoic mittallgeny of California: Geology and Ore Deposits of the American Cordillera. Symposium Proceedings., 1996. 803-822.

RYTUBA, J. J. 2003. Mercury from mineral deposits and potential environmental impact. *Environmental Geology,* 43**,** 326-338.

SAHLMAN, L., WONG, W. & POWLOWSKI, J. 1997. A mercuric ion uptake role for the integral inner membrane protein, MerC, involved in bacterial mercuric ion resistance. *Journal of Biological Chemistry,* 272**,** 29518-29526.

SALMON, K., HUNG, S.-P., MEKJIAN, K., BALDI, P., HATFIELD, G. W. & GUNSALUS, R. P. 2003. Global gene expression profiling in Escherichia coli K12: the effects of oxygen availability and FNR. *Journal of Biological Chemistry,* 278**,** 29837-29855.

SAN MILLAN, A. & MACLEAN, R. C. 2017. Fitness costs of plasmids: a limit to plasmid transmission. *Microbiology spectrum,* 5**,** 5.5. 02.

SANGVANICH, T., MORRY, J., FOX, C., NGAMCHERDTRAKUL, W., GOODYEAR, S., CASTRO, D., FRYXELL, G. E., ADDLEMAN, R. S., SUMMERS, A. O. & YANTASEE, W. 2014. Novel oral detoxification of mercury, cadmium, and lead with thiol-modified nanoporous silica. *ACS applied materials & interfaces,* 6**,** 5483-5493.

SAUER, U., CANONACO, F., HERI, S., PERRENOUD, A. & FISCHER, E. 2004. The soluble and membrane-bound transhydrogenases UdhA and PntAB have divergent functions in NADPH metabolism of Escherichia coli. *Journal of Biological Chemistry,* 279**,** 6613-6619.

SAUPE, F. 1990. Geology of the Almadén mercury deposit, province of Ciudad Real, Spain. *Economic Geology,* 85**,** 482-510.

SCHOBER, P., BOER, C. & SCHWARTE, L. A. 2018. Correlation coefficients: appropriate use and interpretation. *Anesthesia & Analgesia,* 126**,** 1763-1768.

SCHUÉ, M., DOVER, L. G., BESRA, G. S., PARKHILL, J. & BROWN, N. L. 2009. Sequence and analysis of a plasmid-encoded mercury resistance operon from Mycobacterium marinum identifies MerH, a new mercuric ion transporter. *Journal of bacteriology,* 191**,** 439-444.

SELIN, N. E., JACOB, D. J., PARK, R. J., YANTOSCA, R. M., STRODE, S., JAEGLÉ, L. & JAFFE, D. 2007. Chemical cycling and deposition of atmospheric mercury: Global constraints from observations. *Journal of Geophysical Research: Atmospheres,* 112.

SILVER, S. & HOBMAN, J. L. 2007. Mercury microbiology: resistance systems, environmental aspects, methylation, and human health. *Molecular microbiology of heavy metals.* Springer.

SIRONA, D. 2020. Dentsply Sirona: 2020 Annual Report. 140.

SMITH, T., PITTS, K., MCGARVEY, J. A. & SUMMERS, A. O. 1998. Bacterial oxidation of mercury metal vapor, Hg (0). *Applied and environmental microbiology,* 64**,** 1328-1332.

SONG, L., TENG, Q., PHILLIPS, R. S., BREWER, J. M. & SUMMERS, A. O. 2007. 19F-NMR reveals metal and operator-induced allostery in MerR. *Journal of molecular biology,* 371**,** 79-92.

STEAD, M. B., AGRAWAL, A., BOWDEN, K. E., NASIR, R., MOHANTY, B. K., MEAGHER, R. B. & KUSHNER, S. R. 2012. RNA snap™: a rapid, quantitative and inexpensive, method for isolating total RNA from bacteria. *Nucleic acids research,* 40**,** e156-e156.

STRICKS, W. & KOLTHOFF, I. 1953. Reactions between mercuric mercury and cysteine and glutathione. Apparent dissociation constants, heats and entropies of formation of various forms of mercuric mercapto-cysteine and-glutathione. *Journal of the American Chemical Society,* 75**,** 5673-5681.

SUMMERS, A., KNIGHT-OLLIFF, L. & SLATER, C. 1982. Effect of catabolite repression on the mer operon. *Journal of bacteriology,* 149**,** 191-197.

SUMMERS, A., WIREMAN, J., VIMY, M., LORSCHEIDER, F., MARSHALL, B., LEVY, S., BENNETT, S. & BILLARD, L. 1993. Mercury released from dental" silver" fillings provokes an increase in mercury-and antibiotic-resistant bacteria in oral and intestinal floras of primates. *Antimicrobial agents and chemotherapy,* 37**,** 825-834.

SUMMERS, A. O. & LEWIS, E. 1973. Volatilization of mercuric chloride by mercury-resistant plasmid-bearing strains of Escherichia coli, Staphylococcus aureus, and Pseudomonas aeruginosa. *Journal of bacteriology,* 113**,** 1070-1072.

SUMMERS, A. O. & SILVER, S. 1972. Mercury resistance in a plasmid-bearing strain of Escherichia coli. *Journal of bacteriology,* 112**,** 1228-1236.

TRÜMPLER, S., LOHMANN, W., MEERMANN, B., BUSCHER, W., SPERLING, M. & KARST, U. 2009. Interaction of thimerosal with proteins—ethylmercuryadduct formation of human serum albumin and β-lactoglobulin A. *Metallomics,* 1**,** 87-91.

UNO, Y., KIYONO, M., TEZUKA, T. & PAN-HOU, H. 1997. Phenylmercury transport mediated by merT-merP genes of Pseudomonas K-62 plasmid pMR26. *Biological and Pharmaceutical Bulletin,* 20**,** 107-109.

VALKO, M., MORRIS, H. & CRONIN, M. 2005. Metals, toxicity and oxidative stress. *Current medicinal chemistry,* 12**,** 1161-1208.

VEIGA, M. M., MAXSON, P. A. & HYLANDER, L. D. 2006. Origin and consumption of mercury in small-scale gold mining. *Journal of cleaner production,* 14**,** 436-447.

WANG, A. & CROWLEY, D. E. 2005. Global gene expression responses to cadmium toxicity in Escherichia coli. *Journal of bacteriology,* 187**,** 3259-3266.

WANG, F., LEMES, M. & KHAN, M. A. 2012. Metallomics of mercury: Role of thiol-and selenol-containing biomolecules. *Environmental Chemistry and Toxicology of Mercury,* 517.

WESSLER, S. R. & CALVO, J. M. 1981. Control of leu operon expression in Escherichia coli by a transcription attenuation mechanism. *Journal of molecular biology,* 149**,** 579-597.
WIGGINS, A. G., LAVOIE, S. P., WIREMAN, J. & SUMMERS, A. O. 2018. Thinking outside the (pill) box: Does toxic metal exposure thwart antibiotic stewardship best practices? *Plasmid,* 99**,** 68-71.
WILLIAMS, L. E., DETTER, C., BARRY, K., LAPIDUS, A. & SUMMERS, A. O. 2006. Facile recovery of individual high-molecular-weight, low-copy-number natural plasmids for genomic sequencing. *Applied and environmental microbiology,* 72**,** 4899-4906.
WILSON, J. R., LEANG, C., MORBY, A. P., HOBMAN, J. L. & BROWN, N. L. 2000. MerF is a mercury transport protein: different structures but a common mechanism for mercuric ion transporters? *FEBS letters,* 472**,** 78-82.
WU, R., WANG, X., WOMBLE, D. & ROWND, R. 1992. Expression of the repA1 gene of IncFII plasmid NR1 is translationally coupled to expression of an overlapping leader peptide. *Journal of bacteriology,* 174**,** 7620-7628.
XU, F. F. & IMLAY, J. A. 2012. Silver (I), mercury (II), cadmium (II), and zinc (II) target exposed enzymic iron-sulfur clusters when they toxify Escherichia coli. *Applied and environmental microbiology,* 78**,** 3614-3621.
YANKOVSKAYA, V., HORSEFIELD, R., TORNROTH, S., LUNA-CHAVEZ, C., MIYOSHI, H., LÉGER, C., BYRNE, B., CECCHINI, G. & IWATA, S. 2003. Architecture of succinate dehydrogenase and reactive oxygen species generation. *Science,* 299**,** 700-704.
YIN, L., LIN, S., SUMMERS, A. O., ROPER, V., CAMPEN, M. J. & YU, X. 2021. Children with amalgam dental restorations have significantly elevated blood and urine mercury levels. *Toxicological Sciences,* 184**,** 104-126.
YIN, L., YU, K., LIN, S., SONG, X. & YU, X. 2016. Associations of blood mercury, inorganic mercury, methyl mercury and bisphenol A with dental surface restorations in the US population, NHANES 2003–2004 and 2010–2012. *Ecotoxicology and Environmental Safety,* 134**,** 213-225.
YU, R.-Q., FLANDERS, J., MACK, E. E., TURNER, R., MIRZA, M. B. & BARKAY, T. 2012. Contribution of coexisting sulfate and iron reducing bacteria to methylmercury production in freshwater river sediments. *Environmental science & technology,* 46**,** 2684-2691.
ZHANG, J., WANG, F., HOUSE, J. D. & PAGE, B. 2004. Thiols in wetland interstitial waters and their role in mercury and methylmercury speciation. *Limnology and Oceanography,* 49**,** 2276-2286.
ZHENG, N., WANG, S., DONG, W., HUA, X., LI, Y., SONG, X., CHU, Q., HOU, S. & LI, Y. 2019. The toxicological effects of mercury exposure in marine fish. *Bulletin of environmental contamination and toxicology,* 102**,** 714-720.
ZHONGMING, Z., LINONG, L., XIAONA, Y., WANGQIANG, Z. & WEI, L. 2013. Global Mercury Assessment 2013: Sources, emissions, releases, and environmental transport.

APPENDIX A

SUPPLEMENTAL MATERIAL FOR CHAPTER 2

Table A.S1a Summary of steps associated with processing of date for each RNA-Seq library.

Replicon	# Raw Reads	# QC'd Reads	% Passed	% Properly Paired	# Pairs Processed	Annotated	% Features Match
HgS	22,813,104	22,755,656	99.75	97.69	9,277,873	8,265,705	89.09
Plasmid	---	---	---	2.54	261,452	184,822	70.69
HgR + Plasmid	22,149,349	22,046,677	99.54	95.32	8,607,995	7,599,498	88.28

Table A.S1b QC'ed steps associated with processing of date for each RNA-Seq library. The average number of Illumina reads for three biological replicates was calculated at each processing step for each RNA-Seq library: HgS (MG), HgR (NR1), and NR1 plasmid. (A) Summary table for each *E. coli* strain consisting of all read counts for each mercury exposure condition and sampling time point. (B) Total read at each time point for each strain and Hg exposure condition (grey). In green shading are the number of raw reads passing standard quality control criteria. (C) In blue shading are forward and reverse reads properly paired and aligned with Bowtie 2 to MG1655 or MG1655(pNR1) genomes. (D) In orange shading are paired reads aligned with Hg-Seq with a genomic feature on MG1655 or MG1655(pNR1).

Replicon	Condition	Raw Reads	QC'ed & Paired	% Passed	QC'ed Total
HgR	0μM_t0	11,476,936	11,448,956	99.76	22,897,913
Plasmid	0μM_t0	11,476,936	11,448,958	99.76	22,897,916
HgS	0μM_t0	11,025,272	10,994,885	99.73	21,989,770
HgR	0μM_t10	10,790,366	10,762,448	99.74	21,524,896
Plasmid	0μM_t10	10,790,366	10,762,446	99.74	21,524,891
HgS	0μM_t10	12,161,805	12,130,289	99.74	24,260,579
HgR	0μM_t30	12,433,320	12,401,291	99.74	24,802,581
Plasmid	0μM_t30	12,433,320	12,401,292	99.74	24,802,584
HgS	0μM_t30	13,563,652	13,526,447	99.72	27,052,894
HgR	0μM_t60	8,169,483	8,148,672	99.74	16,297,343
Plasmid	0μM_t60	8,169,483	8,148,672	99.74	16,297,344
HgS	0μM_t60	10,663,423	10,631,368	99.70	21,262,736
HgR	0μM_t90	11,040,647	11,013,842	99.75	22,027,685
Plasmid	0μM_t90	11,040,647	11,013,842	99.75	22,027,683
HgS	0μM_t90	11,504,070	11,475,755	99.76	22,951,509
HgR	3μM_t10	8,833,051	8,810,968	99.75	17,621,936
Plasmid	3μM_t10	8,833,051	8,810,968	99.75	17,621,935
HgS	3μM_t10	10,392,847	10,368,724	99.76	20,737,449
HgR	3μM_t30	9,932,997	9,592,022	96.48	19,184,044
Plasmid	3μM_t30	9,932,997	9,910,919	99.78	19,821,837
HgS	3μM_t30	11,781,436	11,753,895	99.77	23,507,790
HgR	3μM_t60	10,882,730	10,859,599	99.79	21,719,197
Plasmid	3μM_t60	10,882,730	10,859,601	99.79	21,719,201
HgS	3μM_t60	11,199,892	11,175,413	99.78	22,350,827
HgR	3μM_t90	14,755,511	14,725,583	99.80	29,451,166
Plasmid	3μM_t90	14,755,511	14,725,584	99.80	29,451,168
HgS	3μM_t90	11,489,179	11,464,130	99.78	22,928,259
HgR	4μM_t10	9,555,903	9,533,577	99.76	19,067,155
Plasmid	4μM_t10	9,555,903	9,533,580	99.76	19,067,159
HgS	4μM_t10	11,017,976	10,993,558	99.78	21,987,115
HgR	4μM_t30	12,070,656	12,039,443	99.74	24,078,885
Plasmid	4μM_t30	12,070,656	12,039,442	99.74	24,078,883
HgS	4μM_t30	11,180,512	11,153,443	99.76	22,306,887
HgR	4μM_t60	12,771,484	12,737,988	99.74	25,475,976
Plasmid	4μM_t60	12,771,484	12,737,990	99.74	25,475,980
HgS	4μM_t60	10,395,331	10,365,259	99.71	20,730,518
HgR	4μM_t90	11,257,686	11,229,009	99.74	22,458,017
Plasmid	4μM_t90	11,257,686	11,229,007	99.74	22,458,014
HgS	4μM_t90	11,909,783	11,878,600	99.74	23,757,199

Table A.S1c Alignment steps associated with processing of date for each RNA-Seq library.

Replicon	Mapped	% Mapped	Properly Paired	% Paired
HgR	22,259,559	97.21	22,141,117	96.69
Plasmid	395,457	1.73	391,463	1.71
HgS	21,627,148	98.33	21,509,946	97.79
HgR	20,836,224	96.79	20,697,352	96.14
Plasmid	362,628	1.69	358,280	1.67
HgS	23,747,049	97.91	23,637,441	97.45
HgR	23,989,578	96.64	23,878,844	96.19
Plasmid	413,225	1.67	409,295	1.66
HgS	26,396,468	97.64	26,227,734	97.01
HgR	15,762,730	96.88	15,700,640	96.51
Plasmid	298,625	1.88	296,367	1.87
HgS	20,781,598	97.41	20,664,884	96.84
HgR	20,749,719	94.61	20,656,282	94.19
Plasmid	532,668	2.32	528,583	2.30
HgS	22,674,364	98.81	22,594,554	98.47
HgR	15,904,855	90.28	15,795,110	89.68
Plasmid	1,183,830	6.62	1,163,951	6.51
HgS	20,270,887	97.72	20,185,679	97.28
HgR	18,427,180	96.02	18,342,469	95.58
Plasmid	451,731	2.29	447,177	2.26
HgS	23,266,233	98.98	23,169,498	98.57
HgR	21,147,999	97.36	21,076,443	97.03
Plasmid	358,676	1.66	355,940	1.65
HgS	22,106,639	98.87	21,994,231	98.33
HgR	28,928,739	98.20	28,845,533	97.91
Plasmid	297,389	1.04	295,684	1.03
HgS	22,755,916	99.23	22,661,198	98.78
HgR	17,586,970	92.28	17,491,969	91.74
Plasmid	1,092,463	5.76	1,079,559	5.68
HgS	21,627,989	98.37	21,534,059	97.95
HgR	22,776,753	94.48	22,653,388	93.91
Plasmid	876,342	3.74	865,394	3.69
HgS	21,914,988	98.22	21,821,084	97.80
HgR	24,809,190	97.20	24,701,327	96.76
Plasmid	321,071	1.43	318,316	1.42
HgS	20,180,497	97.35	20,048,802	96.70
HgR	21,855,531	97.30	21,746,180	96.81
Plasmid	352,102	1.58	348,696	1.56
HgS	23,141,604	97.45	23,025,623	96.96

Table A.S1d Annotated feature steps associated with processing of date for each RNA-Seq library.

Replicon	Total Pairs	Annotated	% Features	No Feature	Ambiguous
HgR	10,725,057	9,207,464	85.85	1,568,935	176
Plasmid	190,513	143,820	75.47	46,693	0
HgS	10,137,093	8,744,562	86.26	1,438,987	180
HgR	9,938,605	8,521,208	85.74	1,465,061	155
Plasmid	174,927	131,756	75.32	43,171	0
HgS	8,783,684	7,615,928	86.71	1,207,301	147
HgR	11,312,687	9,882,853	87.36	1,478,798	191
Plasmid	198,686	153,872	77.44	44,815	0
HgS	12,585,724	10,958,920	87.07	1,683,457	201
HgR	7,283,394	6,513,568	89.43	797,081	121
Plasmid	144,654	114,578	79.21	30,076	0
HgS	9,763,218	8,735,332	89.47	1,063,248	172
HgR	10,003,168	9,029,352	90.26	1,019,711	166
Plasmid	259,928	197,291	75.90	62,637	0
HgS	10,584,154	9,584,162	90.55	1,042,190	173
HgR	7,740,502	7,037,480	90.92	720,189	161
Plasmid	587,354	370,990	63.16	216,363	0
HgS	9,871,238	9,010,320	91.28	880,855	174
HgR	8,025,785	7,079,278	88.21	971,951	137
Plasmid	220,176	160,973	73.11	59,203	0
HgS	11,442,305	10,354,497	90.49	1,115,885	192
HgR	9,510,539	8,271,091	86.97	1,281,472	151
Plasmid	173,475	132,520	76.39	40,955	0
HgS	7,963,558	6,940,086	87.15	1,052,308	132
HgR	7,050,445	6,352,517	90.10	728,165	120
Plasmid	144,371	114,239	79.13	30,132	0
HgS	5,202,647	4,566,504	87.77	658,200	64
HgR	6,426,133	5,834,060	90.79	610,062	210
Plasmid	542,739	351,679	64.80	191,061	0
HgS	7,529,293	6,831,277	90.73	722,375	229
HgR	6,623,345	6,003,538	90.64	647,403	207
Plasmid	435,382	285,352	65.54	150,030	0
HgS	7,444,137	6,735,340	90.48	734,997	238
HgR	7,672,579	6,770,719	88.25	930,635	133
Plasmid	156,325	116,805	74.72	39,520	0
HgS	8,209,939	7,409,049	90.24	825,016	137
HgR	9,591,693	8,290,340	86.43	1,337,967	139
Plasmid	170,345	128,812	75.62	41,534	0
HgS	11,095,353	9,968,186	89.84	1,159,314	238

Table A.S2a: Read counts for genes of the *mer* operon normalized by their gene length in base pairs. (A) 3 µM Hg and (B) 4 µM Hg. Each time point is the average read count and standard deviation of three biological replicates for a given *mer* gene divided by the length of the gene (bp).

3 µM $HgCl_2$	merR		merT		merP		merC		merA		merD		merE		urf2	
Time point	mean	stdv	mean	stdv	mean	stdv	mean	stdv	mean	stdv	mean	stdv	mean	stdv	mean	stdv
0	0.47	0.033	0.03	0.012	0.04	0.016	0.04	0.008	0.04	0.001	0.01	0	0.01	0.004	0.01	0.001
10	2.26	0.705	147.83	71.623	152.72	33.349	128.34	29.256	57.77	11.334	4.67	0.408	3.73	0.632	3.36	0.249
30	0.5	0.271	13.05	8.872	22.5	17.958	17.74	14.625	11.26	9.598	1.89	1.654	1.66	1.524	1.67	1.482
60	0.42	0.072	4.46	1.169	4.83	1.172	3.86	1.018	2.46	0.581	0.38	0.108	0.3	0.059	0.32	0.089
90	0.37	0.266	2.62	1.302	4.2	2.474	3.31	1.892	2.23	1.369	0.39	0.277	0.28	0.191	0.27	0.178

Table A.S2b

4 µM $HgCl_2$	merR		merT		merP		merC		merA		merD		merE		urf2	
Time point	mean	stdv	mean	stdv	mean	stdv	mean	stdv	mean	stdv	mean	stdv	mean	stdv	mean	stdv
0	0.47	0.033	0.03	0.012	0.04	0.016	0.04	0.008	0.04	0.001	0.01	0	0.01	0.004	0.01	0.001
10	1.94	0.71	196.17	76.12	156.59	85.26	128.22	62.79	43.66	16.06	1.49	0.52	0.97	0.25	0.77	0.2
30	1.21	0.55	88.65	49.41	144.32	88.33	93.79	57.08	46.03	23.98	4.5	2.08	3.88	1.46	3.39	1.47
60	0.41	0.18	7.82	3.23	10.8	4.44	8.23	2.37	5.16	2.37	0.9	0.3	0.61	0.17	0.62	0.23
90	0.43	0.03	5.01	1.22	4.97	0.89	3.67	0.62	2.54	0.43	0.34	0.03	0.32	0.03	0.33	0.09

Table A.S3: Pearson correlations for the line graphs of the normalized reads of each *mer* operon gene at each time point. (A) 3 µM Hg and (B) 4 µM Hg.

A.

	merR	merT	merP	merC	merA	merD	merE	urf2
merR	1.000	0.998	0.994	0.995	0.989	0.938	0.923	0.903
merT	0.998	1.000	0.998	0.999	0.995	0.953	0.939	0.920
merP	0.994	0.998	1.000	1.000	0.999	0.969	0.957	0.941
merC	0.995	0.999	1.000	1.000	0.999	0.966	0.954	0.938
merA	0.989	0.995	0.999	0.999	1.000	0.979	0.969	0.955
merD	0.938	0.953	0.969	0.966	0.979	1.000	0.999	0.995
merE	0.923	0.939	0.957	0.954	0.969	0.999	1.000	0.999
urf2	0.903	0.920	0.941	0.938	0.955	0.995	0.999	1.000

B.

	merR	merT	merP	merC	merA	merD	merE	urf2
merR	1.000	0.995	0.940	0.979	0.904	0.494	0.428	0.391
merT	0.995	1.000	0.917	0.966	0.876	0.442	0.370	0.334
merP	0.940	0.917	1.000	0.989	0.995	0.760	0.709	0.680
merC	0.979	0.966	0.989	1.000	0.971	0.657	0.597	0.565
merA	0.904	0.876	0.995	0.971	1.000	0.818	0.772	0.746
merD	0.494	0.442	0.760	0.657	0.818	1.000	0.996	0.992
merE	0.428	0.370	0.709	0.597	0.772	0.996	1.000	0.999
urf2	0.391	0.334	0.680	0.565	0.746	0.992	0.999	1.000

Table A.S4: P-values of the Pearson correlations of the line graphs of normalized reads of each *mer* gene at each time point . (A) 3 µM Hg and (B) 4 µM Hg.

A.

P-value	*merR*	*merT*	*merP*	*merC*	*merA*	*merD*	*merE*	*urf2*
merR		1.33E-04	5.69E-04	4.60E-04	1.48E-03	1.83E-02	2.52E-02	3.60E-02
merT	1.33E-04		8.21E-05	5.09E-05	4.47E-04	1.22E-02	1.80E-02	2.69E-02
merP	5.69E-04	8.21E-05		2.72E-07	3.71E-05	6.64E-03	1.06E-02	1.71E-02
merC	4.60E-04	5.09E-05	2.72E-07		6.32E-05	7.34E-03	1.16E-02	1.84E-02
merA	1.48E-03	4.47E-04	3.71E-05	6.32E-05		3.72E-03	6.55E-03	1.14E-02
merD	1.83E-02	1.22E-02	6.64E-03	7.34E-03	3.72E-03		4.05E-05	3.82E-04
merE	2.52E-02	1.80E-02	1.06E-02	1.16E-02	6.55E-03	4.05E-05		5.99E-05
urf2	3.60E-02	2.69E-02	1.71E-02	1.84E-02	1.14E-02	3.82E-04	5.99E-05	

B.

P-value	*merR*	*merT*	*merP*	*merC*	*merA*	*merD*	*merE*	*urf2*
merR		3.96E-04	1.73E-02	3.57E-03	3.53E-02	3.98E-01	4.73E-01	5.15E-01
merT	3.96E-04		2.85E-02	7.47E-03	5.14E-02	4.56E-01	5.40E-01	5.83E-01
merP	1.73E-02	2.85E-02		1.43E-03	3.68E-04	1.36E-01	1.80E-01	2.06E-01
merC	3.57E-03	7.47E-03	1.43E-03		5.96E-03	2.28E-01	2.88E-01	3.21E-01
merA	3.53E-02	5.14E-02	3.68E-04	5.96E-03		9.05E-02	1.26E-01	1.47E-01
merD	3.98E-01	4.56E-01	1.36E-01	2.28E-01	9.05E-02		3.53E-04	7.87E-04
merE	4.73E-01	5.40E-01	1.80E-01	2.88E-01	1.26E-01	3.53E-04		3.84E-05
urf2	5.15E-01	5.83E-01	2.06E-01	3.21E-01	1.47E-01	7.87E-04	3.84E-05	

Table A.S5: Read counts of differentially expressed chromosomal genes for MG 3 vs 0 µM $HgCl_2$ grouped by COG functional category. Each category is subdivided into up-regulated (upper number) and down-regulated (lower number) genes. Categories defined by COG database update, 2020 annotation (Galperin et al., 2021).

Up- and Down-regulated	10 min.	30 min.	60 min.	90 min.
(A) RNA processing	0	0	0	0
	0	0	0	0
(B) chromatin structure	0	0	0	0
	0	0	0	0
(C) energy production	41	21	15	35
	56	59	60	60
(D) cell cycle control & division	6	7	2	4
	7	7	2	3
(E) amino acids	52	37	84	68
	104	96	23	29
(F) nucleodtides	8	8	20	10
	40	23	5	5
(G) carbohydrates	35	30	12	22
	54	49	11	22
(H) coenzymes	27	24	21	19
	30	22	8	6
(I) lipids	20	25	9	15
	20	11	6	9
(J) translation	20	13	57	81
	91	77	6	6
(K) transcription	66	62	22	15
	35	24	8	13
(L) replication & repair	18	11	11	9
	19	10	1	1
(M) cell wall & membrane	28	37	22	36
	60	31	10	16
(N) cell motility	2	3	1	2
	32	34	7	6
(O) protein processing	54	38	18	8
	15	15	24	14
(P) inorganic ions	34	32	30	22
	47	47	35	26
(Q) secondary metabolites	11	12	1	0
	5	2	2	3
(R) predicted function only	43	38	16	16
	15	16	14	18
(S) function unknown	22	27	6	6
	21	23	12	13
(T) signal transduction	32	27	17	15
	44	25	13	17
(U) intracellular trafficking	4	3	0	9
	18	16	3	2
(V) defense mechanism	14	17	1	2
	16	5	6	10
(W) extracellular structures	2	1	1	3
	3	4	1	0
(X) mobilome	4	1	1	2
	5	4	1	0
(Y) nuclear structure	0	0	0	0
	0	0	0	0
(Z) cytoskeleton	0	0	0	0
	1	1	0	0
Sum	**1281**	**1075**	**625**	**678**
STDV	**24**	**21**	**17**	**17**

Table A.S6: Read counts of differentially expressed chromosomal genes for NR 3 vs 0 µM $HgCl_2$ grouped by COG functional category. Each category is subdivided into up-regulated (upper number) and down-regulated (lower number) genes. Categories defined by COG database update; 2020 annotation (Galperin et al., 2021).

Up- and Down-regulated	10 min.	30 min.	60 min.	90 min.
(A) RNA processing	0	0	0	0
	0	0	0	0
(B) chromatin structure	0	0	0	0
	0	0	0	0
(C) energy production	48	3	21	25
	56	20	62	12
(D) cell cycle control & division	4	2	5	1
	9	1	3	2
(E) amino acids	55	14	74	2
	108	17	24	11
(F) nucleodtides	12	3	16	0
	43	1	6	0
(G) carbohydrates	44	12	12	1
	55	15	18	1
(H) coenzymes	37	3	18	1
	32	5	9	1
(I) lipids	23	8	10	2
	23	1	8	0
(J) translation	25	3	70	2
	101	4	11	0
(K) transcription	71	13	22	1
	40	3	17	4
(L) replication & repair	27	1	10	1
	27	0	1	0
(M) cell wall & membrane	29	10	18	4
	67	4	15	5
(N) cell motility	1	0	10	0
	33	2	2	0
(O) protein processing	60	17	13	8
	16	3	22	0
(P) inorganic ions	32	10	21	5
	47	19	40	5
(Q) secondary metabolites	12	1	1	1
	3	1	4	1
(R) predicted function only	48	7	10	2
	21	3	21	2
(S) function unknown	30	8	7	2
	22	3	18	5
(T) signal transduction	33	6	16	1
	51	2	14	1
(U) intracellular trafficking	5	0	4	0
	17	0	1	0
(V) defense mechanism	19	4	3	0
	17	1	6	3
(W) extracellular structures	1	0	1	0
	4	0	1	0
(X) mobilome	6	1	1	0
	5	0	0	0
(Y) nuclear structure	0	0	0	0
	0	0	0	0
(Z) cytoskeleton	0	0	1	0
	1	0	0	0
Sum	**1420**	**231**	**667**	**112**
STDV	**26**	**6**	**16**	**4**

Table A.S7: Read counts of differentially expressed chromosomal genes for MG 4 vs 0 µM $HgCl_2$ grouped by COG functional category. Each category is subdivided into up-regulated (upper number) and down-regulated (lower number) genes. Categories defined by COG database update, 2020 annotation (Galperin et al., 2021).

Up- and Down-regulated	10 min.	30 min.	60 min.	90 min.
(A) RNA processing	1	1	0	0
	0	0	0	0
(B) chromatin structure	0	0	0	0
	0	0	0	0
(C) energy production	57	50	30	26
	36	59	86	57
(D) cell cycle control & division	6	8	5	2
	11	11	5	2
(E) amino acids	58	67	65	50
	85	103	63	43
(F) nucleodtides	14	10	4	3
	27	39	25	4
(G) carbohydrates	65	88	42	15
	45	47	40	34
(H) coenzymes	42	36	32	19
	41	39	21	7
(I) lipids	23	29	26	19
	22	18	10	5
(J) translation	34	28	22	9
	98	74	15	6
(K) transcription	110	96	68	26
	56	44	23	15
(L) replication & repair	34	31	23	10
	43	40	12	1
(M) cell wall & membrane	37	40	30	9
	87	86	39	11
(N) cell motility	6	10	2	1
	36	36	27	19
(O) protein processing	57	60	53	19
	28	30	28	12
(P) inorganic ions	44	52	51	37
	55	54	41	27
(Q) secondary metabolites	17	20	11	5
	4	7	6	2
(R) predicted function only	63	56	36	17
	30	34	23	21
(S) function unknown	34	43	29	12
	26	25	17	14
(T) signal transduction	40	46	32	20
	70	58	28	14
(U) intracellular trafficking	6	9	5	3
	21	21	7	4
(V) defense mechanism	29	31	14	4
	26	22	9	3
(W) extracellular structures	5	5	1	1
	5	4	1	0
(X) mobilome	8	9	5	0
	7	11	4	1
(Y) nuclear structure	0	0	0	0
	0	0	0	0
(Z) cytoskeleton	0	0	0	0
	1	1	1	0
Sum	**1650**	**1688**	**1117**	**609**
STDV	**27**	**27**	**21**	**14**

Table A.S8: Read counts of differentially expressed chromosomal genes for NR 4 vs 0 µM $HgCl_2$ grouped by COG functional category. Each category is subdivided into up-regulated (upper number) and down-regulated (lower number) genes. Categories defined by COG database update, 2020 annotation (Galperin et al., 2021).

Up- and Down-regulated	10 min.	30 min.	60 min.	90 min.
(A) RNA processing	1	0	0	0
	0	0	0	0
(B) chromatin structure	0	0	0	0
	0	0	0	0
(C) energy production	57	35	19	32
	36	65	55	62
(D) cell cycle control & division	6	6	2	6
	12	8	2	3
(E) amino acids	62	59	64	78
	92	88	19	30
(F) nucleodtides	13	8	15	12
	28	38	4	8
(G) carbohydrates	68	55	10	21
	49	44	11	40
(H) coenzymes	44	30	18	22
	43	26	7	8
(I) lipids	24	20	13	22
	21	11	4	13
(J) translation	33	24	25	101
	98	93	6	12
(K) transcription	105	82	29	25
	58	26	11	17
(L) replication & repair	32	29	6	12
	38	26	0	1
(M) cell wall & membrane	31	35	16	36
	85	58	9	18
(N) cell motility	4	7	0	5
	36	30	4	3
(O) protein processing	60	54	27	12
	26	21	20	22
(P) inorganic ions	47	52	34	29
	46	43	29	36
(Q) secondary metabolites	15	15	3	0
	4	6	3	6
(R) predicted function only	60	47	11	18
	25	29	15	26
(S) function unknown	31	41	5	13
	24	24	14	22
(T) signal transduction	34	33	15	20
	68	35	14	15
(U) intracellular trafficking	7	6	2	8
	21	15	1	3
(V) defense mechanism	30	25	3	4
	25	15	4	11
(W) extracellular structures	3	3	0	2
	6	2	2	1
(X) mobilome	8	6	1	3
	7	5	1	0
(Y) nuclear structure	0	0	0	0
	0	0	0	0
(Z) cytoskeleton	0	0	0	1
	1	2	0	0
Sum	**1624**	**1382**	**553**	**839**
STDV	**28**	**24**	**13**	**20**

Table A.S9: Pearson correlations for the line graphs of the normalized reads of the isocitrate dehydrogenase (*icd*) gene at each time point. (A) 3 µM Hg and (B) 4 µM Hg.

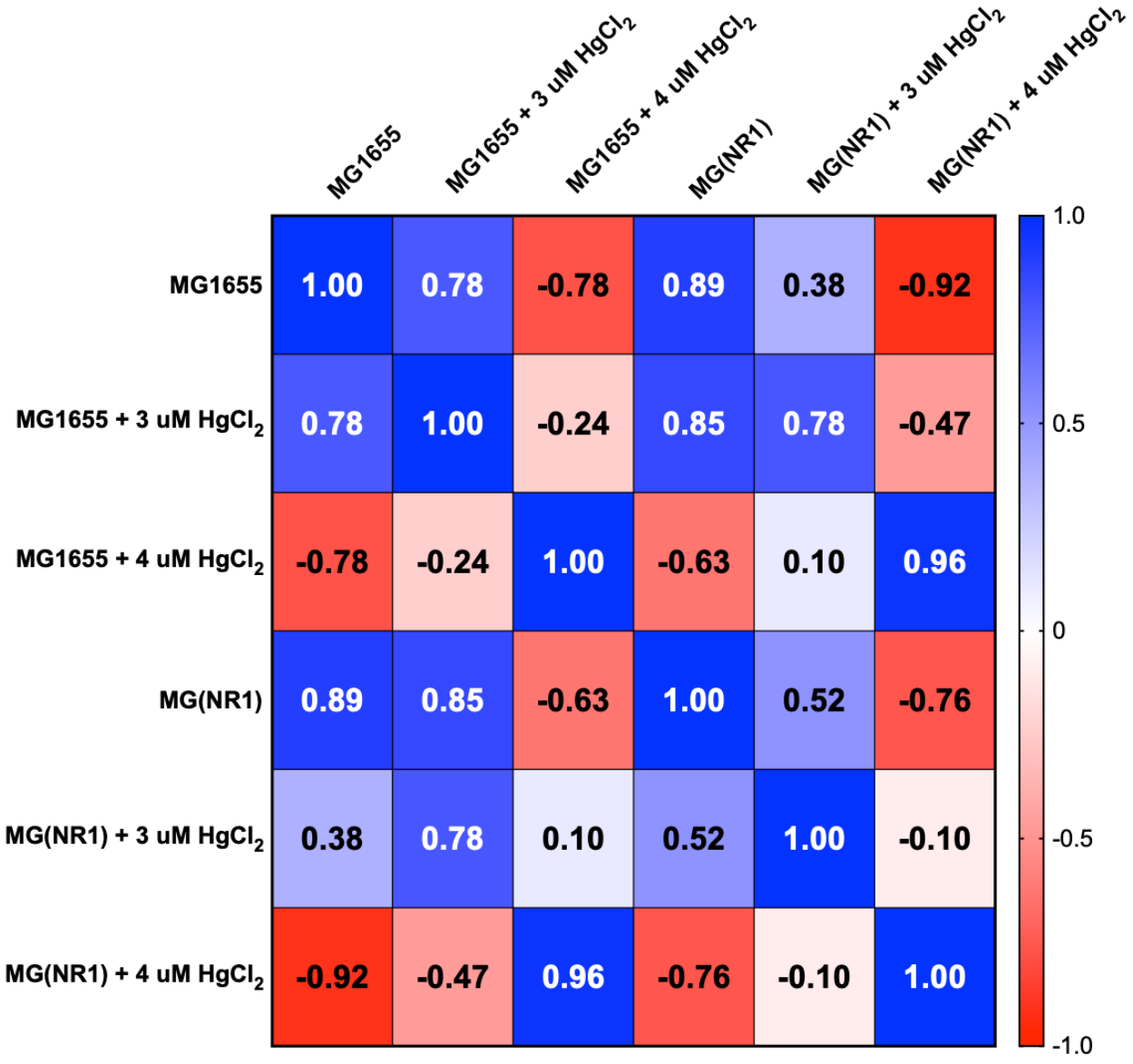

Table A.S10: P-values of the Pearson correlations of the line graphs of normalized reads of each isocitrate dehydrogenase (*icd*) gene at each time point. (A) 3 µM Hg and (B) 4 µM Hg.

P-value for *icd*	HgS + 3 uM $HgCl_2$	HgS + 4 uM $HgCl_2$	HgR + 3 uM $HgCl_2$	HgR + 4 uM $HgCl_2$
HgS + 3 uM $HgCl_2$		0.702	0.119	0.420
HgS + 4 uM $HgCl_2$	0.702		0.867	0.009
HgR + 3 uM $HgCl_2$	0.119	0.867		0.876
HgR + 4 uM $HgCl_2$	0.420	0.009	0.876	

.

Table A.S11: Pearson correlations for the line graphs of the normalized reads of each malate dehydrogenase (*maeB*) gene at each time point. (A) 3 µM Hg and (B) 4 µM Hg.

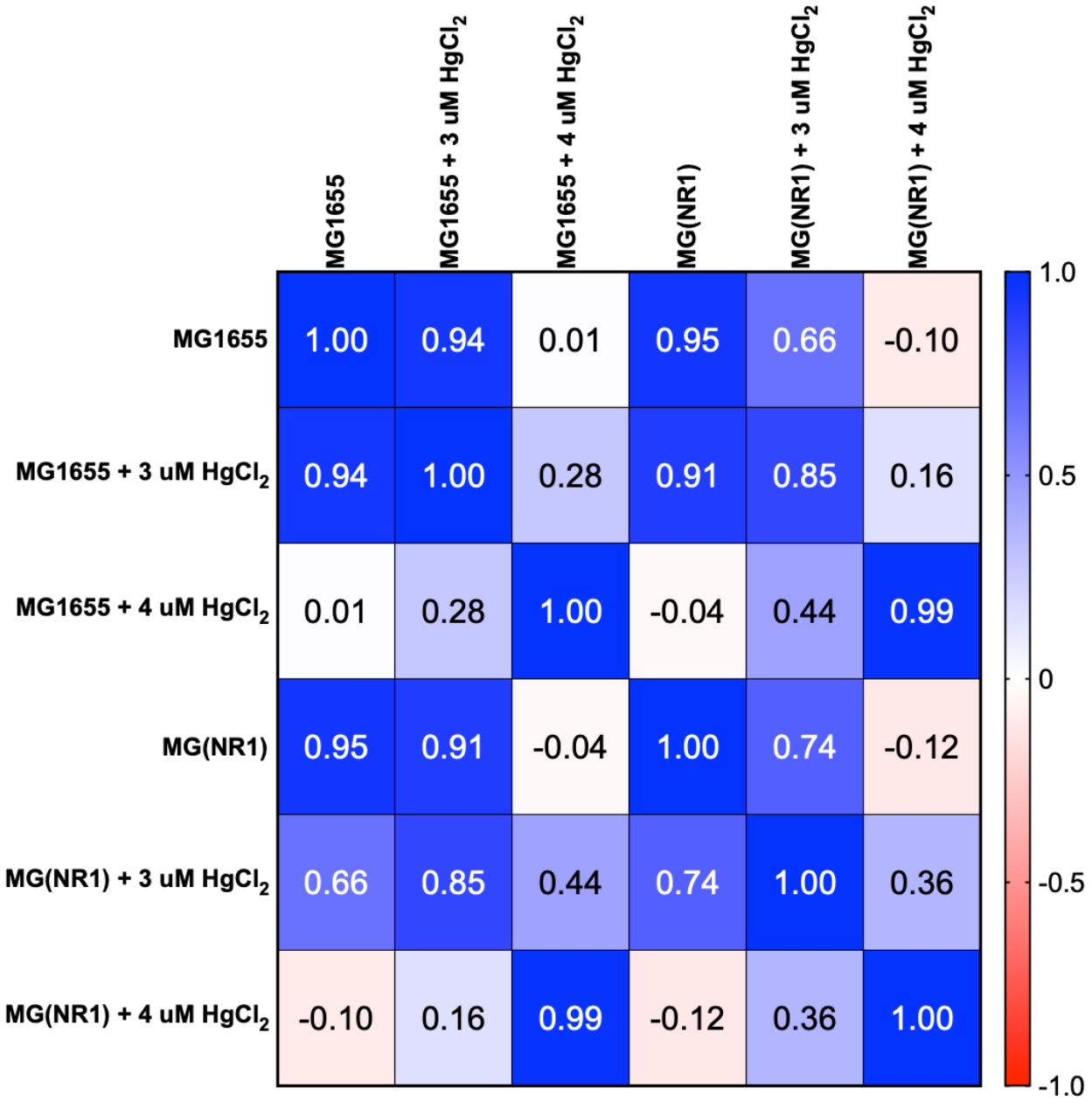

Table A.S12: P-values of the Pearson correlations of the line graphs of normalized reads of each malate dehydrogenase (*maeB*) gene at each time point . (A) 3 µM Hg and (B) 4 µM Hg.

P-value for *maeB*	HgS + 3 uM $HgCl_2$	HgS + 4 uM $HgCl_2$	HgR + 3 uM $HgCl_2$	HgR + 4 uM $HgCl_2$
HgS + 3 uM $HgCl_2$		0.654	0.065	0.803
HgS + 4 uM $HgCl_2$	0.654		0.454	0.002
HgR + 3 uM $HgCl_2$	0.065	0.454		0.550
HgR + 4 uM $HgCl_2$	0.803	0.002	0.550	